CONFORMATIONAL AND FUNCTIONAL ALTERATIONS ON AN ASPARTIC PROTEINASE PROMOTED BY TRIFLUOROETHANOL

ALTERAÇÕES FUNCIONAIS E CONFORMACIONAIS PROMOVIDAS NUMA PROTEINASE ASPÁRTICA POR TRIFLUOROETANOL

CONFORMATIONAL AND FUNCTIONAL ALTERATIONS ON AN ASPARTIC PROTEINASE PROMOTED BY TRIFLUOROETHANOL

ALTERAÇÕES FUNCIONAIS E CONFORMACIONAIS PROMOVIDAS NUMA PROTEINASE ASPÁRTICA POR TRIFLUOROETANOL

Ana Sofia Fraga de Almeida

Dissertation presented to Sciences and Technology Faculty of the University of Coimbra in partial fulfilment of the requirements for a Doctoral degree in Biochemistry (Enzymology).

Dissertação apresentada à Faculdade de Ciências e Tecnologia da Universidade de Coimbra para prestação de provas de Doutoramento em Bioquímica, na especialidade de Enzimologia.

Coimbra 2010

This work was performed at Center for Neuroscience and Cell Biology, Department of Biochemistry, University of Coimbra, under the supervision of Professor Doctor Euclides Pires, and co-supervision of Professor Doctor Marlene Barros. It was supported by Fundação para a Ciência e Tecnologia, Portugal (project POCTI/QUI/60791/2004 and grant SFRH/BD/10754/2002).

Este trabalho foi realizado no Centro de Neurociências e Biologia Celular, Departamento de Bioquímica, da Universidade de Coimbra, sob a orientação do Professor Doutor Euclides Pires, e co-orientação da Professora Doutora Marlene Barros. Este trabalho foi financiado pela Fundação para a Ciência e a Tecnologia, Portugal (projecto POCTI/QUI/60791/2004 e bolsa de doutoramento SFRH/BD/10754/2002).

Ciência.Inovação 2010

Financiamento no âmbito do III Quadro Comunitário de Apoio, comparticipado pelo Fundo Social Europeu e por fundos nacionais do MCES.

TABLE OF CONTENTS

ABSTRACT

The study of aspartic proteases has been gaining interest due to their importance in the development of major concerning human diseases, as Alzheimer's disease, breast cancer, or AIDS. The molecular basis of some of these diseases is associated to folding errors, which disables proteins proper functioning. Stability studies over this class of enzymes are extremely important for characterising the pathology involved mechanisms and to discover therapeutic solutions.

The heterodimeric cardosin A is a plant aspartic proteinase of high yield purification. Besides having been traditionally used as milk clotting agent for cheese making, its characteristics have made it an interesting enzyme for biotechnological applications. This endopeptidase has thus been considered a good model for structural and functional studies of the aspartic proteinases group, and of proteins in general.

Water availability is a fundamental factor for protein stability and conformation flexibility, and these characteristics are imperative for proper functioning. The present approach intends to upgrade the understanding of aspartic proteases native conformation as a mutable form. Along the last few years, cardosin A structural conformation has been characterized in biphasic systems, aqueous solutions saturated by organic solvents, and more extensively in the presence of the organic solvent acetonitrile. In sequence with the work developed by our group, the unfolding of cardosin A was here induced by 2,2,2-trifluoroethanol (TFE), a polar and protic organic solvent with very different properties from the previous organic solvents tested. TFE characteristics promote distinct alterations in water structure, interacting in a particular way with the protein hydration layer and with the protein structure itself. Furthermore, it is known to stabilize well ordered conformations rather than inducing denaturation.

The aim of the present work was to follow the conformational and functional alterations promoted by TFE proximity to cardosin A structure. The function dependence on enzyme structure was related to the availability of water and/or of hydrogen bonds to the protein surface. Different spectroscopic methods (circular dichroism and intrinsic fluorescence), activity measurements, and calorimetric analysis were employed to detect and characterize the organic solvent induced states. Finally, molecular dynamics/molecular mechanics (MD/MM) simulations were applied to the system in order to understand the interaction between protein and solvent molecules.

The TFE in vitro assays with cardosin A promoted folding variations dependent of the alcohol concentration. TFE medium content below 4% decreased protein stability, but reversibly increased its enzymatic rate. TFE medium content over 20%

irreversibly inactivated the enzyme and unfolded its tertiary structure, while secondary helical content was progressively increased (mainly from previously unordered segments). At last, TFE medium content over 70% inactivated the enzyme and promoted a vast increase in structural complexity, taking form as characteristic open helical structures, and these alterations proved to be reversible.

MD simulations with TFE and water described local alterations in protein flexibility, but no large conformational transformations. Instead, the model described an exposition of local competition of TFE with water for solvation surface. TFE molecules were found replacing several hydration molecules in the active site. Despite the catalytic water was not lost in the last acquired conformation of the high TFE content MD simulation, the active site was occupied by several TFE molecules, and this occurrence was proposed to justify the activity loss. The same reasoning can explain the activity recovery upon aqueous dilution, with the release of the active site for substrate binding.

RESUMO

O estudo das proteinases aspárticas tem vindo a ganhar interesse devido à importância desta classe de enzimas na etiologia e evolução de doenças humanas que são hoje fonte duma preocupação crescente, como são os casos da doença de Alzheimer, do cancro da mama ou da SIDA.

A base molecular de algumas destas doenças está associada a erros de folding (enrolamento), que impossibilitam a sua função. Estudos de estabilidade sobre esta classe de enzimas são de extrema importância para a caracterização dos mecanismos patológicos envolvidos, e para a descoberta de soluções terapêuticas.

A proteína heterodimérica cardosina A é uma proteinase aspártica de origem vegetal que pode ser purificada em elevadas quantidades. Apesar de tradicionalmente ser usada como agente coagulante do leite na produção de queijo, as suas características fizeram dela uma enzima interessante para aplicações biotecnoló-

gicas. Esta endopeptidase tem sido considerada um bom modelo para estudos estruturais e funcionais do grupo das proteinases aspárticas e de proteínas em geral.

A disponibilidade de água é um factor fundamental para a estabilidade proteica e para a sua flexibilidade conformacional, características estas essenciais à sua função.

Com o presente trabalho esperamos ter contribuído para a compreensão da conformação nativa das proteinases aspárticas como uma forma mutável. Ao longo dos últimos anos a estrutura conformacional da cardosina A foi caracterizada em sistemas bifásicos, meio aquoso saturado com solventes orgânicos, e mais exaustivamente na presença do solvente orgânico acetonitrilo. Na sequência do trabalho desenvolvido pelo nosso grupo, o unfolding (desenrolamento) da cardosina A foi induzido pelo 2,2,2-trifluoroethanol (TFE), um solvente orgânico polar e prótico com propriedade muito diferentes dos solventes orgânicos previamente usados. As características do TFE promovem alterações distintas na estrutura da água, interagindo de um modo particular com a camada de hidratação da proteína e com a própria estrutura proteica. Além disso o TFE é conhecido por estabilizar conformações complexas em vez de induzir a desnaturação.

Foi objectivo do presente trabalho seguir as alterações conformacionais e funcionais promovidas pela proximidade do TFE à estrutura da cardosina A. A dependência da função enzimática em relação à estrutura proteica foi relacionada com a disponibilidade de água e/ou de pontes de hidrogénio na superfície da proteína. Diferentes métodos espectroscópicos (dicroísmo circular e fluorescência intrínseca), medições de actividade enzimática, e análise calorimétrica foram utilizados para detectar e caracterizar os estados induzidos pelo solvente orgânico.

Finalmente foram aplicadas ao sistema simulações de dinâmica

molecular/mecânica molecular (MD/MM) de forma a compreender a interacção entre a proteína e as moléculas de solvente.

Os ensaios in vitro com a cardosina A em TFE promoveram variações de folding dependentes da concentração do álcool. Concentrações de TFE inferiores a 4% diminuíram a estabilidade proteica, mas aumentaram reversivelmente a actividade enzimática. Concentrações superiores a 20% de TFE no meio inactivaram irreversivelmente a enzima e desenrolaram a sua estrutura terciária, enquanto o seu conteúdo secundário em hélices foi progressivamente aumentado (principalmente de segmentos sem estruturação prévia). Por último, concentrações superiores a 70% de TFE no meio inactivaram a enzima e promoveram um vasto aumento na complexidade estrutural, na forma típica de estruturas helicoidais abertas, alterações estas que provaram ser reversíveis.

As simulações de MD com TFE e água, descreveram alterações locais de flexibilidade proteica, mas sem grandes transformações conformacionais. Em vez disso o modelo expôs os locais de competição entre o TFE e as moléculas de água da superfície de solvatação. Moléculas de TFE foram encontradas a substituir várias moléculas de hidratação no local activo. Apesar da molécula de água catalítica não ter sido perdida na última conformação adquirida na simulação para alto conteúdo em TFE, o local activo apresentava-se ocupado por várias moléculas de TFE, e este facto foi proposto como justificação para a perda de actividade. A mesma lógica poderá explicar a recuperação de actividade após a diluição para sistema aquoso, com a libertação do local activo para interacção com o substrato.

ABBREVIATIONS

AIDS	acquired immunodeficiency syndrome
α-C	alpha carbon
AP	aspartic proteinase
a_w	water activity
BCA	bicinchoninic acid
B value	atomic displacement parameter, or temperature factor
CD	circular dichroism
C_p	heat capacity

CPK	Corey, Pauling and Koltun coloring scheme (CPK)
H-bond	hydrogen bond
ΔH_{cal}	calorimetric enthalpy
ΔH_{vH}	van't Hoff enthalpy
$\Delta\lambda_{max}$	$= \lambda_{max(sample)} - \lambda_{max(NATA)}$
ΔUF	difference in the fluorescence intensity between the substrate and the peptide
DMSO	dimethyl sulfoxide
DSC	differential scanning calorimetry
far-UV CD	CD spectroscopy in the 190-250 nm spectral region
HIV	human immunodeficiency virus
HPLC	high-performance liquid chromatography
KGE	Lys-Gly-Glu domain
λ_{exc}	excitation wavelength
λ_{max}	maximum emission wavelength
MD simulation	molecular dynamics simulation
MM simulation	molecular mechanics simulation
MW	molecular weight
NATA	N – acetyl – L – tryptophanamide

NOE	nuclear overhauser effect
NMR	nuclear magnetic resonance
OS	organic solvent
PDB	Protein Data Bank (Berman *et. al.*, 2000)
PSI	plant-specific insert
RGD	Arg-Gly-Asp domain
RMSD	root mean square deviation
SDS-PAGE	sodium dodecyl sulfate polyacrylamide gel electrophoresis
SEC	size exclusion chromatography
θ	ellipticity
θ_{222}	ellipticity for 222 nm
TFA	trifluoroacetic acid
TFE	2,2,2-trifluoroethanol
T_m	thermal transition temperature
UF	fluorescence units
UV	ultraviolet
Ve	elution volume

1. INTRODUCTION

The study of aspartic proteases has been gaining interest due to their importance in the development of major concerning human diseases, as Alzheimer's disease, breast cancer, or AIDS. The molecular basis of some of these diseases is associated to folding errors, that disable proteins to function properly. Stability studies over this class of enzymes are extremely important for characterising the pathology involved mechanisms and to discover therapeutic solutions. There has been much effort in the development of aspartic proteinase inhibitors as therapeutic agents for treatment of hypertension, AIDS, amyloid diseases, gastric diseases, parasitic infections and cancer (Cooper, 2002).

The heterodimeric cardosin A is a plant aspartic proteinase of high yield purification. Besides having been traditionally used as milk clotting agent for cheese making, its characteristics have made it an interesting enzyme for biotechnological applications.

This endopeptidase has thus been considered a good model for structural and functional studies of the aspartic proteinases group, and of proteins in general.

Water availability is a fundamental factor for protein stability and conformation flexibility, and these characteristics are imperative for proper function. Their characterisation in water reduced environments is of extreme importance. The depletion of water may promote protein unfolding, and through this process non-native conformational states may be stabilised and characterised.

1.1. WATER AVAILABILITY

Biological systems, organisms and cells are currently realised as parts of a whole, related in organic and functional manners. This holistic view of the cell, of its compartments and constituents, is widened to its protein content. Protein conformation has become to be understood as a structure in constant change.

The protein *in vivo* environment is substantially different from the common biochemical experiments conditions. Biochemical rates and equilibria have traditionally been studied in dilute solutions, where the consequences of steric repulsion between solutes are insignificantly small (Minton, 2006a). However, in cells, the total volume of all biological fluid media is jointly occupied by proteins, nucleic acids, and polysaccharides. The concentration of macromolecules inside cells is in the range of 300 – 400 mg/ml, which corresponds to volume occupancy of 5 – 40% (Ellis and Minton, 2006; Homouz *et al.*, 2008). As result, the cell is extremely crowded.

Crowding plays a role in all biological processes that depend on noncovalent associations and/or conformational changes

(Al-Habori, 2001; Ellis, 2001; Sun and Weinstein, 2007). It has been proved that excluded volume effects in such crowded media can result in equilibrium and rate constant alterations by up to several orders of magnitude (Minton, 2006b). Recent works have proved that macromolecular crowding affects the overall "native" protein shape (Homouz *et al.*, 2008) and its folding process (Engel *et al.*, 2008). Biological macromolecules have evolved to function in such crowded environments, where a small change is sensed, allowing the proper cell/organism reaction to occur.

For molecular interactions to occur in such an environment (e.g., for a protein to meet its substrate), effective diffusion needs to take place. But the intermolecular space (1 – 2 nm; Ball, 2008) may be much inferior than the macromolecular dimensions *(*6.5 nm is the approximate diameter of the aspartic protease cardosin A; Frazão *et al.*, 1999). This idea emphasises the importance of protein conformation flexibility.

This narrow confinement was proved to alter the structure of the very immersing liquid[1]. The water hydrogen-bonded network gets significantly perturbed, and this structural change is widespread in the cytoplasm[2]. Water in the cell does not behave as it does in the bulk, suffering altered hydration and hydrophobic association behaviours (Price and Stevens, 1999). Several water molecules occupy cavities in the protein molecules and have approximately four hydrogen-bond partners, performing as glues for stabilizing the tertiary and quaternary structures of proteins (Nakasako *et al.*, 2004). Water plays the hydration role, creating the non-

[1] The water molecule is considered as a biomolecule: without it, other molecules would not only be unprotected and immobile, but also they would stop being biomolecules (they would be deprived of its biological function, given that its peculiar structure would be lost) (Ball, 2002).

[2] Experiments with proton NMR relaxation times of water in cells differ from that in the bulk. Curiously, the relaxation becomes more "bulk-like" in diseased cells, such as cancerous ones (Damadian, 1971).

covalent interactions responsible for the vital three-dimensional structure of proteins (Al-Habori, 2001).

Hydration molecules are located closer than 4 Å from the protein surface, and beyond this distance, water molecules distribute randomly (Nakasako *et al.*, 2004). Proteins may be regarded as entities that not only influence their solvation environments, but are fine-adjusted and modified by these environments, in ways that affect their biological function and behaviour (Ball, 2008). Water acts as solvent, but also mediate enzymatic catalysis, either directly by taking part in the reaction, or indirectly, providing a solvation medium for reactants, transition state, and products (Fersht, 1999). Water levels can be made variable on enzymes studies, and this should surely be a source of useful information about the role of water (Halling, 2004).

1.2. PROTEIN STRUCTURE

> *Any attempt to understand protein function cannot rely on statics (structure) alone but must consider also the dynamical behaviour.*
> *(Ball, 2008)*

1.2.1. Protein stability

Protein stability may be defined as a balance between the forces that determine its natively folded conformation and the forces that promote its structure unfolding (Creighton, 1990). There are two very different aspects of protein stability: one is the chemical stability of the structure, which involves covalent changes and is usually irreversible; the other is the conformational stability of the folded state, usually reversible, where covalent changes are

absent (Pace *et al.*, 1989; Pace and Grimsley, 2001).

To be biologically active, proteins must correctly fold into specific three-dimensional arrangements with structural stability and functional flexibility. Yet the protein genetic information only specifies the primary structure (the linear sequence of amino acids in the polypeptide backbone). Protein folding proceeds from the disordered random coil polypeptide chain, to intermediates with increasing degree of conformation and dynamic order, to the final native state of the protein. When a fully extended unfolded polypeptide chain begins to fold, hydrophobic residues tend to be buried in the interior, and the number of possible conformations the chain can assume begins to decrease. Within milliseconds, the polypeptide chain achieves the molten globule state, a loosely packed hydrophobic core with some secondary structure. Some proteins have one preferred folding pathway, while others seem to have multiple parallel pathways to the native state. The final native state could be described by one predominant conformation, around which local fluctuations of low amplitude occur. There are certain high energy barriers to folding, like the formation of correct disulphide bonds and the isomerisation of proline residues. Cells contain enzymes, such as protein disulfide isomerases and cis-trans-proline isomerases, that catalyse these reactions (Creighton, 1990; Bieri and Kiefhaber, 1999; Daggett and Fersht, 2003; Fleming and Rose, 2005).

Once regarded as a grand challenge, the protein folding problem has seen much progress in recent years. But it is still considered an important and challenging problem in molecular biology (Dill *et al.*, 2007; Zhang *et al.*, 2009).

Several pathologies are due to proteins incorrect folding or low structural stability resulting in aggregation or malfunction. Some examples are acquired spongiform encephalopathies, Alzheimer's

disease, or Parkinson disease. The comprehension of protein folding will allow pharmaceutical industry to develop new therapeutics, such as inhibitors. For instance, inhibitors have shown to act as the best treatment for AIDS, since mature and active HIV protease is essential for virus maturation (Cooper, 2002).

1.2.2. Conformational stability

In physiological conditions, the free energy difference between native and denatured states defines the conformational stability of a protein. This energy difference between a biologically active protein and its inactive denatured state is quite small (approximately 5-15 kcal/mol)[3]. Some forces are responsible for these folded/unfolded energy differences. The major destabilising force is conformational entropy, which opposes to the stabilising forces of hydrogen bonding, hydrophobic effect and close-range electrostatic interactions (Munson *et al.*, 1996; Pace and Grimsley, 2001; Kumar and Nussinov, 2002). The water molecules entropy is increased in the native state, since they no longer solvate the hydrophobic groups, and this is a very important factor favouring the native conformation. In aqueous environment the equilibrium shifts to the native state: despite the higher conformational entropy of the denatured state, its free energy of hydration is also very increased compared to the native conformation. On the other way the native state low conformational entropy is balanced by the low hydration free energy, that forces non-polar groups to concentrate in the molecule hydrophobic interior (Pace and Grimsley, 2001).

The protein stabilisation/denaturation equilibrium may be studied

[3] For comparison, the energy contribution of a single hydrogen bond is of the order of 2-5 kcal/mol.

by changing the physical and chemical properties of the environment. When a new equilibrium state is reached, it is possible to quantify native and denatured molecules, and to calculate the equilibrium constant, assuming that the denaturation is reversible. When the denaturation is irreversible, the enzymatic activity can be used to quantify the active enzyme concentration (Melo, 2003). The kinetic unfolding mechanism has also been characterised for some oligomeric proteins in order to understand the sub-units interaction and folding. In these cases the unfolding intermediates may only be indirectly detected by the non-coincidence of denaturation curves that follow different events (Neet and Timm, 1994). Some proteins may adopt stable and partially folded conformations. This capacity is considered intrinsic to the polypeptide chain, and depends on its charge and hydrophobicity. These conformations appear to be stabilised mainly by nonspecific interactions between hydrophobic side-chains (Uversky, 2002). Different intermediate or partially unfolded conformations may perform important roles on synthesis, folding, function and degradation of globular proteins. (Baldwin, 1991; Fink, 1995).

Irreversible denaturation may be originated by covalent causes (peptidic bond hydrolysis or intramolecular bond formations) or non-covalent sources (aggregation and misfolding). A variety of conditions can promote unfolding with some ease, such as extremes of pH, heating, and addition of organic solvents, detergents, chaotropic agents, or high concentrations of denaturants such as urea or guanidium chloride. Loss of the three dimensional structure of the folded protein can be monitored by changes in spectroscopic parameters, measured by techniques such as circular dichroism or fluorescence, and also, in the case of enzymes, by the alteration of catalytic activity (Price and Stevens, 1999).

But the correlation between correct folding and function is not a rule, since there are a number of proteins that lack intrinsic globular structure in their normal functional form. Intrinsically unstructured or natively unfolded proteins are extremely flexible, non-compact, and under physiological conditions reveal little, if any, secondary structure. They are implied in the development of some neurodegenerative diseases, as their unstructured states play important roles in the development of fibrillar stages. This fact further supports the importance of investigations in detailed structural and dynamics of proteins nonnative states (Wirmer *et al.*, 2005).

The described fragile stability of the native state over the denatured state is biologically very important. Living cells need proteins to be easily degradable and synthesised, and to readily respond to changes in environmental conditions (Lazaridis and Karplus, 2003). Catalytic activities, transport across membranes, ligand binding and allosteric regulation are protein functions that require structural flexibility (Závodszky *et al.*, 1998; Matouschek, 2003; Schimmele and Plückthun, 2005).

In its native state, proteins are not static, but flexible and dynamic. Changes in conformation may be subtle, reflecting molecular vibrations and small movements of residues throughout the protein. All atoms are subjected to small temperature-dependent fluctuations, being in constant motion, which is reflected in the molecule as a whole. These atomic movements are generally random, but sometimes can be collective and cause groups of atoms to move in the same direction. Side chains can flip, loop regions may not be fixed in one single conformation, helices may slide in relation to each other, and entire domains can change their packing contacts, increasing or decreasing the distance between them. Some conformational alterations may be quite dramatic, with major segments of the protein structure moving

several nanometres between different functional states. These large collective movements are reflected in X-ray and NMR studies (Branden and Tooze, 1999; Ma *et al.*, 2000).

Small differences in the environment, as pH modification, the presence or absence of ligands or the enhancement of media hydrophobicity, can stabilise different conformational states. The promoted structural movements are essential for function, for enzyme catalysis, binding of antigens to antibodies, receptor-ligand interactions and energy transduction, among others (Branden and Tooze, 1999; Tsai *et al.*, 1999; Henchman and McCammon, 2005; Dobbins *et al.*, 2008).

1.3. CONFORMATIONAL CHANGES PROMOTER

Alcohols are frequently considered minimal models for mimicking hydrophobic interactions, protein proximity environment, and proximity to biological membranes (Baskakov *et al.*, 1999; Perham *et al.*, 2006; Ball, 2008).

The water available for the protein depends on several characteristics of the medium. Considering the presence of an organic solvent (OS), its polarity is an important factor to consider. A more polar solvent holds more water molecules in solution, making a lower amount of molecules available for binding to the enzyme (Bell *et al.*, 1995).

In alcohols, the hydroxyl group enhances tetrahedral structure in water surrounding it. The polar interaction with the water -OH group is bigger than water restructuring effect induced by hydrophobic CH_3- groups, and has stronger influence on the thermodynamic properties. Thus, simultaneous hydrophobic and hydrophilic hydrations occur, with water reorganizing around alcohol non-polar groups (Kiselev *et al.*, 2001; Dixit *et al.*, 2002).

There are no sharp boundaries between polar and non polar solvents. Trifluoroethanol (TFE) is comparable to acetonitrile in terms of its bulk solvent polarity parameter (only slightly higher), but demonstrates a stronger hydrogen bonding ability (Jamison *et al.*, 2006). Mixed in water, both OS promote a lowering in the dielectric constant of the water mixture, and create a new disposition of the bulk water molecules. Acetonitrile (C_2H_3N) contains a large bond dipole (cyanide) and does not contain a hydroxyl group, being a dipolar aprotic solvent, while TFE (CF_3CH_2OH) is a polar protic solvent (figure 1.1).

1.3.1. The fluoroalcohol TFE

2,2,2-Trifluoroethanol (TFE) is a fluoroalcohol with nine times the size of a water molecule (Buck, 1998). Alcohols are small organic molecules that induce partially folded intermediates of proteins, and stabilize otherwise unstable folding intermediates. They are categorized as denaturants that tend to stabilize well-ordered conformations, from which TFE is considered to promote stability rather than inducing denaturation (Dill *et al.*, 1995; Viseu *et al.*, 2004). The effectiveness of alcohols in inducing conformational transition varies substantially among its class. Besides several important characteristics, TFE is also popular for its relatively strong effects on protein conformation and low absorbance in the far-ultraviolet region, making far-UV circular dichroism measurements feasible (Hamada and Goto, 2005).

1.3.1.1. Application and mechanisms of action

TFE is commonly used in several experimental conditions. TFE is extremely useful to analyse the intrinsic conformational propensity of protein fragments and peptides with no appreci-

Figure 1.1 – Molecular representations of acetonitrile, water and TFE solvent molecules (molecular representations from Wikipedia c1).

able ordered conformation in aqueous solution since it induces the formation of secondary structures (Sönnichsen *et al.*, 1992; Luo and Baldwin, 1997). In order to optimise its sequence to be structurally rigid, newly designed proteins with low structural properties in aqueous media have also been characterised using this solvent (Reiersen *et al.*, 1998).

In many other situations, TFE transforms proteins into molten globule-like intermediates (Buck *et al.*, 1993; Gast *et al.*, 1999). Although these structures are recognised by some authors as being locally alcohol-induced, and hence as off-pathway products (Bhakuni, 1998), they are frequently accepted as kinetic molten globules (Hamada and Goto, 2005).

The protein early folding stage occurs before fixed strong tertiary interactions are formed, and when backbone conformational preferences neutralise long-range interactions (Schönbrunner *et al.*, 1996; Sanz *et al.*, 2002). TFE decreases the strength of hydrophobic interactions, diminishing native tertiary contacts. On the other hand, it increases the number of intramolecular hydrogen bonds, stabilizing local interactions (Dill *et al.*, 1995; Luo and Baldwin, 1998). Thus, TFE can induce states of folding similar to the *in vivo* early and intermediate ones. This was proved for several proteins such as lysozyme from hen egg-white

(129 residues), whose TFE induced conformation was shown to be nearly identical to an early folding intermediate (Buck *et al.*, 1993), and β-lactoglobulin (162 residues), whose non-native α-helical structure was transiently accumulated during refolding in the absence of TFE (Shiraki et al., 1995). By the same reasons, small amounts of TFE are also used to accelerate folding kinetics (Lu *et al.*, 1997).

Another common use for TFE is as dissolvent for protein aggregates, for peptide during protein synthesis and for prion and Alzheimer's amyloid β-peptide when these aggregate or form amyloid fibrils (Yamamoto *et al.*, 2005). But it also has shown to induce protein aggregates at neutral pH, probably due to the reduced electrostatic repulsion between molecules (Hamada and Goto, 2005). On the other hand, for the formation of fibrils, while hydrophobic interactions contribute to the intermolecular association of peptides through side-chain–side-chain interactions, polar interactions contribute to the intermolecular hydrogen bonds substantiating the cross-β-structure (Yamaguchi *et al.*, 2006). TFE is also known to induce well-ordered fibrillar structures similar to amyloid fibrils (Zerovnik *et al.*, 2007; Marcon *et al.*, 2005).

Although proteins assume significant levels of nonnative α-helical conformations at high concentrations of TFE, several short peptides form β-turn or β-hairpin structures (Roccatano *et al.*, 2002), β-strands (Zhao and Liu, 2006), and there are also some examples of longer polypeptides or proteins showing stabilization of β-sheet structures (Schönbrunner *et al.*, 1996). The exact type of secondary structures stabilized in TFE/water solvent depend on the protein amino acid sequence, since these secondary structures are stabilized by local hydrogen bonds (Hamada and Goto, 2005). Moreover, several peptides do not follow the predicted

behaviour (Luidens *et al.*, 1996).

Besides all the referred characteristics and actions of this fluoro-alcohol, several authors defend TFE as being able to simulate some physiological environments. Providing hydrophobic surface areas and decreasing the medium dielectric constants, TFE mimics the close contact of the polypeptide chain with the inner part of membranes (Torta *et al.*, 2008). The structural properties of membrane proteins can be analysed in TFE/water solvent (Akitake *et al.*, 2007), as well as soluble protein behaviour during membrane translocation (Gast *et al.*, 1999). By similar reasons, TFE can mimic the environment in the protein interior (Waterhous and Johnson, 1994; Umezaki *et al*., 2008). Moreover, alcohols have been used to mimic the proximity to biological membranes (Perham *et al.*, 2006) and the *in vivo* conditions under which a disordered domain interacts with a target molecule (Baskakov *et al*., 1999).

Despite the numerous publications, the detailed mechanism by which alcohols induce protein conformational alterations is still in debate. Alcohols have very similar chemical properties to detergents: both exhibit hydrophobic (hydrocarbon or halogenated hydrocarbon) and hydrophilic (hydroxyl) groups. Theoretical studies on the effect of TFE on protein structure suggest two different mechanisms:

(1) destabilisation of intramolecular hydrophobic interactions between side chains, by displacing water and modifying its structure (Cammers-Goodwin *et al.*, 1996), and indirectly disrupting the solvent shell of α-helices (Luo and Baldwin, 1999). The hydrophobic part of the molecule, formed by the CF_3-group, may preferentially bind to hydrophobic residues and hydrophobic portions of proteins, thus modifying or disrupting hydrophobic interactions (Buck, 1998).

(2) promotion and/or strengthening of local backbone hydrogen bonds formation. TFE is a less polar solvent than water, and a less potent hydrogen bond competitor (Buck, 1998).

So, in aqueous media containing TFE, hydrophobic interactions stabilizing the native structure are weakened, while local hydrogen bonds are strengthened. The result is unfolding and simultaneous formation of "open helical conformations" or "open helical coils", i.e., solvent-exposed helices (Hamada and Goto, 2005). It has also been stated that TFE destabilizes unfolded species and, thereby, indirectly enhances the kinetics and thermodynamics of folding of coiled coils (Kentsis and Sosnick, 1998). Therefore, TFE effect on a polypeptide is a sum of all these effects and capacities, which will be dependent on the specific sequence of the chain.

A subject of discussion is whether TFE attains its effects by direct binding to the polypeptide chain (Jasanoff and Fersht, 1994; Luo and Baldwin, 1997), or by indirect mechanism, over the peptide solvent shell (Cammers-Goodwin *et al*., 1996; Walgers *et al.*, 1998). Gast *et al.* (2001) defend that an indirect mechanism is more probable, and that replacement of water by alcohol molecules is the most important process.

1.3.1.2. Miscibility and concentration effects

Although TFE is miscible with water at any concentration, alcohol molecules form cluster structures (Iwasaki and Fujiyama, 1977; Kuprin *et al.*, 1995). However, the exact nature of these clusters is not easily characterized by experimental techniques.

Gast *et al.* (1999) studied the TFE/water mixture properties by dynamic light scattering. TFE/water mixtures (at 20ºC) behave like ideal solutions, where $(H_2O)_{18}$TFE clathrates are present. Clathrate hydrates are structures in which small non polar

molecules are trapped inside "cages" of hydrogen bonded water molecules. At concentrations higher than 20% TFE a new type of clathrate hydrates $(H_2O)_l(TFE)_m$ (where *l* and *m* are integers) are dispersed. The decrease in light scattering above 50% TFE is explained by the breakdown of the larger clathrate hydrate structures (10 Å) (Gast *et al.*, 1999). Hong *et al.* (1999) have shown by solution X-ray scattering that clusters are formed between 0 and 80% TFE (v/v), being maximal at about 30%. However, no macroscopic phase separation takes place.

In 2000, Reiersen and Rees proposed a cluster model to explain the TFE-induced conformational transitions, in which the clusters size varies according to alcohol concentration (figure 1.2). At low concentrations, these clusters will not be fully developed or stabilized, and can pull the water molecules from the proteins surface. In subsequent steps, the clusters can directly associate with hydrophobic side chains, which will lower their conformational entropy, a key factor for α-helices folding. At higher concentrations, TFE clusters are smaller, but present a higher local intra-cluster TFE concentration (Reiersen and Rees, 2000). NMR studies involving small peptides in TFE provide some support for this thesis (Díaz *et al.*, 2002).

More recently, Yamaguchi *et al.* (2006) described these TFE clusters as micelle-like clusters instead of clathrate hydrates. In these clusters, alcohol molecules associate dynamically via hydrophobic interactions through hydrocarbon groups, although no macroscopic phase separation takes place. The transition phase from a dispersed TFE monomeric state to the clustered state, defined as the alcohol clustering concentration value, is 35% (v/v). These hydrophobic clusters of TFE are much more dynamic than micelles. They can reduce the polarity around protein molecules, strengthening the hydrogen bonds more effectively than dispersed alcohol molecules.

At higher concentrations of alcohol, the micelle-like clusters disappear, resulting in a homogenous solution. Yet, peptides remain in α-helical conformation, because the increased bulk hydrophobicity is enough to stabilize them (Yamaguchi *et al.*, 2006).

The existence of clusters was also confirmed by several molecular dynamics simulations (Fioroni *et al.*, 2000; Chitra and Smith, 2001; Roccatano *et al.*, 2002), and by other techniques, such as FTIR (Scharge *et al.*, 2006, 2007), resonant two photon ionization spectroscopy (Giardini *et al.*, 2007), Raman spectroscopy and simple force field approaches (Scharge *et al.*, 2007).

All the previous theories imply that local concentration of TFE in these clusters is many times larger than the bulk concentration. According to the proposed clathrate hydrates type of clusters, involvement of water molecules in its formation can result in a drastic decrease of water activity in the mixed solvent (Gast *et al.*, 1999). This can justify the special characteristics of TFE as a secondary conformation inducer. Other molecular simulations, along with intermolecular NOE (nuclear overhauser effect) measurements, showed that, in a TFE/water mixture the alcohol aggregates around the peptide and forms a matrix that partly excludes water. This matrix promotes formation of local interactions and, thus, of ordered secondary structure. By displacing water from the surface, TFE removes alternative hydrogen-bonding partners, providing a lower dielectric constant environment, and favouring the formation of intrapeptide hydrogen bonds (Díaz *et al.*, 2002; Roccatano *et al.*, 2002).

Despite those theories, calorimetric and spectroscopic results, obtained in the work of Banerjee and Kishore (2005), suggest that solvent-mediated effects dominate in the TFE-protein interaction, since its binding appeared to be very weak. Some authors defend that the fluoro-alcohols cluster formation cannot be the

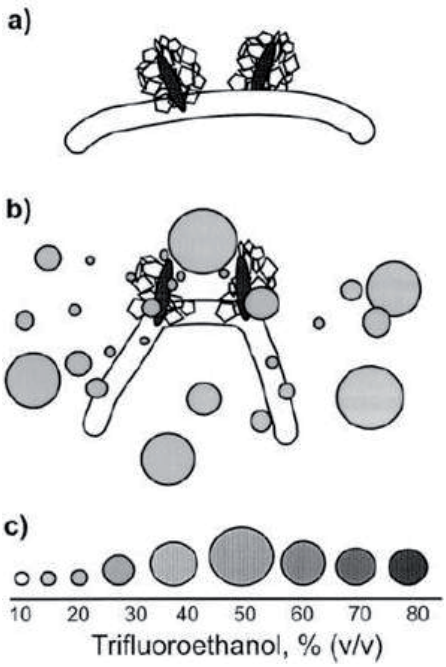

Figure 1.2 – Model for TFE effect on local side chains of a short peptide, and the concentration-dependent cluster size. a) - A peptide backbone with two hydrophobic groups; each group is hydrophobically hydrated with water molecules forming polygons. b) – The same peptide is shown after addition to a TFE/water mixture; the TFE clusters are shaded, and have destroyed the water structure on the side chains, providing a solvent matrix for side-chain-side-chain interactions. c) – Relative cluster size of TFE as a function of concentration; the intra-cluster TFE concentrations are indicated by the grey intensity (light to dark equals low to high). Reproduced from Reiersen and Rees, 2000.

primary cause of the induced structural changes, because these often happen before the critical concentration is reached (Gast *et al.*, 2001). Lately, NOE measurements proved that there are no indications that the aggregation of fluoro-alcohol molecules is necessary for the interactions of TFE with the tested peptides. Rather, these strong and long-lived interactions are primarily the result of the greater hydrogen-bonding ability and hydrophobicity of this solvent (Chatterjee and Gerig, 2007).

Although the existence of clusters can be unnecessary for most of the observed structural changes, the ability to form clusters and the efficiency to induce structural changes are correlated, since both phenomena are based on the same effect: the hydrophobic interactions between halogenated alcohol molecules either with itself or with hydrophobic groups of the polypeptide chain.

On the other hand, some authors claim that the low dielectric constant of this solvent is the main reason that justifies TFE induction of secondary structures and loss of native folding (Buck, 1998; Walgers *et al.*, 1998; Zhao and Liu, 2006; Akitake *et al.*, 2007). Alcohols exhibit lower dielectric constant than water and are much weaker hydrogen bond acceptors, promoting perturbation of the proteins water shell (Walgers *et al.*, 1998), attenuation of intramolecular hydrophobic interactions, strengthening of intraprotein hydrogen bonding, and decreased shield of electrostatic interactions. These types of effects are dependent of the solvent concentration (Akitake *et al.*, 2007).

Javid *et al.* (2007) measured the dielectric permittivity for different water/TFE concentration mixtures, at 25ºC, and described a multiphasic effect of TFE. Dielectric permittivity value decreases from 79.8 (aqueous buffer) to 77 at 10% TFE. According to the authors, this variation can be translated in diminution of intramolecular hydrophobic interactions in the protein. But at higher TFE concentrations

(35%), medium dielectric permittivity drops drastically to 58.8 and, hence, the solvent hydrophilicity decreases markedly. At these TFE concentrations, the attractive as well as the repulsive part of the interaction are enhanced. Protein molecules start to change their conformation and more hydrophobic residues of the protein molecules become exposed to the solvent (Javid *et al.*, 2007).

It is than clear that TFE effects result from the effects superposition of its different intrinsic properties (such as solvent polarity, dielectric constant, length of the carbohydrate chain, number of OH groups, degree of halogenation), which can hardly be adequately separated.

1.4. CARDOSIN A

1.4.1. General characteristics

Cardosin A (EC 3.4.23.-) is an aspartic proteinase (AP) present in large amounts in *Cynara cardunculus flavescens* L.. The pistils of this cardoon have been traditionally used as milk-clotting agent for cheese production in the Iberian Peninsula. Cardoon APs are encoded by a multigene family, which also comprises cardosins B, C, D, E, F, G, H and cyprosins 1, 2 and 3 (Brodelius *et al.*, 1995; Pimentel *et al.*, 2007; Sarmento *et al.,* 2009a).

APs are proteolytic enzymes, generally characterised as having low optimal pH values, and being competitively inhibited by the bacterial peptide pepstatin A. The catalytic centre is formed by two aspartic acid residues (Asp32 and Asp215), with conserved catalytic triads (Asp-Thr-Gly or Asp-Ser-Gly), and has preference for bonds between residues with bulky hydrophobic side chains. APs show high sequence homologies, and their molecular weights are typically in the 35,000 dalton region (Dunn, 2002).

They show bilobated structures, with two similar domains, each one contributing with a catalytic aspartate. The APs most studied families are A1 (pepsin-like family, that includes cardosin A) and A2 (retroviral APs), and belong to the clan AA (Barrett *et al.*, 1998). In the A1 family, different oligomeric structures can be found, despite the high structural homology. Monomeric structures as pepsin and plasmepsin, or heterodimeric, as cathepsin D and phytepsin. Retroviral proteases are smaller and require dimerisation for catalytic function, since each molecule only presents one catalytic residue (Barrett *et al.*, 1998).

This class of proteases has high biological relevance since their members are present in organisms from all kingdoms. They are involved in numerous physiologic processes, such as digestion, intracellular proteolysis and extracellular matrix degradation (Cooper, 2002). Important class members are partly responsible for nowadays major concerning diseases, as renin (in hypertension; Cooper, 2002), β-secretase (in Alzheimer's disease; Stockley and O'Neill, 2008), cathepsin D (in breast cancer; Liaudet-Coopman *et al.*, 2006), and HIV-1 proteinase (in AIDS; Kohl *et al.*, 1988).

1.4.2. Structure

Cardosin A is an heterodimeric protein composed by two polypeptide chains with an apparent molecular weight of 31 and 15 kDa (Veríssimo *et al.*, 1996). It has been the first plant AP to have its three dimensional structure determined (figure 1.3, Frazão *et* al., 1999). Both active site aspartates are located in the heavy chain. Nine sugar rings are distributed over the protein surface in two glycosylation sites, one in each chain (Asn67 and Asn257), away from the active site. These glycosilations may be important for conformational stability and for correct enzyme processing.

Three disulfide bridges are found in the cardosin A mature form, two within the heavy chain and the third within the light chain, at conserved positions. These three covalent bridges do not link the two peptide chains, which are held together by hydrophobic interactions and hydrogen bonds. As representative of the AP family, cardosin A is essentially formed by the duplication of a motif of four anti-parallel β-strands and one helix, which is repeated twice in each domain (Frazão *et al*, 1999).

1.4.3. Active site and catalytic mechanism

Cardosin A is active between pH 2.5 and 7.5 with maximum activity at pH 5 (Veríssimo *et al.*, 1996; Pina *et al.*, 2003). Unlike other APs that show narrower pH activity preferences that restrict them to a specific cellular compartment function, cardosin A could remain active in most cellular environments (Oliveira, 2007).

Its active site cleft is located between the two domains, and accommodates substrate residues in specificity sub-sites S3 to S'3 (Frazão *et al.*, 1999). Catalytic aspartates belong to the well preserved triads Asp32-Thr-Gly and Asp215-Ser-Gly (Barrett *et al.*, 1998).

Over the active site, a loop region with high mobility can be found. This region (Tyr75-Gly-Thr), known as "flap", presents highly conserved sequence among the AP class, and its residues participate in the specificity sub-sites (Frazão *et al.*, 1999). Residues 76 and 77 are known to contribute to the active site hydrogen bonds wire, responsible for substrate alignment and catalysis efficiency (Okoniewska *et al.*, 2000).

The accepted catalytic mechanism for all pepsin-like aspartic proteinases assumes that Asp215 is charged while Asp32 is protonated (Pearl and Blundell, 1984). Adjacent regions to the

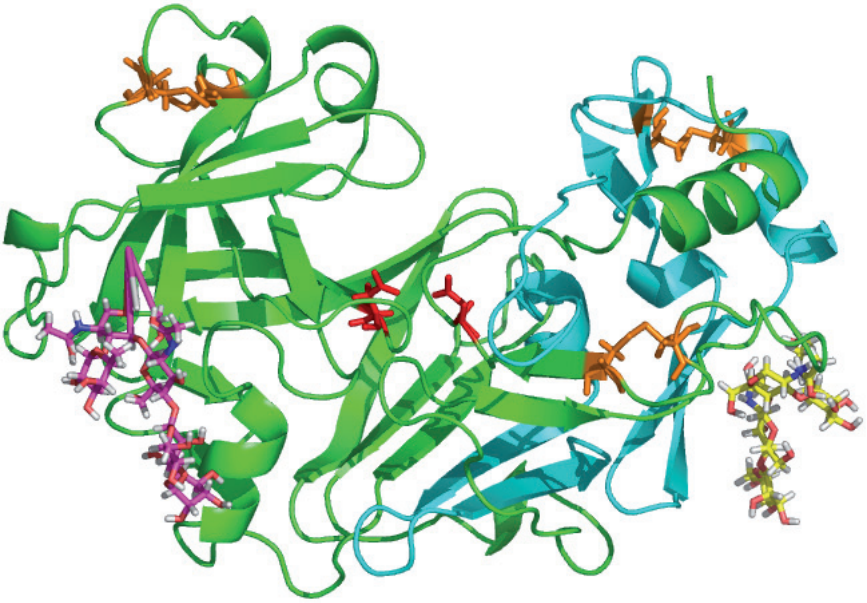

Figure 1.3 – Cardosin A three-dimensional structure representation (PDB 1B5F). Cartoon representation exhibiting large (green) and small (light blue) chains, catalytic aspartates (red), cysteine residues participant in disulfide bridges (orange) and glycosilations represented as sticks (yellow and pink). The representation was created using PyMOL software (DeLano Scientific LLC).

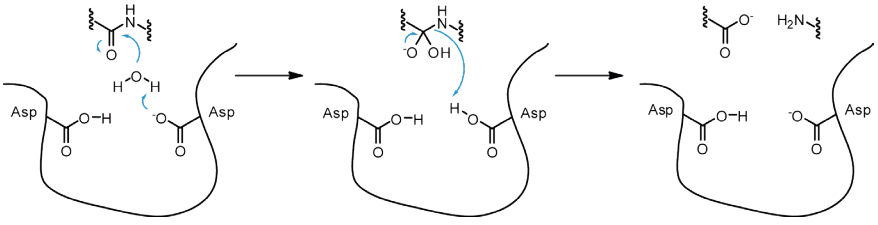

Figure 1.4 - Mechanism of peptide cleavage by aspartic proteases according to Suguna et al., 1987 (image credits: Wikipedia c2).

catalytic centre preserve the charged and protonated states. The water molecule located between the active carboxyls plays the role of nucleophile, becoming deprotonated on substrate binding, in order to initiate the general base catalysis (figure 1.4; Suguna *et al.*, 1987). Another water molecule at the vicinity of the active groups was found to be completely conserved. This second water molecule plays an essential role in the formation of a chain of hydrogen-bonded residues between the active site flap and the active carboxyls on ligand binding (Andreeva and Rumsh, 2001).

The active site aspartates side chains in the crystallised cardosin A were found coplanar, with hydrogen bonds involving main chain and conserved side chain groups. A possible catalytic water molecule is maintained hydrogen-bounded to both aspartate carboxyls (Frazão *et al.*, 1999).

1.4.4. Processing, localization and function

Being synthesised as a preproenzyme with 66 kDa, cardosin A is cotranslationally translocated to the ER, where the signal peptide is excised and the protein becomes glycosylated (Costa *et al.*, 1997), prior to Golgi processing (Duarte *et al.*, 2008a). This precursor form is catalytically inactive towards its natural substrates. Alignment with prophytepsin[4] (PDB[5] 1QDM; Kervinen *et al.*, 1999) suggests that its N-terminal pro-sequence wraps around the enzyme, sterically blocking the active site. But the proform inactivation of cardosin A may not occur in the exact same way (Simões and Faro, 2004). Besides the regulatory function,

[4] Phytepsin (EC 3.4.23.40) is considered to be a plant homologous to mammalian cathepsin D and yeast vacuolar proteinase A. It has very high structural and sequence homologies with cardosin A (1.918 Å RMS, 1.82 E-78 E-value).

[5] Protein Data Bank (PDB) code (Berman et. al., 2000).

the propeptide is important for zymogen folding, stability and intracellular location (Khan and James, 1998).

Cardosin A auto-activates at acidic pH by proteolysis of the activation segment (Khan *et al.*, 1999; Castanheira *et al.*, 2005). Besides the propeptide, most APs of plant origin present a plant-specific insertion (PSI) in their primary structure, a domain of about 100 amino acids that is removed upon activation of the zymogen, yielding the two mature subunits (Simões and Faro, 2004). The PSI sequence has high similarity with mammalian saposins (sphingolipid-activator proteins) (Egas *et al.*, 2000). Several PSI functions have been proposed, such as controlling exit from the endoplasmic reticulum and targeting to the vacuole, vesicle leakage, and a structure–function role (Egas *et al.*, 2000; Törmäkangas *et al.*, 2001; Payie *et al*., 2003; Simões and Faro, 2004).

After glycosylation, cardosin A maturation continues with the cleavage at the N-terminus of the PSI preceding the prosegment removal. The formed 35 kDa intermediate is believed to be the secreted form, and the final step in its processing should occur after sorting from the trans-Golgi, to the vacuolar or secretory pathways (Duarte *et al.*, 2008a). Cardosin A localisation and deposition appears to be organ dependent. Procardosin A form is observed inside protein bodies in embryo cells, and in cell walls in cotyledonary and endosperm cells (Pereira *et al.*, 2008).

As the great majority of plant APs, no definitive biological function has been attributed to cardosin A. Cardosin A presents the binding sequence RGD (Arg176-Gly-Asp) in the surface opposing the active site (Faro *et al.*, 1999). Plant phospholipase Dα was identified as cardosin A binding protein through RGD and KGE (Lys278-Gly-Glu) interaction sequences (Simões *et al.*, 2005). This association has been proposed to facilitate vacuoles disin-

tegration during the dismantling phase of vacuolar-type cell death (Simões e*t al.*, 2005). The accumulation of the enzyme, in mature cardoon flowers, may indicate roles in the senescence of this organ as an effector in programmed cell death, in pollen-pistil interaction through its RGD binding domain, or in an adhesion-mediated proteolytic mechanism associated with pollen recognition and tube growth (Ramalho-Santos *et al.*, 1997, 1998; Faro *et al.*, 1999; Simões and Faro, 2004; Duarte *et al*., 2006). Several functions were proposed for cardosin A in the seed, namely in the membrane reorganisation and lipid transformation (necessary for water uptake, tissue reorganisation, radicle and cotyledon growth), and senescence during seed germination. In addition, their proteolytic activities and/or processing of seed protein reserves should be crucial to embryo nourishing (Pissarra *et al.*, 2007; Pereira *et al.*, 2008).

1.4.5. Biotechnological interest and applications

The research interest in cardosin A started with its purification and characterisation as a protease responsible for milk-clotting capacity of cardoon pistils, traditionally applied in Iberian cheeses production (Veríssimo *et al.*, 1996). Cardosins contribution to the alimentary industry continues to be explored (Barros and Malcata, 2006). Several reasons make cardosin A a very interesting candidate for various kinds of biotechnological experiments.

Cardosin A can be directly purified from fresh biological material using a simple and high yield technique (Sarmento *et al.*, 2004), or it can be synthesised in a recombinant form (Castanheira *et al.*, 2005). Along the last decade cardosin A has been characterised structurally (Frazão *et al.*, 1999) and functionally, in terms of catalytic specificity (Sarmento 2002, 2004), peptidic synthesis

potential (Sarmento *et al.*, 1998, 2004), and activity in non--aqueous media (Sarmento *et al.*, 2003, 2004b, 2006).

The fact of being a two chain enzyme belonging to the important AP class increased interest on stability and unfolding studies. Its functional characterisation in organic media makes of cardosin A a good probe in limited proteolysis studies (Sarmento *et al.*, 2006).

Cardosin A uses a mechanism of collagenolytic activity similar to the mammalian cathepsin K (Duarte *et al.*, 2005). This activity has been used in pre-clinical studies, where the enzyme acts as prevention and reduction agent of peritoneal post-surgical fibrosis and adhesions (Pereira *et al.*, 2005). Another biotechnology practice using cardosin A tissue disaggregation capacity is the isolation of neuronal cells from embryonic rats, with superiors neurite outgrowth and dendritic extension (Duarte *et al.*, 2008b).

Other studies focused on the conformational changes promoted by the presence of denaturing agents, as urea and guanidine hydrochloride (Pereira, 2007), and organic solvents, namely acetonitrile (Pina *et al.*, 2003; Shnyrova *et al.*, 2006; Oliveira *et al.*, 2009; Sarmento *et al.*, 2009b). However, the relationship between cardosin A conformational structure and physiologic function still needs to be clarified. Comprehension of this relation will be essential to elucidate its biochemical and biological role, and to open new biotechnological perspectives.

2. OBJECTIVES

Along the last few years, cardosin A structural conformation has been characterized in biphasic systems, aqueous solutions saturated by organic solvents, and more extensively in the presence of the organic solvent acetonitrile. Following the work developed by our group, the unfolding of cardosin A was here induced by 2,2,2-trifluoroethanol, a polar and protic organic solvent with very different properties from the previous organic solvents tested.

TFE characteristics promote distinct alterations in water structure, interacting in a very particular way with the protein hydration layer and with the protein structure itself. Furthermore, it is known to stabilize well ordered conformations rather than inducing denaturation (Dill *et al.*, 1995), and several authors refer TFE as a mimetic agent for some physiological environments, as membrane proximity (Perham *et al.*, 2006) or polypeptide chain close contact (Torta *et al.*, 2008).

The aim of the present work was to follow the conformational and functional alterations promoted by TFE proximity to cardosin A structure. Different spectroscopic methods (e.g., circular dichroism, intrinsic fluorescence), activity measurements, and calorimetric analysis were employed to detect and characterize the organic solvent induced states. Finally, molecular dynamics/ molecular mechanics simulations were applied to the system in order to understand the interaction between protein and solvent molecules.

The comprehension of this process may give light on the flexibility of the native state structure, and on the structural plasticity of tertiary and secondary structural elements. The understanding of the native conformation as a mutable form may be upgraded for aspartic proteases by the present approach. The relation between proteases structure and function is essential to elucidate the biochemical and biological role of these enzymes, and to open new perspectives for biotechnological application and pharmaceutical purposes.

3. MATERIALS AND METHODS

3.1. CHEMICALS

Fresh flowers from *Cynara cardunculus* L. *flavescens* were collected in Ansião (Coimbra, Portugal) in July of 2000 and 2007. Pistils were harvested and frozen at -20ºC until enzyme purification.

Acetonitrile (HPLC grade) was purchased from *Romil*. 2,2,2-Trifluoroethanol (TFE) was purchased from *Merck* (Darmstadt, Germany). All other chemicals were of analytical grade and were obtained from *Sigma* or *Amresco*.

3.2. ENZYME PURIFICATION

Cardosin A was purified according to Veríssimo *et al.*, 1996 with minor alterations (Sarmento *et al.*, 2004). Briefly, frozen pistils

were disrupted with a mortar in 100 mM sodium citrate, pH 3.5. After being centrifuged at 14,000 rpm for 10 minutes, the supernatant was filtered. The sample was injected in a *HiLoad 26/60 Superdex™ 75 preparation grade* gel filtration column, equilibrated in 25 mM Tris/HCl pH 7.6 at room temperature, and coupled to an *ÄKTA Basic 10* (*GE Healthcare*). The fraction containing cardosins was collected and applied to an *anion exchange HiPrep 16/10 QFF*, Q Sepharose. Elution of cardosin A was achieved by a gradient of NaCl. After desalted (*HiPrep 26/10 Desalting*), the enzyme was lyophilized, and stored at -20ºC or used immediately. Cardosin A purity was assessed by SDS-PAGE (Laemmli, 1970).

3.3. PROTEIN CONCENTRATION DETERMINATION

Protein concentration was determined by the *BCA protein assay* (*Pierce*) according to the manufacturer's instructions. Alternatively, protein concentration was determined spectrophotometrically at 280 nm, using an extinction coefficient of 43.8×10^3 M/cm and considering 42 kDa as cardosin A molecular weight (Veríssimo, 1996).

3.4. ACTIVITY DETERMINATION

3.4.1. Discontinuous assay

The synthetic peptide Lys-Pro-Ala-Glu-Phe-Phe(NO_2)-Ala-Leu was used as cardosin A substrate as described before (Veríssimo *et al.*, 1996). Hydrolysis occurs between the two phenylalanine residues, and the rate of hydrolysis was followed by HPLC to avoid results distortions by the OS (Sarmento *et al*., 2009b).

Cardosin A was incubated at 25ºC for 1 hour, in 0.2 M sodium

chloride, 50 mM sodium acetate, pH 4.7, with the adequate concentration of TFE. Enzyme concentration was typically 0.0292 mg/ml. The reaction started by adding an aliquot of this enzyme solution (146 ng) to 0.3 ml of the same buffer with 4% DMSO, and 0.063 mg of the substrate (1:19,000, enzyme:substrate molar ratio). At 5, 10, 20 and 30 minutes an aliquot (0.06 ml) was removed and reactions stopped by adding 0.54 ml TFA (1,5% v/v). Samples were centrifuged and injected by an *autosampler A-900* into a C_{18} column (*Teknokroma*) coupled to an *ÄKTA Basic 10* (*Amersham Biosciences, GE Healthcare*). The elution was carried out by an acetonitrile gradient (30 - 100% v/v) acidified with 0.1% TFA. Detection was made continuously at 257 nm.

Data handling

A calibration curve was built for correlation of the product peak area with product concentration.

At least 3 replicates of each condition were analysed and substrate hydrolysis velocities calculated (mol/min).

3.4.2. Continuous assay

Alternatively, rates of hydrolysis were followed by fluorimetry (Simões *et al.* 2007) using the synthetic peptide (MCA-Lys)Lys-Pro-Ala-Glu-Phe-Phe-Ala-Leu(Lys-DNP) (*Genosphere Biotechnologies*).

In order to validate the method for the presence of TFE, some controls were run. The deviations of the peptide emission spectra and maximum intensity emission wavelengths were followed for the different percentages of TFE used. The fluorescence intensity at the emission wavelength (393 nm) was followed for substrate (intact peptide) and products (completely digested peptide), at different substrate and TFE concentrations. The variations

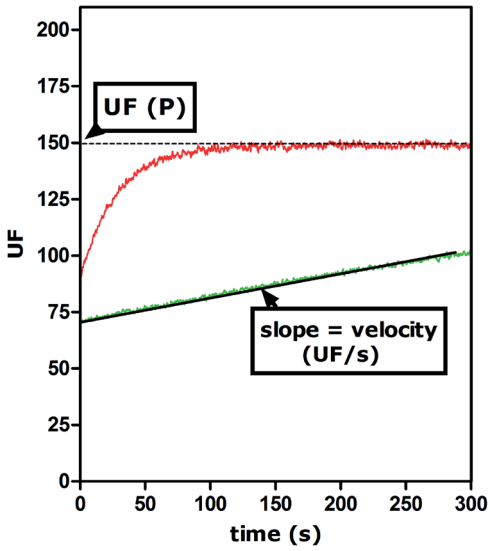

$$activity = \frac{slope \times m(S)}{[UF(P) - UF(S)] \times m(E)} \quad (3.1)$$

Figure 3.1 – Typical digestion spectra. The curve represented in red corresponds to a complete digestion of the substrate; in green it can be found a typical digestion time course.

detected by the presence of TFE were not significant.

In order to determine cardosin A activity typically assay was carried out as follows: cardosin A was incubated at 0.0292 mg/ml, at 25º C, for 1 hour, in 0.2 M sodium chloride 50 mM sodium acetate pH 4.7, with the adequate concentration of TFE. Reaction started by adding the peptide (450 ng/ml) to the enzyme (15 ng/ml) solution (1:800, enzyme:substrate molar ratio). Digestion rate was followed in a *Perkin Elmer LS50B luminescence* spectrometer, with the sample excitation wavelength at 328 nm and emission recorded at 393 nm.

Data handling

All spectra were corrected for background signal; the rate of hydrolysis (*slope*, in UF/s) was determined for each reaction, averaged with least 3 replicates; the maximum fluorescence

emission (*UF(P)*, see figure 3.1), produced for the complete digestion of the peptide, was determined for each percentage of TFE tested, as well as the minimal one [for the intact substrate, *UF(S)*]. The specific activity, in ng/s/mg E, was calculated according to equation 3.1 (where *m* stands for mass and E for enzyme).

3.4.2.1. Reactivation studies

After incubated in the presence of TFE (1 hour at 25ºC, as described in section 3.4.2.), cardosin A was diluted (100 fold) in aqueous buffer (1 h at 25 ºC) and assayed for activity (section 3.4.2).

3.5. HYDRODYNAMIC STUDIES

Proteins can be separated based on their hydrodynamic volume by size exclusion chromatography (SEC). This technique is based on the existence of a good correlation between the retention time in a gel filtration column, and the Stokes radius of the protein molecule (Uversky, 1993). Cardosin A volume variation promoted by the presence of TFE in the media was followed by SEC (Oliveira, 2007).

Cardosin A (1.54 mg/ml) in 10 mM sodium phosphate buffer, pH 5, with the required TFE concentration, was incubated for 1 hour at 25ºC. The protein (1.5 mg) was injected in a *Superdex 75 HR 10/30 FPLC column* coupled to an *ÄKTA Basic 10* (*GE Healthcare*) previously equilibrated in the same buffer, and eluted at a flow rate of 1 ml/min. The elution was monitored at 280 nm, and at least 3 replicates were run per condition. A *Gel Filtration LMW Calibration Kit* (*GE Healthcare*) was used according to the manufacturer's instructions, and blue dextran (2,000 kDa) elution

volume was used in order to determine the column void volume.

Data handling

The apparent molecular weight was calculated according to manufacturer's instructions, using the standard curve plotted of log(MW) versus K_{av}; this parameter was calculated according to equation 3.2, where V_e is the elution volume, V_0 is the void volume determined by the elution of blue dextran, and V_g is the geometric column volume (Whitaker, 1963).

$$K_{av} = \frac{V_e - V_0}{V_g - V_0} \tag{3.2}$$

3.6. INTRINSIC FLUORESCENCE

Optical spectroscopy provides standard techniques for measuring the conformational stability of proteins, and for following the kinetics of unfolding and refolding reactions. Practically all unfolding and refolding reactions can be followed by changes in absorbance, fluorescence, or optical activity (usually measured by CD). Proteins fluorescence spectra derives from the aromatic amino acids (Trp, Tyr and Phe), but, at 295 nm, it is usually dominated by the contribution of tryptophan residues. During protein unfolding, Trp fluorescence wavelength shifts and intensity changes can be followed (Schmid, 2005).

Cardosin A intrinsic fluorescence was measured in a *Jasco FP-777 Spectrofluorometer* (*Jasco Co.*), in the laboratory of Professors Adelaide Almeida and Angela Cunha, from the Department of Biology of the Centre for Environmental and Marine Studies, in the University of Aveiro, Portugal. Protein samples at 0.2 mg/ml in 10 mM sodium phosphate buffer, pH 5, with different concentrations of TFE, were incubated at 25ºC for 1 hour.

After being centrifuged, protein in solution was quantified by spectrometry (section 3.3). The excitation wavelength was set at 295 nm, in order to avoid the emission contribution of other residues than tryptophan, and emission spectra were recorded from 275 to 400 nm. All measurements were performed with a 5 nm bandwidth for both the excitation and emission monochromators.

N – Acetyl – L – tryptophanamide (NATA) was used as control and measured in the same conditions described for cardosin A. At least 3 replicates were measured per condition.

Data handling

All spectra were corrected for background signal and for protein concentration; emission fluorescence intensity variation was followed at the wavelength where it showed to vary the most through the different conditions tested (326 nm); the maximum emission wavelength was calculated as the average between the wavelengths in which the emission intensity was 80% of the major one (Pina *et al.*, 2003); $\Delta\lambda_{max}$ stands for the difference between the maximum emission wavelength for the condition, subtracted by the correspondent maximum emission wavelength for NATA ($\Delta\lambda_{max} = \lambda_{max(sample)} - \lambda_{max(NATA)}$).

3.6.1. Tertiary structure reversibility

In order to assess to the reversibility of the alterations induced by TFE, another set of experiments were run. After incubation in the presence TFE, 1 hour at 25ºC (as described in section 3.6.), cardosin A was diluted (100 fold) in aqueous buffer, (1 h at 25 ºC) and intrinsic fluorescence was measured as described previously (section 3.6).

3.7. CIRCULAR DICHROISM SPECTROSCOPY

The different types of regular secondary structure found in proteins give rise to characteristic circular dichroism (CD) spectra in the far-UV (van Holde *et al.*, 2006). This technique was used for examining the structure of cardosin A in the different conditions tested, and was performed in the laboratory of Professor Rui Brito, from the Department of Chemistry of the Center for Neurosciences and Cell Biology, in the University of Coimbra, Portugal.

Far-UV CD measurements were carried out in a *DMS20 Olis® CD Module* (*On-Line Instrument Systems, Inc.*) in a 1 mm path-length cell, in the range of 190 to 260 nm, and under constant nitrogen flow at 25ºC. Protein samples (0.25 – 0.27 mg/ml) in 10mM sodium phosphate buffer, pH 5, with different concentrations of TFE, were incubated for 1 hour at 25ºC. Afterwards, samples were centrifuged and protein concentration was determined spectrofotometrically as described before (section 3.3.).

Data handling

Each scan was subtracted to the correspondent baseline; the molar ellipticity ($[\Theta]_{MRW}$) was calculated using equation 3.3 (Schmid, 2005), where θ_{obs} stands for the ellipticity (degrees) measured at the wavelength, *Mr* is the protein molecular mass (Da), *C* is the protein concentration (mg/ml), *l* is the optical path-length of the cell (cm), and N_A is the number of amino acids of the protein; the ellipticity values at 222 nm were analysed in order to follow the variation of the protein α-helical content (Kelly *et al.* 2005); secondary structure percentage calculation was done using *CONTIN* software (Provencher, 1982) and comparing with a 43 soluble proteins database.

$$[\Theta]_{MRW} = \frac{\theta_{obs} \times 100 \times Mr}{C \times l \times N_A} \qquad (3.3)$$

Far-ultraviolet circular dichroism spectroscopy was also run upon different time incubations. Cardosin A samples in 5% TFE in 10 mM sodium phosphate buffer, pH 5, were incubated for various times from 20 minutes to 114.5 hours at 25ºC, before being prepared for the CD scan, as explained in the previous section.

3.8. DIFFERENTIAL SCANNING CALORIMETRY

Differential scanning calorimetry (DSC) is an experimental technique to directly measure the heat energy uptake that takes place in a sample during controlled variation of temperature. It is very useful for studying the thermodynamics of unfolding transitions of proteins (Cooper, 2004).

The calorimetric experiments were performed on a high-sensitivity *MicroCal VP-DSC calorimeter* (*MicroCal Inc.*, Northampton, MA), in the laboratory of Professor Alan Cooper, from the WestChem Department of Chemistry, in the University of Glasgow, Scotland, UK. All solutions were degassed by stirring under vacuum prior to being carefully loaded into the calorimeter cells. A scanning rate of 60ºC/h was used, and protein (0.55 mg/ml in 10 mM sodium citrate buffer, pH 5, with different concentrations of TFE) was incubated for 1 or 24 hours at 25ºC.

Data handling

Calorimetric data were converted to excess heat capacity by subtracting the instrumental baseline, normalizing for molar concentration, and subtracting the sample baseline. Data were analyzed by non-linear regression statistical fitting using the non-two-state folding/unfolding model (*Origin* software, supplied by *MicroCal*). The following variables were calculated: thermal transition temperature (T_m), the temperature at which, in an ideal dynamic reversible two-state equilibrium, any molecule spends

50% of its time folded and 50% unfolded; calorimetric enthalpy (ΔH_{cal}), determined by the area under the transition peak; and van't Hoff enthalpy (ΔH_{vH}), determined by the shape of the curve. Transition reversibility was tested by promoting a new transition after the first one (by reheating the sample after cooling it down).

3.9. MOLECULAR DYNAMICS SIMULATIONS

3.9.1. System setup

These experiments were run by Doctor Nuno Micaêlo (Molecular Modelling and Simulation Group, Minho University, Braga, Portugal). The general simulation methodology applied in the MD/MM simulations of cardosin A in TFE was similar to the one done by Micaêlo and Soares (2007). The cardosin A X-ray structure with PDB ID: 1B5F was used (Frazão *et al.*, 1999), and the protonated state of tritable residues was estimated accordingly to their protonation state at pH 7. Three systems were prepared, a fully hydrated cardosin A, a 90% and a 10% (weight of water / weight of protein) hydrated cardosin A in TFE. Sodium ions were added until full system neutrality was reached. The system was built in dodecahedral box with a minimum distance between the protein and box wall of 0.8 nm, and solvated with an equilibrated configuration of water or organic solvent molecules at 298 K.

3.9.2. Molecular dynamics simulations

MD/MM simulations were performed with the GROMACS package (Hess *et al.*, 2008) using the GROMOS 53a6 force-field (Oostenbrink *et al.*, 2004). Bond lengths of the solute and TFE molecules were constrained with lincs (Hess *et al.*, 1997), and those of water with

settle (Miyamoto and Kollman, 1992). Non-bonded interactions were calculated using a twinrange method (van Gunsteren and Berendsen, 1990) with short-range and long-range cut-offs of 8 Å and 14 Å, respectively. The SPC water model (Hermans *et al.*, 1984) was used in aqueous and in non-aqueous simulations. A reaction field correction for electrostatic interactions (Barker and Watts, 1973; Tironi *et al.*, 1995) was applied, taking a dielectric of 54 for the fully hydrated system with SPC water (Smith and van Gunsteren, 1994). For the TFE system, the dielectric constant was 18. The simulations were started in the canonical ensemble with initial velocities from a Maxwell–Boltzmmann distribution at 300 K, and run for 100 ps with position restraints applied to all heavy atoms of the protein (force constant of 10^6 kJ•mol^{-1}/nm^{-2}) and a temperature coupling constant of 0.01 ps, allowing the equilibration of the organic solvent and water molecules. A second step of 100 ps was done with restraints only applied to the α-C carbons of the enzyme and a temperature-coupling constant of 0.1 ps. The unrestrained simulations were done in the isothermal–isobaric ensemble with an integration time step of 2 femtoseconds. The protein, organic solvent, and water and ions, were coupled to three separated heat baths (Berendsen *et al.*, 1984) with temperature coupling constants of 0.1 ps and a reference temperature of 298 K. The pressure control (Berendsen *et al.*, 1984) was implemented with a reference pressure of 1 atm and relaxation times of 0.5 ps and 1.0 ps, for water or TFE / water solvent simulations, respectively. The aqueous simulation was simulated for 10 ns and the organic solvents system for 100 ns.

4. THE TFE-INDUCED UNFOLDING OF CARDOSIN A: RESULTS AND DISCUSSION

4.1. STRUCTURAL CHARACTERISATION

The lyophilised native protein was diluted in several solutions with different TFE contents. To visualize this event, one can imagine the solvent molecules penetrating the space between the protein molecules, separating them, and contacting with the protein hydration layers that survived to the lyophilisation procedure. During this process the protein recovers its mobility, and the proper native folding. The protein hydration shell is recreated, considering that the freeze-drying process did not promote considerable aggregation, inactivity or permanent unfolding of the protein. The presence of the organic solvent (OS) in the solution will produce new and different effects in this solubilisation process. The TFE molecules will possibly compete with water in this contact layer, promoting new interactions with

protein groups, and/or between them. This new interactions may promote small and local changes, but also big conformational changes in the protein. It is the aim of this section to follow and to characterise these alterations.

4.1.1. Tertiary structure

An easy way to follow conformational changes is by using the intrinsic fluorescence of the protein. Cardosin A intrinsic fluorescence was measured in the laboratory of Professors Adelaide Almeida and Angela Cunha, from the Department of Biology of the Centre for Environmental and Marine Studies, in the University of Aveiro, Portugal. The five tryptophans present in cardosin A responded to an excitation beam of UV light with the proper wavelength (λ_{exc}), and gave rise to a characteristic emission of fluorescence, with a meaningful maximum wavelength (λ_{max}). The other aromatic amino acids (tyrosine and phenylalanine) are also fluorescence emitting residues, but their contribution to the global spectra is usually masked by the tryptophan emission. Moreover, the samples were analysed with an λ_{exc} of 295 nm, where only tryptophan residues absorb. This amino acid changes its λ_{max} and intensity according to environmental factors as solvent polarity, pH, and the presence or absence of quenchers, making this technique perfect to follow unfolding processes (Daughdrill *et al.*, 2005). The λ_{max} is the most straightforward interpretation parameter to follow molecular environment changes. In contrast, fluorescence intensity values variation is less informative in terms of solvent exposure of fluorophoric groups, for it may either increase or decrease upon protein unfolding (Schmid, 1990, 2005).

Cardosin A is represented in the figure 4.1, with the tryptophan

residues highlighted in yellow, and from those only Trp299 is present in the small chain. All exhibit low temperature factor (B) values (see discussion below), and only Trp154 seems to be partially at the protein surface, while all the others present very low or null relative solvent accessible surface area values (table 4.1).

Fresh lyophilised cardosin A samples were sequentially solubilised in the presence of increasing amounts of TFE, and incubated for 1 hour at 25ºC before being analysed in the fluorimeter. Along with the protein samples, a free modified tryptophan control (N–acetyl–L–tryptophanamide, or NATA) was scanned in order to minimize the direct effects of solvent polarity and viscosity on the tryptophan emission analysis. It can be seen that the λ_{max} for NATA decreases steadily with increasing TFE content (see figure 4.2 inset), which validates the sample results, proving the fluorescence alterations to occur only by OS effect over the protein structure.

Following the difference between the maximum wavelength value for each condition and the correspondent maximum wavelength for NATA ($\Delta\lambda_{max}$), along the increasing TFE concentrations tested (figure 4.2), a clear transition can be observed from 20 to 30% TFE. The cardosin A λ_{max} suffered a red shift to higher values, consequence of a change in tryptophan residues exposition. The λ_{max} values became closer to the free tryptophan ones, and the $\Delta\lambda_{max}$ decreased. This transition is interpreted as a protein tertiary structure unfolding promoted by the OS, where any/some tryptophan residue(s) become exposed to a more polar environment. Before this transition, there was no significant variation in the $\Delta\lambda_{max}$ of the sample, and for higher TFE concentrations these values were gradually reduced. But even at 90% TFE, the highest concentration tested, the tryptophan residues did not show a complete exposition to the solvent.

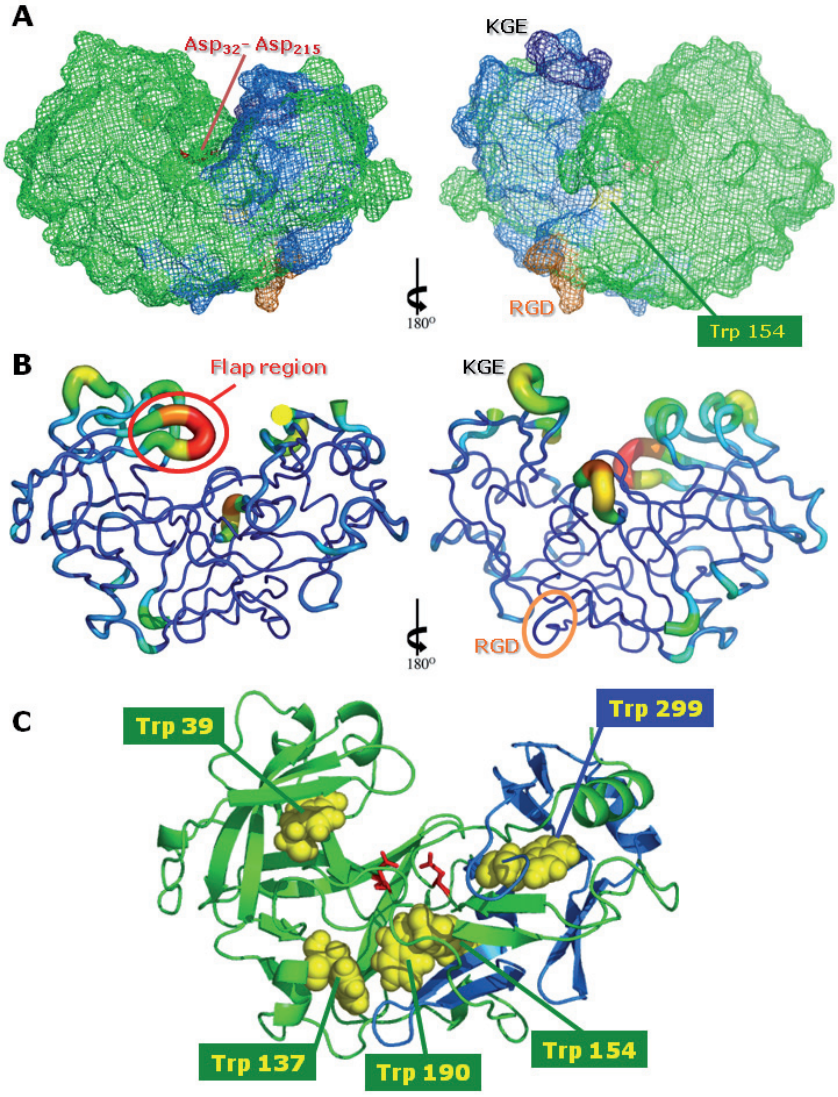

Figure 4.1 – Cardosin A three-dimensional structure representations (PDB 1B5F). A – Front and back scheme of the protein structure, with the large (green) and small (light blue) chains, the catalytic aspartates (red), the tryptophans (yellow), the KGE (Lys278-Gly-Glu) (dark blue) and the RGD (Arg176-Gly-Asp) (orange) domains represented. B – Front and back representations of cardosin A according to the B values: warmer colours and thicker cartoon segments represent residues with higher mobility. The protein is represented with the exact same rotation as in A. C – Cartoon representation of cardosin A with numbered tryptophans (same corresponding colours as in A). The representations were created using PyMOL software (DeLano Scientific LLC).

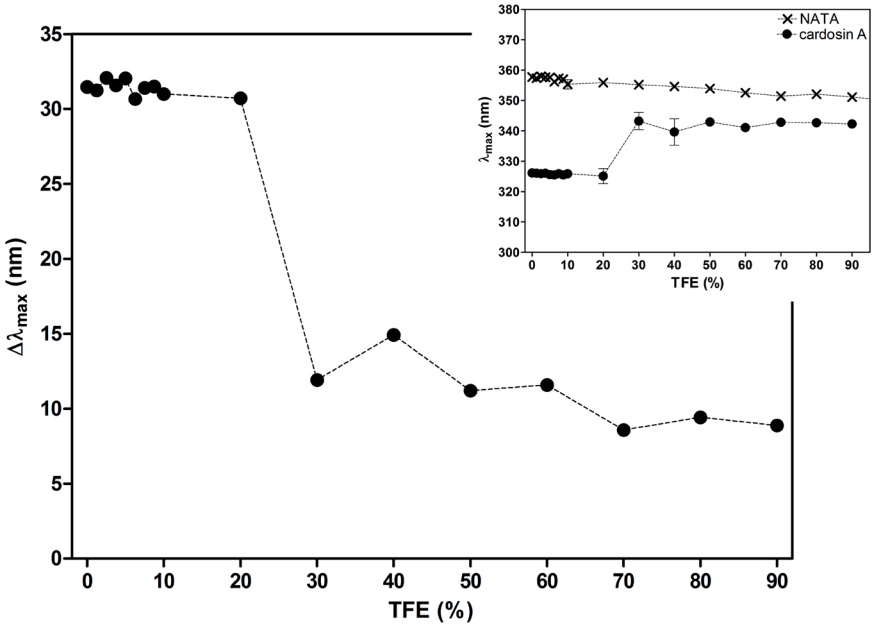

Figure 4.2 – TFE effect over cardosin A intrinsic fluorescence. Oscillation of the emission maximum wavelength variation ($\Delta\lambda_{max}$), which corresponds to the sample emission maximum wavelength ($\lambda_{max\ (sample)}$) subtracted by the corresponding value for NATA ($\lambda_{max(NATA)}$), promoted by the presence of TFE. Protein (at 0.2 mg/ml) and NATA samples, in 10mM sodium phosphate buffer, pH5, with different amounts of TFE, were incubated for 1 hour at 25ºC, before running the spectra (see section 3.6). Each point corresponds to a minimum of 3 replicates. The inset presents the original wavelengths variation.

TFE is typically expected to disrupt the native tertiary structure of proteins. The present results reflect this effect, with the clear opening of cardosin A tertiary structure. This transition occurred at the same TFE concentration described for the maximum X-ray scattering of the TFE/water mixture (Hong *et al.*, 1999), interpreted by Reiersen and Rees (2000) as the concentration where TFE clathrates start to significantly enlarge. In the micelle-like cluster theories, 35% TFE is the lower concentration from which the alcohol molecules start to cluster (Yamaguchi *et al.*, 2006). It should be noticed that no macroscopic phase separation was observed under our experimental conditions.

At lower concentrations (where clusters, if present, would be smaller in size and less stable), TFE molecules could compete with the hydration layer ones, but this interaction would not be strong enough to attack the tertiary structure of cardosin A. TFE exhibits lower dielectric constant than water, and is a much weaker hydrogen bond acceptor (section 7, table 7.1). Increasing in concentration, alcohol molecules could have bound directly to the protein, disturbing protein water shell, increasing local hydrophobicity, and decreasing intramolecular hydrophobic interactions, leading to tertiary structure unfolding (Buck, 1998; Corrêa and Farah, 2007; Javid *et al.*, 2007). These effects may be magnified by local high concentrations, sustained by clusters. Placing the dried enzyme in 90% TFE seemed to promote an unfold similar to the observed for TFE concentrations higher than 30%. Despite the disappearing of clusters at higher alcohol concentrations, the increased bulk hydrophobicity is enough to stabilize the not completely unfolded tertiary structure (Yamaguchi *et al.*, 2006).

Cardosin A disulphide bonds (two in the large chain and one in the small) may hold up the total unfolding of the molecule. The comparison between the various tryptophans and their exposure

Table 4.1 - Cardosin A tryptophans. Relative solvent accessible surface area values calculated (in %) for cardosin A tryptophan residues, based on the native PBD structure, using *ASAView* and *GETAREA 1.1* application servers (Ahmad *et al.*, 2004, and Fraczkiewicz and Braun, 1998, respectively). Residues secondary structure localization and a carbon temperature factor (B) according to the crystal structure (Frazão *et al.*, 1999). Distance to disulfide bonds calculated using *PyMOL* software (DeLano *Scientific LLC*). Numbers in brackets quantify distances between elements in different chains.

	Relative Solvent Accessible Surface Area (%)				
	Trp39	Trp137	Trp154	Trp190	Trp299
ASAView	0.0	0.8	6.2	0.4	0.0
GETAREA 1.1	0.2	0.8	8.0	0.5	0.0
Secondary structure	β-sheet	α-helix	β-sheet	loop	loop
α-carbon B value (Å^2)	20.79	19.18	18.74	18.00	16.53
	Distance to Disulfide Bonds (Å)				
C_{45} – C_{50}	11.77	24.73	30.08	28.82	(31.32)
C_{206} – C_{210}	32.49	29.57	25.66	16.17	(7.45)
C_{249} – C_{282}	(34.51)	(37.14)	(23.28)	(30.40)	23.50
	Primary structure proximity (number of amino acids)				
C_{45} – C_{50}	6	87	104	140	-
C_{206} – C_{210}	167	69	52	16	-
C_{249} – C_{282}	-	-	-	-	17

probabilities is done in table 4.1, using relative solvent accessible surface area values, secondary structure in which the residue is involved, distance values from the disulfide bonds in the quaternary and primary structures, and residue α-carbon B values. The temperature factor or B value (atomic displacement parameter) in protein crystal structures reflects the fluctuation of an atom about its average position. Therefore, its distribution along the protein sequence is an important indicator of the protein structure, reflecting its flexibility and dynamics (figure 4.1 – B). A large B value indicates high mobility of individual atoms and side chains (Yuan *et al.*, 2005). The presented tryptophan B values are pretty close to each other, and low when compared, for instance, to Gly76 (B: 124.76) or Thr77 (B: 133.34)[1]. Comparing among them, the Trp39 has the higher mobility, in spite of its interaction in a β-sheet structure, and its relative proximity to a disulfide bridge. Trp154, the most natively exposed, is also in a β-sheet structure and is one of the most distant to the two disulfide bridges in its chain. Trp137 belongs to an α-helix, and it is probable to continue interacting in this structure, since TFE is known to protect and induce helical configurations. The tryptophans number 190 and 299 are in more mobile structures (loops), despite of their low B values. Trp190 is closer to a disulfide bridge and to a beta structure, while Trp299 is pretty far from its chain disulfide bridge, and has additional distance from any secondary structure. Thus, cardosin A tryptophan residues incomplete exposition would have been expected.

In the same way, cardosin A did not undergo complete unfolding when submitted to denaturing environments promoted by urea or guanidine hydrochloride (Pereira, 2007), nor upon thermal denaturation (Pina *et al.*, 2003). In all these studies, and also

[1] These are two of the most mobile residues of the cardosin A structure, located in the highly conserved flap region, that projects out over the active site cleft and interacts with the protein substrate.

in the presence of acetonitrile (Oliveira, 2009), the tryptophans were more effectively exposed than in TFE.

To sum up, under the presence of TFE, cardosin A tertiary structure showed to be partially unfolded (from 20 to 30%), but the tryptophans exposition was not complete, not even for the highest TFE concentration tested.

4.1.2. Secondary structure

The tertiary structure loss may have occurred with changes in the secondary one. The far-UV circular dichroism is the perfect technique to follow these alterations (Kelly and Price, 2000). This technique was performed in the laboratory of Professor Rui Brito, from the Department of Chemistry of the Center for Neurosciences and Cell Biology, in the University of Coimbra, Portugal. CD results for cardosin A in the presence of TFE can be observed in figure 4.3. In this UV range (170 - 250 nm), the peptide backbones chirality (in the amidic bond) is employed to analyze the secondary elements present in the protein sample.

Cardosin A is a characteristic representative of the AP family, essentially formed by the duplication of a motif of four anti-parallel β-strands and one helix, which is repeated twice in each domain. The crystallographic analysis showed a structure composed of 45.3% of β-strands and 13.5% of helical motifs (table 4.2; Frazão *et al.*, 1999). In the far-UV spectra, β proteins show weaker and more dissimilar spectra compared to helical proteins. The shape of the CD spectrum of a β protein depends, among other factors, on the length and orientation of the strands, and on the twist of the sheet, but most spectra show a positive ellipticity (θ) between 190 and 200 nm (Schmid, 2005). The aqueous cardosin A spectrum fits under this description, with negative ellipticity

values from 210 to 240 nm, a minimum at 217 nm, and a single maximum at 196 nm (figure 4.3 – A; Pina *et al.*, 2003; Shnyrova *et al.*, 2006).

Mixtures with increasing amounts of TFE were used to solubilise fresh lyophilised cardosin A samples. After an incubation of 1 hour at 25ºC, samples were run in the spectropolarimeter (section 3.7). Incubations during lower and higher periods (from 20 minutes to 24 hours) were run in the presence of 5% TFE, but did not show considerable variation in ellipticity (section 4.2, figure 4.15).

The far-UV profile changed progressively. At 20% TFE the θ values became closer to the origin, indicating loss in protein stability (Kelly *et al.*, 2005). Moreover, the profile maximum and minima changed, corresponding to a change in the structural elements proportion. Increasing TFE concentrations remarkably increased the helicity content of the sample, resulting in a typical α-helical profile for 60% TFE and beyond, with a maximum at 192 nm, and minima at 209 and 221 nm (figure 4.3 – A). It was therefore confirmed that TFE induces α-helical conformations, even in proteins consisting predominantly of β-sheets.

This TFE effect is usually justified by two types of action. The hydrogen bonds between the alcohol-rich medium and the protein would become weaker, making the hydrogen bonds within the polypeptide chain comparatively stronger. This would weaken the hydrophobic interactions within protein chains, resulting in destabilization of their folded state (Thomas and Dill, 1993). Additionally, the decreased polarity of the medium could be relieved by transition of the secondary structure into α-helices, that have less polar groups exposed to the solvent. In this way polar peptide groups would become less available for hydration, and non-polar groups would remain on the surface of

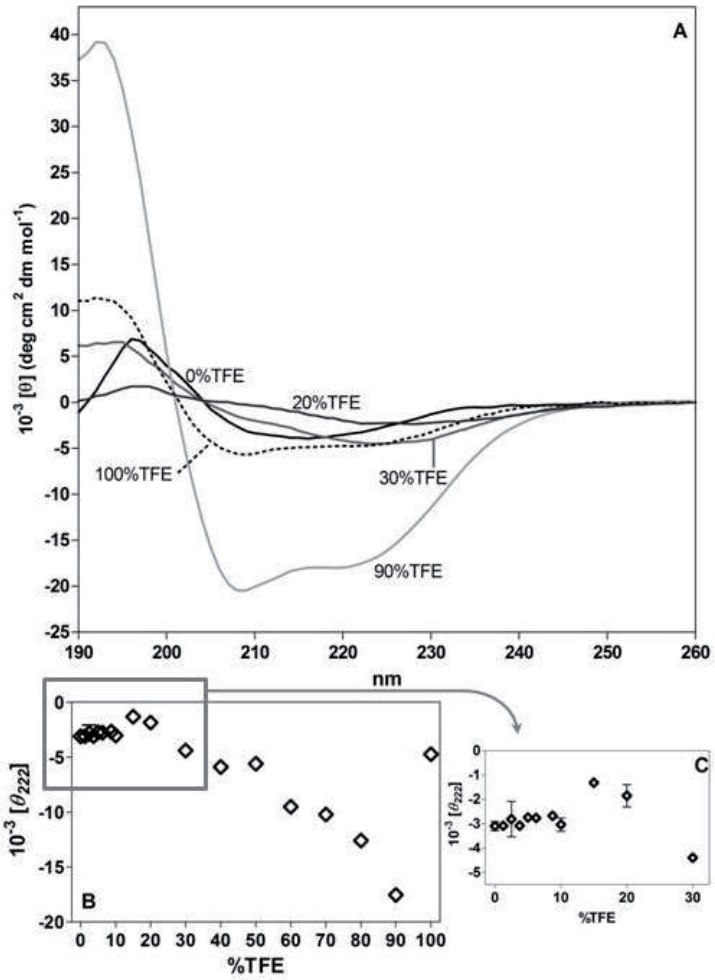

Figure 4.3 – TFE effect over cardosin A CD spectra. Cardosin A was incubated for 1 hour at 25ºC, in the absence and in the presence of increasing TFE concentrations. A - selected far-UV CD spectra. B - ellipticity values at 222 nm for all tested TFE concentrations. C - θ_{222} for the lower TFE percentages. Each spectrum was produced by solubilisation of a new sample in a medium with the mentioned concentration (section 3.7). In A and B, each point corresponds to a minimum of 3 replicates.

the helix (Fatima *et al.*, 2006). Thus, the progressive addition of TFE destroyed the native structure of cardosin A and induced the formation of α-helices.

The various resulting spectra were compared using the value for 222 nm ellipticity (θ_{222}) (figure 4.3 – B and C). The polypeptide chain θ_{222} is considered as an index of its secondary structures content. This wavelength is also a characteristic minimum for helical structures (along with another minimum at 208 nm, and a maximum at 195 nm). In proteins with helices and sheets, is common for the helical contributions to dominate the CD spectrum (Kelly and Price, 2000). For these reasons 222 nm was the chosen wavelength to follow the ellipticity of our system.

At lower TFE concentrations, the θ_{222} values did not significantly vary, but beyond 10% TFE, the values slowly came near the origin (figure 4.3 – B and C). Observing the spectra for 20% TFE the loss of structure is clear. Solubilising the enzyme in 30% TFE increased its secondary elements content to values higher than for 20% TFE and water. Nevertheless, the spectrum presented a reasonably different profile than the native one, with a new minimum at 223 nm. This new minimum decreased its θ values along with TFE enhancement in the medium content until 90% TFE, where the spectrum presented a typical α-helical profile.

Several studies approached the TFE effect over protein conformation. The analysis of several types of proteins, with different secondary structures in TFE, using θ_{222} variations, was done by Goto and co-workers (Shiraki *et al.*, 1995). They found a good correlation between the α-helical content of proteins in the presence of TFE, and their predicted propensities to form α-helix based on the amino acid sequence. In the obtained transition curves two phases could be told. After the initial transition, proteins with a relatively low propensity for α-helices showed

Table 4.2 – Comparison between cardosin A relative secondary structure content (PDB 1B5F) and predicted values. *PSIPred* (Jones, 1999; McGuffin *et al.*, 2000) is a secondary protein structure predictor algorithm. It is based on the submitted primary sequence and uses neural networks. *AGADIR* is an algorithm that predicts the helical content of peptides (Muñoz and Serrano, 1997, 1994a, b).

	Chain	β-sheet	α-helix	other	total
PDB	Large	78	21	146	239
		32.6%	8.8%	59.6%	
	Small	30	10	47	87
		34.5 %	11.5 %	54.0 %	
PSIPred	Large	50.6 %	8.4 %	47.7 %	
	Small	50.6 %	8.0 %	41.4 %	
AGADIR	Large		36 %		
	Small		40 %		

a low helical content, which gradually increased in the second stage with further increases in TFE. This post transitional helical content increase was less obvious for proteins with intrinsic high propensity for α-helices, in which the helical content was already high after the first transition. Cardosin A helical propensity is relatively low, as shown in table 4.2. Besides the crystallographic data, the results from protein secondary structure predictors and from a helical content predictor are presented. The method of Muñoz and Serrano for helix prediction (*AGADIR*) considers short range interactions, and conditions such as pH, temperature and ionic strength are used in the calculation (Muñoz and Serrano, 1994a, b, 1997). It suggested a higher helicity than the observed cardosin A helical content. The results obtained for cardosin A in TFE seem to confirm the previous idea: placing cardosin A in the non-helical tendency group, only in a second phase the α-helical

content increase is noticeable. However, Wu and co-workers studied another β-sheet protein, snake venom cardiotoxin (60 residues), and defended that the TFE-induced structural transition is governed by protein stability, rather than by the intrinsic α-helix formation propensity (Chiang *et al.*, 1996).

The figure 4.4 graph was built using *CONTIN* software for estimating protein secondary structure fractions from CD spectra (Provencher, 1982). The predicted proportion calculated for the native aqueous cardosin A (11% of α-helices to 63% of β-sheets) was considered close to the crystallographic calculated proportion (13.5% of helical motifs to 45.3% of β-strands). From the native aqueous environment till 10% TFE, the θ_{222} values, together with the $\Delta\lambda_{max}$ ones (figure 4.2), did not present significant variations. Meanwhile a subtle decrease in the helical and β-sheet content was noticed. This structure loss tendency was maintained up to 20% TFE, along with an increase in θ_{222} values. But from 20 to 30% TFE, another transition occurred, with a strong decrease in the $\Delta\lambda_{max}$ values, a decrease in the ellipticity, on with an increase in the helical content. From then on, the helical content of the protein increased in a remarkable extent, transforming a native 13.5% α-helical structure in a 63% one. The major contribution of residues to take part in these newly α structures seem to come from previously unordered ones, despite of the noticed increase in the tryptophans exposition to polar environments.

The final TFE concentration tested was approximately 100%. The results for cardosin A in this medium showed not to follow the tendency of the remaining samples tested. Instead of a high helical content, the 99.9% sample protein presented a spectrum closer to the origin than the previous ones, and a less negative θ_{222} value, similar as the registered for the 30 – 40% TFE range. The predicted secondary structure contents also exhibited a soft

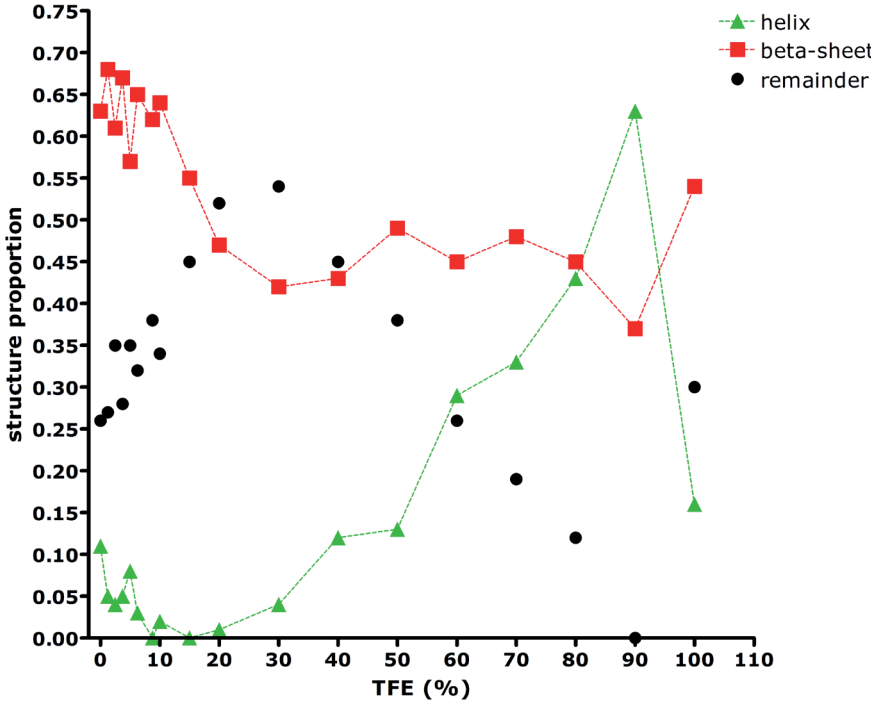

Figure 4.4 – Secondary structure calculation from the far-UV CD spectra of cardosin A, in different concentrations of TFE, using *CONTIN* software (Provencher, 1982).

structural alteration when compared to other high TFE concentrations. When the dried protein is submerged in a solution where only TFE molecules are in interaction with each other, the solvent competition proposed for the water/OS media would only happen in the remaining structural water molecules. The cardosin molecule was probably trapped in a more rigid conformation (Klibanov, 2001), not suffering such an extensive unfolding as in other high TFE concentrations.

In order to better compare the structural modifications followed by CD and fluorescence techniques, the figure 4.5 graph was built. The major structural distortion modifications were considered to occur in the presence of 90% TFE. The tryptophans exposition showed an abrupt transition for lower TFE levels, comparing to a slow and progressive increase in the secondary structure content read by far-UV CD. At 30% TFE, for instance, the tryptophans exposition was already 87% of the final exposition, while only 8% of the total newly formed secondary structure was built.

NMR studies showed that the secondary structures formed in the TFE state are mobile and rapidly converted to the extended configurations (Hamada and Goto, 2005). This fact, along with small-angle solution X-ray scattering results, lead the TFE state to be considered an "open helical configuration", in which the α-helical rods are exposed to the solvent because of the absence of strong hydrophobic attraction between them (Hamada and Goto, 2005). This kind of structure may explain the obtained results, where high helical content was observed with large solvent exposition, with non-overlapping transitions.

Traditionally it was accepted that TFE would help the polypeptide chain to express its local and intrinsic conformational preference (Buck, 1998). But, as cardosin A, predominantly β-sheet proteins, such as β-lactoglobulin (162 residues; Hamada *et al.*, 2000; Gast

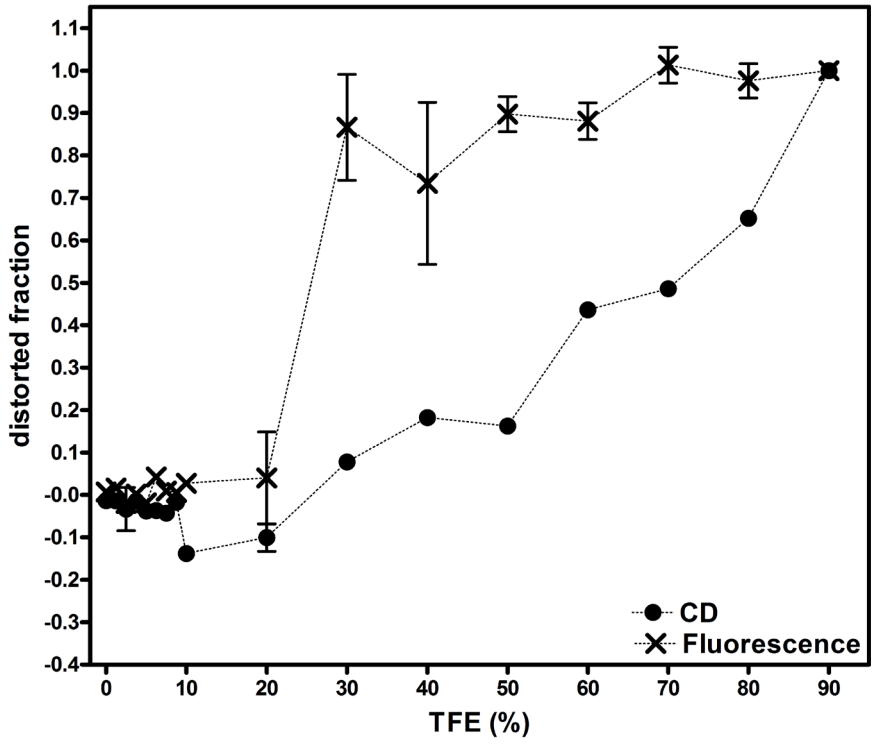

Figure 4.5 – Changes in structural properties of cardosin A upon exposure to growing concentrations of TFE for 1 hour at 25ºC, as detected by CD and fluorescence.

et al., 2001), concanavalin A (237 residues; Jackson and Mantsch, 1992), cardiotoxins (60 residues; Chiang *et al*., 1996; Lo *et al*., 1998), monellin (94 residues; Fan *et al.*, 1993), and cellular retinoic acid binding protein (Liu *et al.*, 1994), among others, have shown to exhibit high helical tendency in TFE. The induced partially folded states have lost the specific side-chain interactions, being largely stabilized by local backbone interactions. Based on these observations, some authors defend that the folding mechanism of some β-proteins might be explained by a non-hierarchical model in which the transient formation of a helical structure preceded the native β-sheet structure (Shiraki *et al.*, 1995). The formation of such structures might be less effective in terms of rapid folding since the structure would need to be disrupted at a later stage of folding. Probably the formation of these non-native α-helical segments would be useful for preventing intermolecular aggregation, since the polypeptide chain would become relatively compact (Hamada and Goto, 2005).

Contrary to this, for another β-sheet protein, tendamistat (a specifically mammalian alpha-amylases inhibitor with 74 amino acid residues long), a native-like β-structure was observed in the partially folded state induced by a high concentration of TFE. Far UV-CD results presented a clear increase in the helical content upon TFE addition, while amide hydrogen exchange and FTIR measurements proved that most of the native β-sheets were still intact. The α-helical induction appeared to be located mainly in regions corresponding to loops or random structure in the native state. So, although the shape of the CD spectrum is dominated by a small amount of helical structure, β-sheets contribute significantly to the CD spectrum of the tendamistat TFE state (Schönbrunner *et al.*, 1996). As cardosin A, tendamistat also has a low intrinsic helix-forming propensity. Also the aspartic protease apparently presents the TFE induced helical portions formed from

native non-structured elements of the protein. Similar effect was observed in studies over peptide fragments of the α-spectrin SH3 domain (62 residues), where non-native α-helical structure could be induced by addition of TFE in unordered regions of the native state, but not in β-strand or β-turn regions (Viguera *et al.*, 1996). So we should not exclude the hypothesis of a similar situation occurring for cardosin A. The obtained high helical content results would not translate an exchanging from β strands to α-helices. Instead, unordered segments would get their helicity increased, masking the maintained β-sheet structures dichroic contribution.

Moreover, studies on β-lactoglobulin (162 residues) and α-chymotrypsin (141 residues), both predominantly β-sheet proteins, under high TFE content medium showed that the non-native α-helical structure is unstable and converts readily to an intermolecular anti-parallel β-sheet aggregate. This transition was a gradual and time dependent process, and apparently independent on the protein concentration. Aggregates with a large content of intermolecular β-sheet seemed to be the thermodynamically favoured states for these β-sheet proteins in the presence of high concentrations of TFE (Dong *et al.*, 1998). This tendency for aggregation was not observed in cardosin A results, though it could be happening.

4.1.3. Hydrodynamic behaviour

Many properties can be used to monitor folding-unfolding equilibrium, including the large volume changes associated with it. Although intrinsic viscosity remains the most theoretically straightforward method for determining such volume changes, gel filtration techniques offer an alternative approach (Corbett and Roche, 1984; Oliveira, 2007). Size exclusion chromatog-

raphy (SEC) can be applied to the study of protein unfolding, since it is able to resolve changes in the hydrodynamic properties along the denaturation pathway. Besides it can detect the presence of intermediate states, provided they are kinetically stable within the time scale of the chromatographic run (Reyes *et al.*, 2003).

SEC was the technique used to follow cardosin A volume changes in the presence of TFE. The protein was maintained for 1 hour in the incubation buffer (10 mM sodium phosphate buffer, pH 5) with the TFE percentage to test, and applied to a gel filtration FPLC column equilibrated with the same buffer (section 3.5). The SEC elution profiles and the correspondent apparent volume variation are presented in figure 4.6.

Increasing the content in TFE produced a slight increase in the protein *Ve* (elution volume), with a bigger shift around 10%. The cardosin A apparent Stokes radius decreased, which by definition means a decrease in the radius of a hard sphere that diffuses at the same rate as the molecule, whose behaviour includes hydration and shape effects. Among these TFE concentrations, the apparent MW was slowly reduced in 9,7 kDa (apparent $MW_{10\%TFE}$=24.1 kDa). This decrease in the apparent molecular weight was not followed by alterations in the tryptophans exposition, nor in the far-UV CD results.

This behaviour may describe loss in hydration layer molecules, given that they should be accounted in the hydrodynamic data analysis (Koenig *et al.*, 1975). At this low TFE percentage, TFE cluster formation is not found to be reported in the literature. This attack to the protein hydration layer would happen with no direct effect over the protein structure. Nevertheless, a competition between water and solvent molecules would happen, resulting in the observed decrease of the protein hydrodynamic volume.

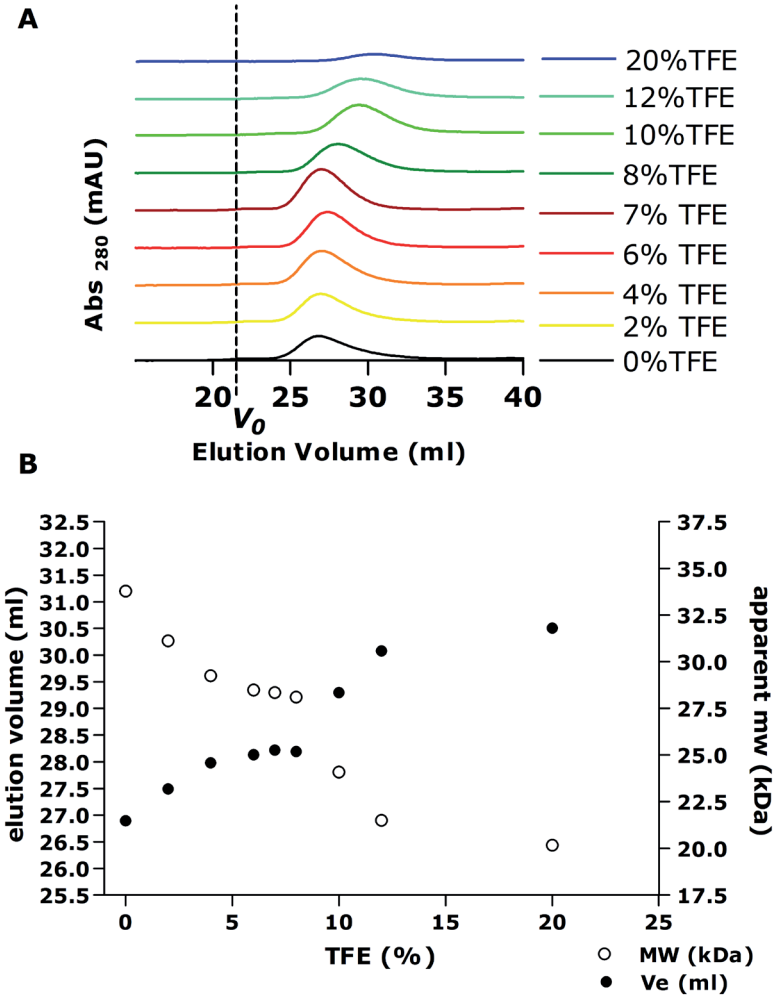

Figure 4.6 - TFE effect over cardosin A hydrodynamic volume. A - SEC elution profiles of cardosin A at different TFE concentrations: from bottom to top TFE concentrations are 0, 2, 4, 6, 7, 8, 10, 12 and 20%; V0 indicates the column void volume. B - Elution volumes (*Ve*) and estimated molecular weight values of cardosin A as a function of TFE concentration. Each point corresponds to a minimum of 3 replicates (section 3.5).

For TFE percentages of 12 and higher the protein elution peaks became to have weaker definition, and from 20% on the protein became attached to the column matrix, promoting an unfeasible elution. Besides, the same adherence may justify the elution described for lower TFE concentrations. The *Superdex* matrix is produced by covalently bonded dextran to highly cross-linked porous agarose beds, where the dextran is the principal responsible for the separation properties. The manufacturers declare it can be used in the presence of polar organic solvents, like 20% acetonitrile, with no damage to the medium. To our knowledge, the only reported remark in the literature that relates dextran with TFE describes that, when put together in a solution, turbidity is produced, and from this observation it was suggested the formation of a complex between these two chemicals (Naseem and Khan, 2004). If the TFE present in the media would associate itself with the matrix, this would decrease the interaction of the protein with the column, which would decrease the *Ve* of the protein, whereas the opposite was observed.

The unfolding of cardosin A from 10 to 20% TFE, followed by fluorescence and far-UV CD, would expect an increase in the apparent MW of the protein. As an example, TFE molecules penetrated the β-rich protein β-lactoglobulin matrix (162 residues), and magnetic relaxation dispersion data were consistent with a strong accumulation of TFE at the surface as well as in the interior of the protein (Halle *et al.*, 2005). TFE transformations from native, to intermediate, and to helical structures, are characterised as being accompanied by a progressive expansion of the protein and loss of specific long-lived hydration sites (Gast *et al.*, 2001). Molten globule states and kinetic molten globule states also present higher Stokes radii than the native conformation (Gast *et al.*, 1998).

Supposing the imperfect elution in the gel filtration column, where samples were not separated according to molecular weight and volume, the presence of the OS would be responsible for increasing the interaction between the protein and the matrix. This would happen in such a way that the elution started to be delayed, and lately becoming not possible. In fact, the column was effectively clean by 0.5 M NaOH application, which denotes a non-specific or hydrophobic interaction of the protein to the polymer, and the elution ended out to be impossible for percentages of TFE higher than 20%.

This approach was also performed for cardosin A in the presence of another OS, acetonitrile (Oliveira, 2007). The results also showed a decrease in the apparent molecular weight of 28 kDa from 0 to 50% acetonitrile, but they were characterised as incongruent.

Some conclusions might be made regarding this technique. From aqueous to 10% TFE media, the protein may have lost some of its hydration layer thickness. This occurrence would characterise the first step in the TFE attack to the protein structure, while no other changes were observed in the secondary and tertiary conformations. But these conclusions are not certain due to doubt on data reliability.

4.1.4. Thermal stability

There are many different ways in which the changes in conformation of a macromolecule can be observed experimentally. Some of these methods, such as the calorimetric techniques, give thermodynamic information directly. A thermodynamic study characterises the structure and the behaviour of biological systems, and it is ruled by the interplay between thermal motion of molecules and the various interaction forces between them (Cooper, 2004). Differential

scanning calorimetry (DSC) is the method of choice to study the conformational stability of biological molecules. The calorimetric experiments were performed in the laboratory of Professor Alan Cooper, from the WestChem Department of Chemistry, in the University of Glasgow, Scotland, UK. Through this technique the heat capacity of the sample is calculated, and using this numeric value the enthalpy is obtained. At constant temperature, the enthalpy describes the heat effects promoted by reactions like folding/unfolding (Makhatadze, 2005).

The normalized thermograms for cardosin A incubated with increasing percentages of TFE are presented in figure 4.7 - A (for details, see section 3.8). Each thermogram shows a sharp and single endothermic peak, nearly but not quite symmetric: the changes in the heat capacity (C_p) look slightly more gradual at lower temperatures and more abrupt at higher temperatures. This asymmetry tends to be enhanced with the increase in TFE concentration. For percentages higher than 5%, the post transition profile appears to be typical of an exothermic reaction, as occurs during aggregation. The thermal transition scans showed to be nearly independent of incubation time.

Aggregation of protein alcohol-induced states during thermal denaturation has also been reported earlier for concanavalin A (237 residues; Jackson and Mantsch, 1992) and hen egg white lysozyme (129 residues; Bhakuni, 1998), to give some examples. For cardosin A in the presence of 15 and 20% TFE, no transition was observed in the temperature range (0 to 100ºC), only an exothermic fall in the thermogram. Hence, at 25ºC, the temperature at which all the other experiments were run, the protein would already present some kind of open structure for TFE percentages as 15 and 20% (higher TFE concentrations were not tested). These subtle open conformations did not

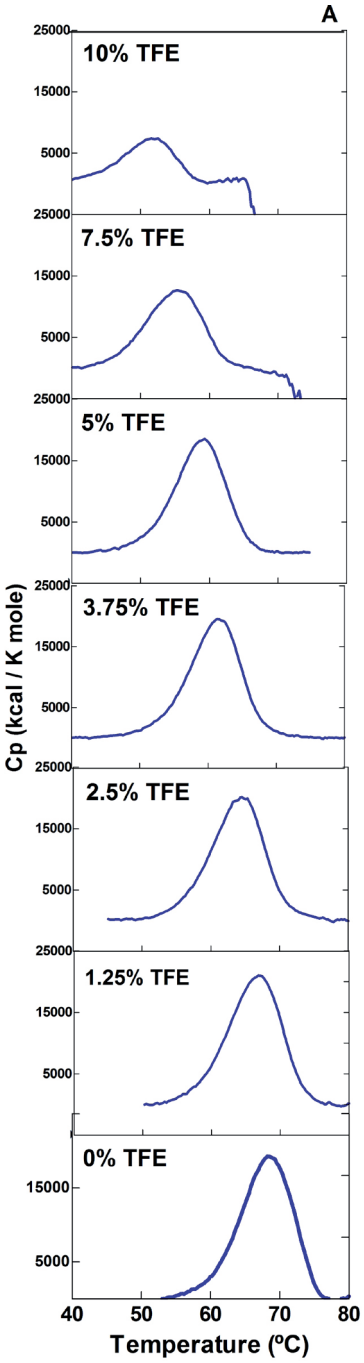

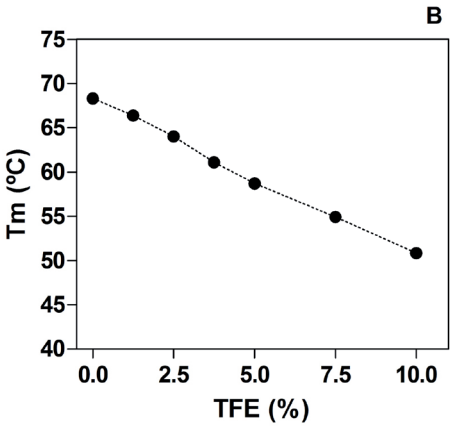

C

%TFE	$\Delta H_{cal}/\Delta H_{vH}$
0	2
1.25	2
2.5	2
3.5	2
5	2

Figure 4.7 – DSC thermograms of cardosin A in the presence of different concentrations of TFE, upon 24h incubation at 25ºC. A - Experimental data obtained after subtraction of instrumental baseline, concentration normalization, and sample baseline, for different percentages of TFE. B – Thermal transition temperature values variation according to TFE content; each point corresponds to a minimum of 3 replicates. C - Table C presents the $\Delta H_{cal}/\Delta H_{vH}$ ratio values for the different TFE percentages (see section 3.8). C_p – excess heat capacity; T_m - thermal transition temperature.

present enough structure damage to be observed through the remaining used techniques. The TFE presence in the polypeptide chain proximity promoted the aggregation capacity. This may resolve the previously questioned hypothesis from the hydrodynamic results, confirming the protein hydration volume decrease.

The thermal transition temperature values (T_m) decreased with the raise in the OS content (figure 4.7 - B), denoting a clear weakening of the protein structure. It was not expected any improvement on the thermal-stability of cardosin A, since water is not only a reactant in nearly all thermal degradative reactions, but also a facilitator in protein mobility leading to thermo-unfolding and aggregation of enzymes. Irrespective of the type of alcohol or protein studied, a clear decreasing trend of T_m, with increasing alcohol concentration, has been observed (Bhakuni, 1998).

None of the tested and presented transitions was reversible. This is in agreement with previous studies over cardosin A, during pH variation (Pina *et al.*, 2003), and in the presence of 10% acetonitrile (Shnyrova *et al.*, 2006), in which the thermal transitions also showed to be irreversible. Even in the absence of aggregation, thermal unfolding is rarely completely reversible, since exposure of the unfolded polypeptide to higher temperatures can lead to improper refolding, aggregation, improper disulfide bond formation, proline isomerization, de-amidation, hydrolysis of peptide bonds at aspartic acid residues, or other chemical changes that give rise to mis-folded forms (Lepock *et al.*, 1992). Heating the samples using different scan rates (30, 60 and 90ºC/h) promoted a T_m medium variation of approximately 1ºC. These variations, as well as the ones promoted by varying protein concentration, are usually accounted for kinetic

irreversible processes occurring during the transition (such as aggregation or chemical degradation at higher temperatures). The system was not in equilibrium, as it was proved by the transitions irreversibility, the scan rate dependence, and the post-transitional aggregation. Therefore, a correct thermodynamic description on the protein stability was unfeasible (Privalov, 1979).

The cooperative index H_{cal} /ΔH_{vH} for each transition is present in figure 4.7 - C. In a simple two-state denaturation process, carried out under equilibrium conditions, ΔH_{cal} should be equal to ΔH_{vH}. But, if the denaturation involves the formation of a relatively long-lived intermediate structure, the resulting DSC curve will be a convolution of the heat capacities and enthalpies of all relevant forms of the protein, ending in a broader peak. This would create a higher cooperative index, as happens in the present case (Sturtevant, 1987). Distortion of the thermograms, due to irreversible phenomena, disabled the cooperative index calculation for percentages of TFE higher than 5%, since the enthalpy changes would be unreliable. However, the present results comparison cannot be made with much confidence in the absence of supporting evidence from other methods, since factors as aggregation and others (incorrect baseline correction, wrong estimation of protein concentration) can affect the shape of the transition (Cooper *et al.*, 2000).

To sum up, TFE induced a decrease on cardosin A thermal stability, and also in the denatured protein solubility. The loss of the hydration layer integrity could be one of the justifications for this behaviour. Small amounts of the OS disrupted and/or weakened the effects responsible for maintaining the natively ordered state of the protein, without provoking measurable unfolding.

4.1.5. Structural analysis conclusions

While in small quantities in the medium, TFE may have gently attacked cardosin A hydration layer, as suggested by the protein hydrodynamic volume results and supported by the DSC ones. Meanwhile no other changes were observed in the secondary and tertiary conformations, but clearly its rising presence was decreasing the structural stability of the enzyme. Further increasing the OS content promoted a clear tertiary structural transition from 20 to 30% TFE, with tryptophan residues being exposed to the solvent. At the same time, some secondary structure alterations were observed, beginning with an increase in the protein helical content, and progressively creating new helical structures in this predominantly β-sheet protein. The presented results suggest that these new α-helical structures were formed from previously unordered segments, but also from some β-sheet ordered forms, implying partial destruction of the native secondary conformation. These new α–helical forms may be claimed as open structures, in which the tryptophan residues are maintained in contact with the solvent, though not completely exposed.

4.2. FUNCTIONAL CHARACTERISATION

All the structural alterations observed must have an effect over the active site cleft and neighbouring conformation, reflecting changes in the enzyme function. In fact, enzyme activity evaluation is fairly expedited in recognizing slight conformational perturbations in the active site and other structural elements implicated in catalysis. For this reason enzymatic activity variations usually occur prior to global protein unfolding. Peptidolytic activity assays were run on cardosin A in the presence of increasing percentages of TFE.

The presence of the OS disables the use of a common absorbance substrate cleavage reading, since it deforms the relation between the absorbance and the substrate quantity in a non linear way. The chosen method to follow cardosin A activity in TFE was developed to overcome this problem (Sarmento, 2002), and uses the Lys-Pro-Ala-Glu-Phe-Phe(NO_2)-Ala-Leu peptide as substrate. It is cleaved by cardosin A at one peptide bond (Phe-Phe(NO_2)) (an essential requisite for kinetic studies), and the product formation is quantified by HPLC. This same method had already been used to study cardosin A activity under other unfolding conditions such as temperature, pH (Pina *et al.*, 2003), use of denaturants, as urea and guanidine hydrochloride (Pereira, 2007), and other organic solvents (Oliveira, 2007; Sarmento *et al.*, 2004b, 2008). At pH 5 and 25ºC, after one hour of enzyme incubation in the presence of the OS, the reaction started by adding substrate. Samples were collected at different times (5, 10, 20 and 30 minutes), the reactions were stopped, and the product formation was quantified using a C_{18} column (section 3.4.1). In this way, the OS present during the hydrolysis could not interfere in the results analysis, since its quantity was extremely depleted.

The hypothesis of TFE increasing the peptide secondary structure was refuted by far-UV CD (figure 4.8). The peptide aqueous secondary conformation proved to be clearly unordered, with weak signal after 210 nm, and a pronounced minimum between 195 and 200 nm. Within the TFE range in which cardosin A presented activity (see below), there was a progressive loss in the peptide secondary structure content, responsible for the decrease in the absolute ellipticity values for 195 and 222 nm. It is thus concluded that any activity variation would not be owed to peptide availability alterations.

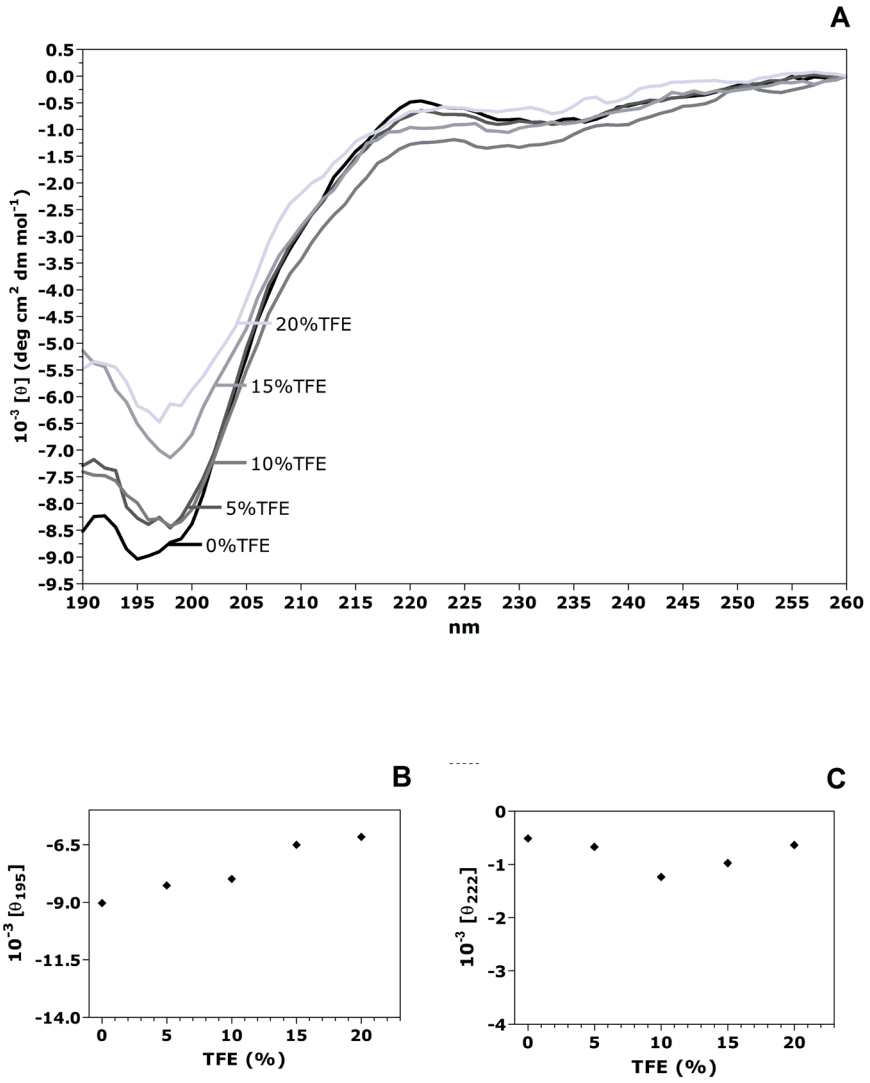

Figure 4.8 - Circular dichroism results for Lys-Pro-Ala-Glu-Phe-Phe(NO_2)-Ala-Leu peptide, in the absence and in the presence of increasing TFE concentrations. A - Far-UV CD spectra. B - ellipticity values at 195 nm. C – ellipticity values at 222 nm. The peptide was incubated at 0.80 – 1.40 mg/ml for 1 hour at 25ºC, and read in a cuvette with a 0.2 mm path length.

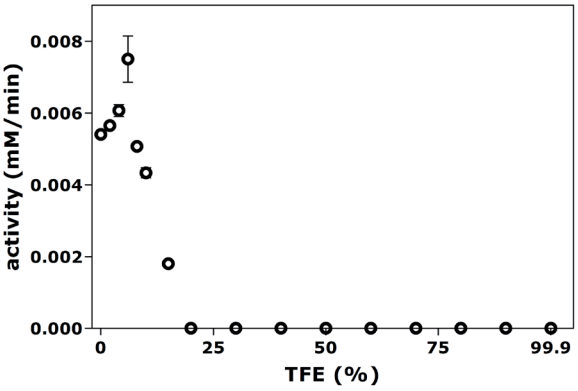

Figure 4.9 – Cardosin A peptidolytic activity in the presence of TFE, analysed by HPLC. Each point corresponds to a minimum of 3 replicates (section 3.4.1).

Figure 4.9 presents the peptidolytic activity of cardosin A for increasing TFE content in the media. Some would expect the catalytic activity to be higher in aqueous medium, where the enzyme is in its native conformation (Ulijn *et al.*, 2002). But for low OS concentrations the enzyme was not inhibited. Instead, an increase in cardosin A activity was observed until 6% TFE. The maintenance of catalytic activity indicates retention of the native conformation of the active site. The hypothetical enzyme hydration layer attack took by TFE (proposed by thermostability and hydrodynamic results), could be responsible for enhancing the enzyme flexibility and consequently increasing the activity (Halling, 2004). By increasing the mobility of the flap and active site regions, the accessibility for the substrate would be increased and its interaction enhanced. The decrease in the hydration shell thickness could also provide a similar effect, since the contact between substrate and enzyme would occur closer.

The electrostatic forces between the reacting species depend on

the solvents dielectric constant, and their degree of solvation is known to affect rate constants (Levine, 1995). As examples, off all the steps in hexokinase turnover, glucose binding is the step with the major conformational change and most affected by solvation (hexokinase is a glucokinase (transferase); Rand *et al.*, 1993). For glutaminyl-tRNA synthetase (glutamine-tRNA ligase), the active site preorganisation and its slow solvation dynamics were recognised as important factors for molecular recognition and enzyme specificity (Guha *et al.*, 2005). The electrostatic stabilisation promoted by the lysozyme cleft over the substrate molecule has been described to be reinforced in a low dielectric constant medium, enhancing 3×10^6 fold its rate (lysozyme is an O-glycosyl hydrolase; Price and Stevens, 1999).

The increase in the medium TFE content could promote a decrease in the substrate solvation. This would increase the activity values, since less driving force would be necessary for association with the enzyme (Gupta and Roy, 2004). Nonetheless, this alteration could also be reflected in a more difficult conformational change to the transition state, thus providing a decrease in the velocity of catalysis instead of the observed increase (Wangikar *et al.*, 1995). For a proper discussion on this subject a more profound understanding of cardosin A machinery is required. The access of the substrate to the active site may be facilitated, or the conformational alterations may have stabilised the transition intermediate state, or still the resulting products may be released rapidly.

This increased activity for low TFE percentages was also observed in other proteins, as bovine carbonic anhydase II (carbonate dehydratase; Wei *et al.*, 2006), ervatamin C (cysteine protease; Sundd *et al*., 2004), horseradish peroxidase (Zhou *et al*., 2002) and calf intestinal alkaline phosphatase (Zhang *et al*., 2000).

The initial activity raise was followed by a linear decrease, which progressively led to the loss of protein activity when at 20% TFE. This was the expected behaviour, since OS are often reported to decrease rates of enzyme-catalyzed reactions (Klibanov, 1997). The functionality of an enzyme should be maximal at an optimum level of water, beyond which the enzyme performance is declined due to the loss in enzyme stability (Rezaei *et al.*, 2007). This activity loss occurs before any detectable structural alteration.

From these 20% TFE on, the tryptophans exposition was also observed (figure 4.2), as well as the major loss of cardosin A secondary structures (figures 4.3 and 4.4). These facts point to severe disarrangements in the protein integrity with subsequent functional loss. Increasing the media TFE content would provide an effective attack to the protein hydration layer. Being clustered, the TFE molecules get their unfolding capacity enhance, destroying the H-bonds between the protein and the water molecules, destabilizing intramolecular hydrophobic interactions, but also strengthening or inducing the formation of local backbone hydrogen bonds (Hamada and Goto, 2005). So the structure would become looser, disabling the formation of an effective enzyme-substrate complex.

Another important condition to provide an active performance is the presence of water in the microenvironment of the catalytic cleft. TFE lowers the dielectric constant of the medium, which modifies the stabilization of the overall structure and reduce the residues motion. This decrease can also directly affect catalytic activity by disturbing the active site hydration. Moreover, water is one of the reactants in hydrolysis, and as a result its presence is of vital importance to the reaction kinetics. Besides the water molecule located between the active carboxyls, which plays the role of nucleophile during catalytic reaction, another

water molecule is essential to form a chain of hydrogen-bonded residues between the active site flap and the active carboxyls on ligand binding (Pearl and Blundell, 1984; Andreeva and Rumsh, 2001). The progressive substitution of water for TFE molecules could reach a value upon which the presence of these catalytic essential water molecules would be compromised. Competitive inhibition has also been hypothesised (Valivety *et al.*, 1994), as observed for subtilisin in acetonitrile (serine protease; Schmitke *et al.*, 1998).

There is no question that enzymes can function in the absence of bulk water. They frequently show sufficient catalytic activity and unique selectivity, and are exploited as synthesis promoters in the non-aqueous environment (Klibanov, 2001). In fact, this study was already done for cardosin A in aqueous–organic biphasic systems of n-hexane/ethyl acetate and sodium phosphate buffer. The aspartic protease stability was characterised under the referred conditions (Barros *et al.*, 1992), and it proved to be successfully used as a biocatalyst in peptide synthesis (Sarmento *et al.*, 1998). But the activity loss presented here for such a low OS content should not be due to the functional transition just referred.

Despite the increase in the secondary structures content for TFE percentages higher than 20% TFE, the functionality of the enzyme could not be recovered.

TFE promoted a denaturation in the cardosin A molecules that can be described in different phases. Initially, the gentle attack of the hydration layer may have decreased its thickness and protein thermal resistance, but also improved its catalytic performance. These changes occurred in the absence of global conformational changes. Increasing amounts of the OS led the protein to a second phase where activity was lost, but where structural changes were

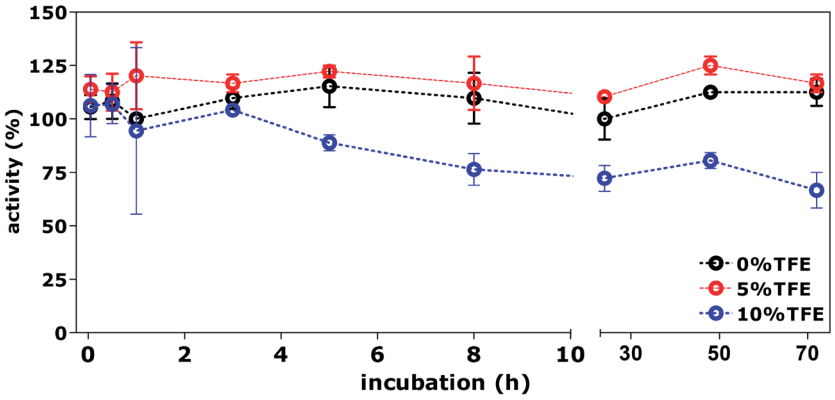

Figure 4.10 – Effect of incubation time over cardosin A enzymatic activity. Cardosin A was incubated in 0.2 M sodium chloride, 50 mM sodium acetate, pH 4.7, in 5 and in 10% TFE (black, red and blue open circles, respectively) and activity determined by HPLC, according to section 3.4.1. Each point corresponds to a minimum of 3 replicates.

not significant enough to be observed by the chosen sensible techniques. For percentages higher than 20% TFE, a series of events occurred in the protein structure that could explain the catalytic loss, while new conformations arose.

To ensure that 1 hour incubation time was long enough to allow the protein to reach the equilibrium of its new conformation, another assay was performed. The effect of the incubation time was followed for three TFE concentrations. The results are presented in figure 4.10, and confirm that 1 hour incubation is an appropriate duration for analysing the peptidolytic activity of the sample, since the results obtained for this period fairly characterise the slight variations observed beyond. This incubation period was also convenient for comparing results with the other techniques employed.

Throughout this work, different protein concentrations were used for each procedure, depending on the technique characteristics and limitations, and also on the available protein. In order

to verify if this activity profile was dependent on the enzyme concentration, different enzyme concentrations were incubated previously to the assay, in the presence of the TFE concentration under study. The protein amounts tested (0.003 mg/ml, 0.0292 mg/ml, and 0.3 mg/ml) resembled the concentrations used in CD experiments (0.267 mg/ml) and intrinsic fluorescence (0.020 mg/ml). The digestion assays were run in TFE using the same amount of enzyme and the same enzyme:substrate ratio (figure 4.11). It would be expected that the different enzyme concentrations in the incubation would not have any effect in the activity results, since these were run in the same conditions. However, there was some variation separating each condition. The curve tendency described in figure 4.9 is observed for all the enzyme concentrations tested. However, the complete inactivation did not occur at the same TFE concentrations. The most concentrated samples still presented some activity at 20% TFE, while the others failed to act. This could mean that, for TFE concentrations equal to 20%, the drastic structure effects that inactivate the enzyme are kind of shielded by the higher protein concentrations. Notice that all of the conditions tested are more than 1000 times diluted compared to the *in vivo* one (400 mg/ml) (Homouz *et al.*, 2008).

The activity increase for low TFE concentrations also showed to be dependent of the enzyme concentration in the incubation previous to the assay. If this variation would translate an effect dependent on the number of protein molecules in the proximity of each other, some kind of protection from TFE effect for higher protein percentages would be expected. This would lead to a minor increase in the activity for low TFE values. But the variation occurred in the opposite way: the higher protein concentration tested in the incubation, presented the higher increase in activity for lower TFE values. This result would make sense if some character, improved by the presence of low amounts of TFE, would

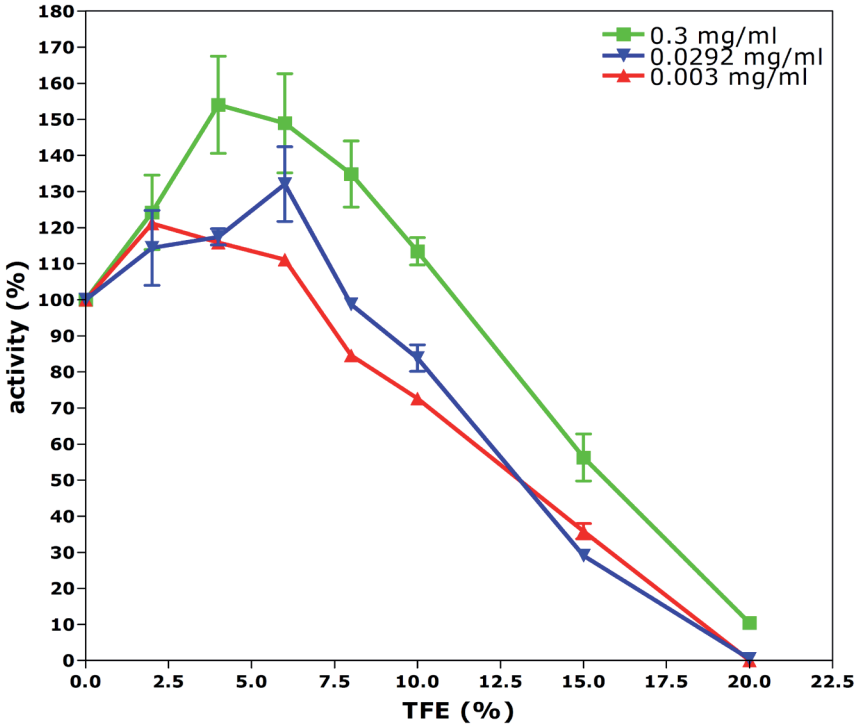

Figure 4.11 – Peptidolytic activity in the presence of TFE for different protein concentrations in the incubation. Results analysed by HPLC. Each set of experiments, presented in a different colour and connected by a line, corresponds to assays preceded by enzyme incubations with the following concentrations: 0.003 mg/ml in red, 0.0292 mg/ml in blue, and 0.3 mg/ml in green. All the assays were done with the same enzyme concentration and the same enzyme: substrate proportion. Each point corresponds to a minimum of 3 replicates (section 3.4.1).

be encouraged by the proximity of other protein molecules. To understand this trend, additional experiments need to be run.

In similar work run for cardosin A in the presence of acetonitrile, the opposite tendency was observed, with higher activity increase for lower protein concentrations. The meaning attributed to the variation was the same as explained before for 20% TFE (Oliveira, 2007).

4.2.1. Functional characterisation using a continuous method

Since we were using a discontinuous method to access for cardosin A activity, with possible sample errors and considerable work in separation and estimation of the products, a continuous method was established. Most conditions of the activity assay were maintained, and the reaction was carried out using the same buffer and temperature. These new method included another peptide, (MCA-Lys)Lys-Pro-Ala-Glu-Phe-Phe-Ala-Leu(Lys-DNP), with the same residues sequence, but presenting a fluorophore (MCA-Lys) and a quencher (Lys-DNP). Cleavage of the susceptible bond (Phe-Phe) was detected as an increase of reaction medium fluorescence over time, due to increase in the product content, allowing the determination of hydrolysis rate (section 3.4.2; Simões *et al.*, 2007).

To validate this method for the presence of the OS used in this study, several controls were run. At first it was necessary to prove that the fluorescence emission wavelength (λ_{max}) for the peptide and for its degradation product would not significantly vary with the presence of TFE (figure 4.12). Besides being small, only 2 nm in cardosin A activity range, the substrate and product λ_{max} variations occurred in broad emission spectra, which reduces their meaning (see figure 4.12 inset as an example).

Upon these observations, the reading emission wavelength was considered appropriate to follow the product formation along the TFE percentages tested.

Since the method is based on following emission intensity variations, it was necessary to test them under several conditions. The intact peptide and its product emission fluorescence were read for different concentrations in the presence of 3 percentages of TFE. Figure 4.13 - A presents how the emission fluorescence intensity varies for each tested condition. As expected, the products revealed higher emission intensity values. Assembling these results, it was shown that the difference in the emission fluorescence intensity between the substrate and the peptide (ΔUF) was not constant for the same peptide concentration along the TFE tested concentrations (figure 4.13 - B). For the same TFE concentration, the ΔUF increased with the increase in peptide concentration, as would be expected and necessary (figure 4.13 - C). This increase was not always linear (still smaller than the typical equipment variations), and so it was necessary to perform a normalization for each replicate (equation 3.1, section 3.4.2). There it is considered the emission fluorescence intensity of the intact substrate and of the completely degraded substrate. These substrate and product emission intensities (minimal and maximal emission intensities respectively; figure 3.1, section 3.4.2), besides normalizing the OS effect, convert the activity values from emission fluorescence intensity per second (UF/s), in nanograms of degraded peptide per second (ng/s). In this way the only varying aspect is the one we are interested in: the normalized slope of the increasing product formation, i.e., the protein activity.

The variation of cardosin A activity in the presence of increasing contents of TFE in the medium was once more characterised, this time using this fluorescence based approach. The activity

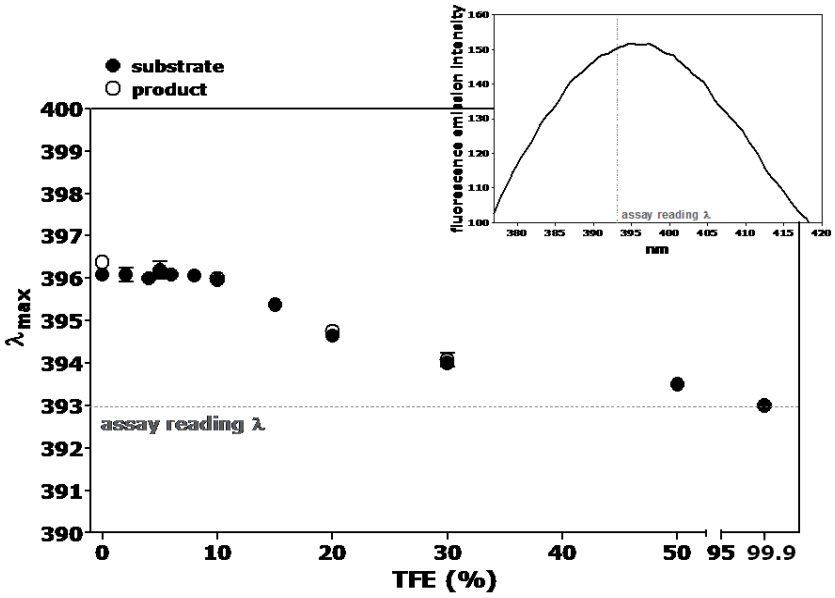

Figure 4.12 – Fluorescent peptide and product maximal emission wavelength variation along the increasing media content in TFE. Conditions: excitation wavelength - 328 nm; emission wavelength - 393 nm. Each point corresponds to a minimum of 3 replicates. Inset – emission fluorescence intensity variation upon excitation of the substrate at 328 nm for 5% TFE. The complete peptide degradation was performed before the addition of TFE to the medium. The emission wavelength used in the assay (393 nm) is indicated (section 3.4.2).

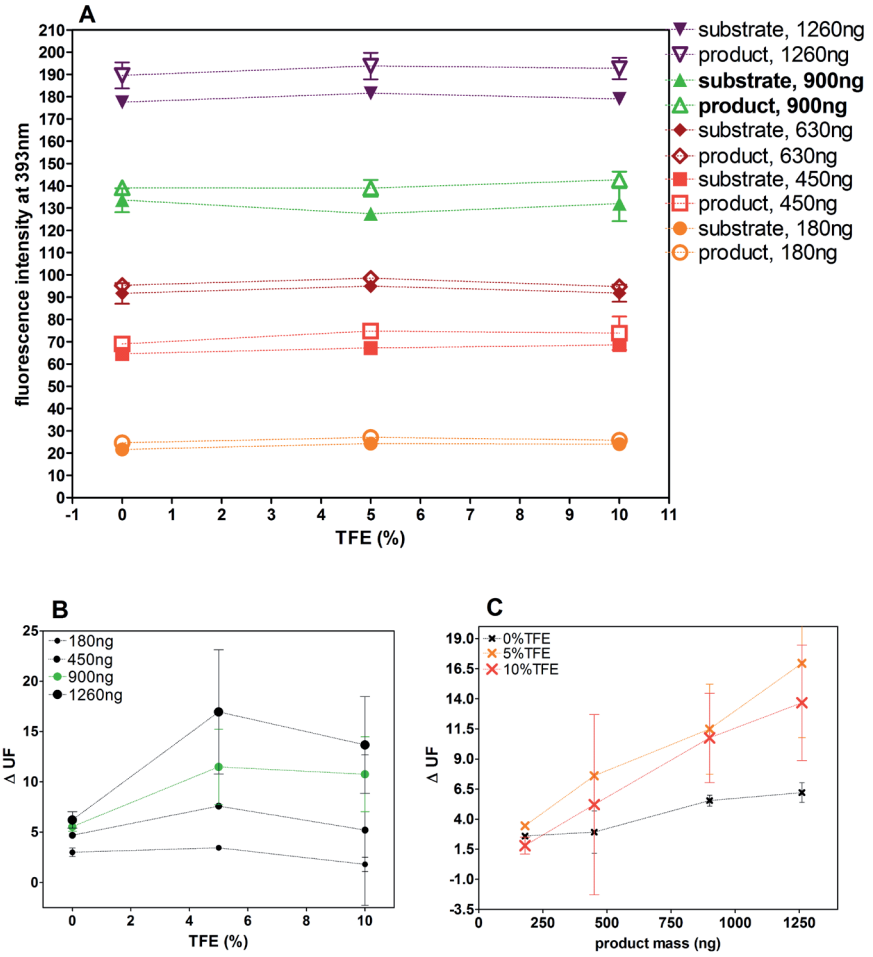

Figure 4.13 – Emission intensity variation of the fluorescent peptide and its product in the presence of TFE. A – Intensities of fluorescence emission at 393 nm of the peptide and its product in five different concentrations depending on the TFE medium content. B – ΔUF variation for 4 peptide concentrations according to TFE medium content. C - ΔUF variation according to their concentration for 3 TFE percentages. The complete peptide degradation was performed before the addition of TFE to the medium. Conditions: excitation wavelength - 328 nm; emission wavelength - 393 nm. At least 3 replicates were run per each represented point (section 3.4.2). ΔUF – emission fluorescence intensity difference between the substrate and the product.

profile presented in figure 4.14 (in black, continuous method) was obtained using the same enzyme incubation conditions performed in the discontinuous method. The figure also compares both data obtained for cardosin A activity. In this new approach the activity increase was even more pronounced: the activity for 4% TFE presented medium values 59% higher than the native ones, versus an increase of 17% in the discontinuous method. After this maximum, the activity was lost more abruptly, with a residual activity for 20 and 30% TFE, and a complete loss over these concentrations. Despite the difference in the activity profile, the curve tendency was similar, and the activity increase for lower TFE values, as well as for the other OS percentages was confirmed. Some variations among results proceeding from both methods were expected, since we are comparing activity assays using completely different enzyme concentrations and enzyme:substrate ratios. Being less laborious, and less disposed to mistakes, the continuous method was chosen to continue the present study.

Maintaining the low TFE percentage (5%), and increasing the incubation time, secondary structure variation was studied using the far-ultraviolet CD technique (figure 4.15). From 30 minutes to 1 hour incubation, cardosin A secondary structure suffered an adaptation, with a small loss in the minimum ellipticity (216 nm). For longer incubations, the spectra maintained its tendency, and the structural loss was very small (figure 4.15 - A). These structural variations were better analysed by following the ellipticity values for 222 nm. For incubations higher than the chosen one, these values presented some variation among them, but confirmed very slight structural modifications (figure 4.15 - B). It was not observed a marked structural loss nor a helicity increase, as could be observed for TFE concentrations like 20 or 40% (figure 4.3). This secondary analysis presumes the enzyme functional preservation already confirmed (figure 4.9).

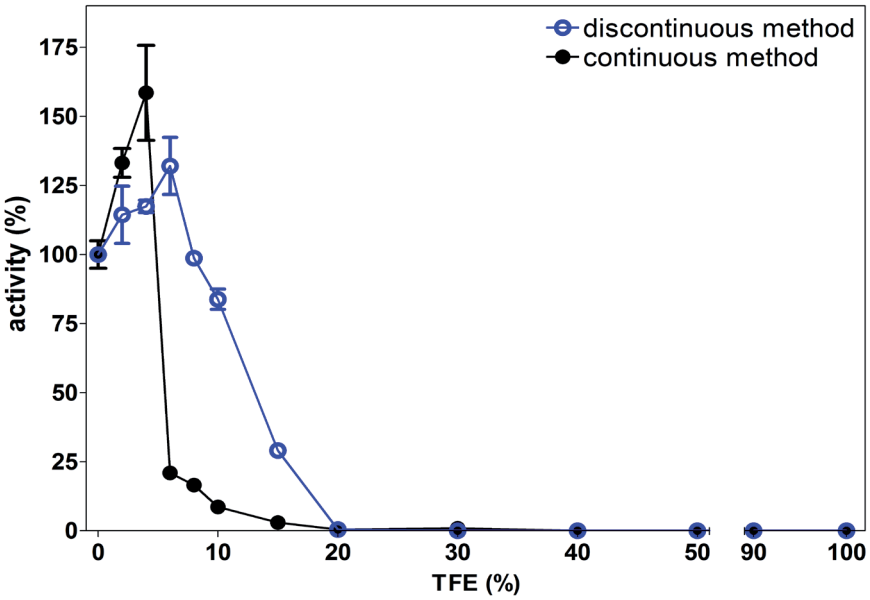

Figure 4.14 – Cardosin A activity profile in the presence of TFE accessed by fluorimetry and HPLC. Activity results obtained by continuous and discontinuous methods are plotted in closed black circles, and in open blue circles, respectively. Each point corresponds to a minimum of 3 replicates (sections 3.4.1 and 3.4.2).

4.3. Reversibility assays

The presence of the OS around cardosin A molecules promoted a specific alteration for each condition tested. The subsequent purpose was to follow the reversibility extent of these conformational changes. The protein return to an aqueous environment was reproduced through the 100 fold dilution with buffer of the TFE incubated sample, followed by another incubation of 1 hour (sections 3.4.2.1 and 3.6.1). The figure 4.16 presents the activity (using the fluorimetry assay) and the intrinsic fluorescence results for these reversibility conditions, and compares them with the previous data.

The lower TFE percentages, that allowed the increase in the activity, were found to have their activity profile completely reversible. For these TFE values the intrinsic fluorescence technique did not sense any alteration. From 4 to 10% TFE diluted samples, there was some activity recovered, with an increase from 8.6% to 52.5% activity when returned to aqueous environment. Beyond 20% TFE, the tryptophans exposition appears to be partially recovered, even for the higher percentages. However, the vestigial activity for 20 and 30% TFE did not recover with the return of the enzyme to the aqueous environment. In these OS ranges, the CD experiments proved an extensive loss of the protein secondary structure (figure 4.3). This loss, even if regained in some extent, as intrinsic fluorescence showed, should have been severe enough to turn out impossible any activity recovery.

Higher TFE percentages, as 70% TFE, produced severe effects in the protein secondary and tertiary structures, with an extraordinary increase in the helical content (figure 4.4) and tryptophans exposition to the medium. Intrinsic fluorescence reversibility for

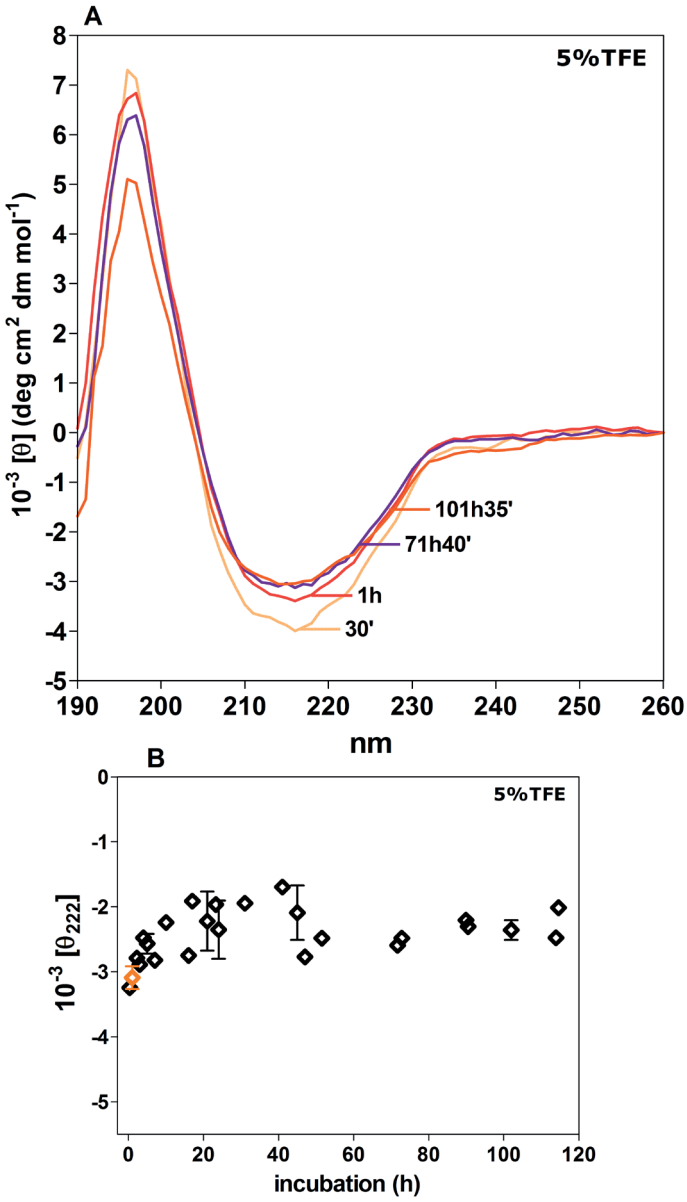

Figure 4.15 - Far-ultraviolet CD monitoring of the conformational changes of cardosin A during incubation with 5% TFE. A – Selected cardosin A CD spectra after different incubation times. B - Ellipticity changes at 222 nm for cardosin A at various incubation times (section 3.7.1). Results for 1 hour incubations are highlighted in orange.

this range would guess enzyme activity loss, since the tryptophans exposition recovery was similar to the one obtained for 30% TFE. Nonetheless, the enzyme partially regained its activity (48% for 70% TFE, and 47.5% for 99.9% TFE). Again, the partial functional recovery occurred without the total reburying of tryptophans, as maintained for functional TFE range. The partial activity recovery was only obtained for the highest TFE concentrations. Several reasons for these occurrences were hypothesised. The lyophilised enzyme placing in high TFE concentrations may have not resulted in a successful solubilisation (although precipitation was not observed). The posterior effective dilution with aqueous buffer would thus justify the activity recovery. On the other way, cardosin A could be trapped in a more rigid conformation for these high OS concentrations. This fact would hold it back from undergoing to an irreversibly unfolded state. The wash out of TFE would result in native-like active conformation recovery.

Observing figure 4.4, the highest content in unstructured secondary structures is achieved at 30% TFE. When returning to aqueous environment, a large recovery of β and α structures would be necessary to obtain an activity recovery. For 70% TFE, high helical content was formed with loss in unstructured elements but also in β-sheets. The removal to aqueous environment with some activity recovery admits the loss of this structure. Cardosin A active site is located between the two lobes of the molecule at the bottom of a large cleft. The base of the active site cleft is made of β-strands forming two contiguous ψ-like structures, where the two catalytic aspartates are located, with no disulfide bridges near it. Probably these β structures were not lost during the 70% TFE promoted unfolding, but could have been in 30% TFE. The TFE promoted helical state has been proposed as an open helical structure, which would enable it to regain an active and near-native like form. Moreover, NMR studies showed that the secondary structures

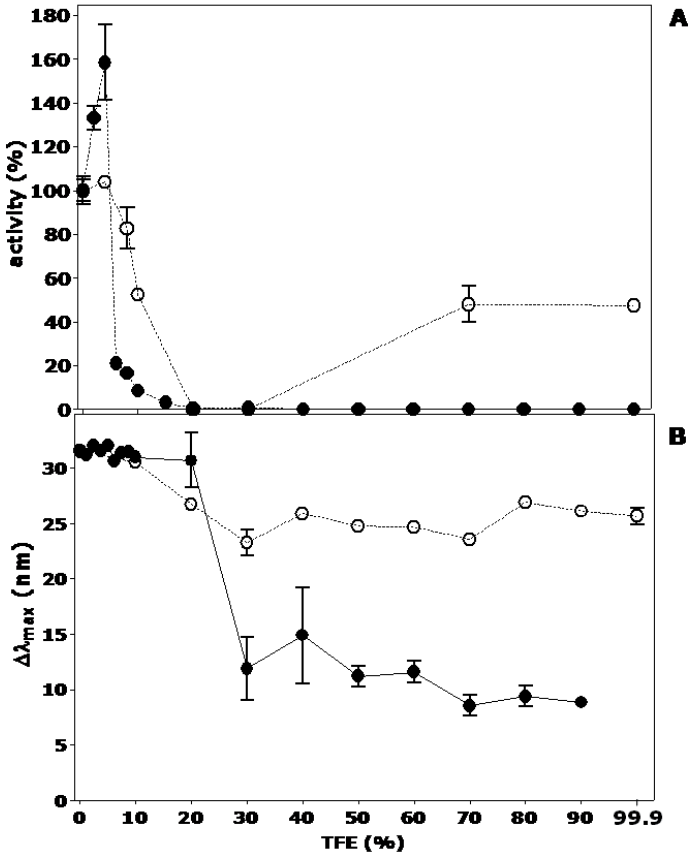

Figure 4.16 – Cardosin A TFE induced effects and their reversibility monitored by activity and fluorescence experiments. A - Initial rates of hydrolysis of the fluorescent peptide catalysed by cardosin A in the presence of varying TFE concentrations. Residual activity was measured after 1 hour incubation at 25ºC (closed circles) and also after 100 fold dilution of the TFE in cardosin A incubation solution (opened circles) (Section 3.4.2.1). B - Changes in intrinsic fluorescence maximal emission wavelength variation for cardosin A incubated at different TFE concentrations, measured in the presence of TFE (closed circles) and after dilution (up to 100 fold) with buffer (open circles) (Section 3.6.1). Each point corresponds to a minimum of 3 replicates.

formed in the TFE state are mobile and rapidly converted to the extended configurations (Hamada and Goto, 2005). The presented structural results appear to be in accordance to those descriptions. The increase in the helicity would have occurred within the more flexible native structures, not unfolding the more rigid and functional important ones, as the active site and surroundings. The last hypothesis would be the 70% TFE state non activity to be due to an excessive decrease in the water content of the media, disabling the catalytic function. The return to an aqueous medium would allow the recovery of enzyme functions.

Note that all the studies run in this work were independently handled: each sample was only used in one recorded condition. Other results would certainly be obtained if the same sample was hydrated without TFE, and subsequently submitted to growing concentrations of the OS. Probably the enzyme in 70% TFE, which had already been submitted to 30%, would not recover its activity after the re-hydration.

Cardosin A in 99.9% TFE showed a slight loose in the β content and an increase in the helical content compared with the native structure (figure 4.4). When its UV-spectrum was analysed by *CONTIN*, the β content was close to the 15% one, but with larger content in α-helices. The almost absence of water could have promoted the described changes in the protein structure and the inactivity. Replacing TFE by water would unfold the new α-helical structures, resulting in a conformation similar to the 15% TFE one, which would allow for some proteolytic activity regaining. Far-UV CD analysis of these reversibility tested samples would enlighten this discussion.

Previously, in a similar approach, cardosin A was also submitted to increasing concentrations of acetonitrile (Oliveira, 2007). For

low percentages (10% acetonitrile), the activity also increased to even higher values (up to 182% for 5% acetonitrile), and was completely lost for concentrations over 30%. The reversibility was nearly total until 20%, in activity and in the intrinsic fluorescence emission. For 90% acetonitrile, cardosin A showed to be reversible, with a new 85% activity, and a complete recovery of the tryptophans exposition. It was proved that the activity raise for low acetonitrile concentrations was not due to an increase in the catalytic efficiency. TFE is comparable to acetonitrile in terms of its bulk solvent polarity parameter (only slightly higher), but demonstrates a stronger hydrogen bonding ability (Jamison *et al.*, 2006). In the presence of hydrophobic solvents, a higher amount of water remains associated with the enzyme structure, leading enzymes to exhibit higher activity levels in hydrophobic solvents than in hydrophilic solvents (Rezaei *et al.*, 2007), and this characteristic could justify the bigger increase in cardosin A activity for acetonitrile. Besides, TFE would compete with water for enzyme surface interactions, namely for the active site hydration molecules, impairing cardosin A function.

Using another approach, cardosin A hydrolytic behaviour in the presence of other organic solvents was also run (Sarmento, 2002; Sarmento *et al.*, 2004b, 2008). Ethyl acetate, n-hexane and isooctane (ordered by growing hydrophobicity) were used in aqueous saturated media, and the enzyme showed to be active under all the tested conditions, with slight changes in specificity. It was concluded that the most hydrophilic solvents induced the lowest activity of cardosin A along with a higher destabilising structural effect. More hydrophobic solvents are less soluble in the aqueous phase, and therefore less solvent molecules can interact with the protein (Sarmento *et al*., 2008). In addition to the alteration of active enzyme concentration, a factor affecting cardosin A affinity for the substrate could be an alteration of its

ionisation state (of the catalytic cleft or of the enzyme as a whole) induced by the solvent. But this alteration would imply an alteration of the pH profile, which was not observed (Sarmento *et al*., 2004b). In the present work the activity profile in the presence of TFE also presented lower values for the same OS range when compared to the more hydrophobic OS acetonitrile.

Since TFE can exert its effect via different ways, it could be interesting in the future to determine kinetic constants for cardosin A activity. This would allow getting further insights on the enzyme catalytic performance modifications in the presence of this OS.

5. GENERAL DISCUSSION

The aim of the present work was to comprehensively study the cardosin A conformational changes induced by the presence of the fluoro-alcohol 2,2,2-trifluoroethanol (TFE) in the media.

The folding variations described by TFE *in vitro* results can be resumed in the following items:

- TFE medium content below 4% reversibly decreased protein stability, and reversibly increases its enzymatic rate.

- TFE medium content over 20% irreversibly inactivated the enzyme and unfolded tertiary structures, while secondary α-helices were progressively increased in content (mainly, but not always, from previously unordered segments).

- TFE medium content over 70% inactivated the enzyme and promoted a vast increase in structural complexity, taking form as open helical structures. These alterations proved to be reversible.

Upon analysing these conformational and functional results one question remains. How did the solvent molecules interact with the protein to justify the obtained results?

To answer that question it would be important to measure, characterise and localise the number of water molecules bound to the enzyme (Bell *et al.*, 1997; Halling, 2004). For these purposes Doctor Nuno Micaêlo has kindly performed molecular dynamics/molecular mechanics (MD/MM) simulations of the system.

5.1. UNDERSTANDING STRUCTURAL ALTERATIONS

Computer simulations provide detailed atomic information of processes that would be difficult (if not impossible) to study experimentally. One of those processes is the solvation mechanism of biomolecules in aqueous and non-aqueous environments. MD simulations studies of enzyme dynamics in water/cosolvent mixtures have provided molecular evidences that support solvent mediated effects as water stripping, reduced protein mobility, and the pH memory effect (Roccatano, 2008).

The MD/MM simulation approach used in this work simulates one cardosin A molecule in a box of organic solvent and water mixtures. This probably corresponds to a situation that is harder on the protein than the real one (possibility of aggregation and adhesion to support material), but various works with similar approaches have been proved to capture the overall physical features of the system (Colombo *et al.*, 1999; Soares *et al.*, 2003; Micaêlo and Soares, 2007). The simulations where run for 0, 10 and 90% of TFE, representing absence, low and high amount of the OS molecules relatively to the water ones. The root mean square deviations[1] (RMSD) of the alpha carbon atoms (α-C) of the protein fitted against the X-ray

[1] The root mean square deviation (RMSD) is a frequently-used measure of the differences between values predicted by a model or an estimator and the values actually observed from the thing being modeled or estimated.

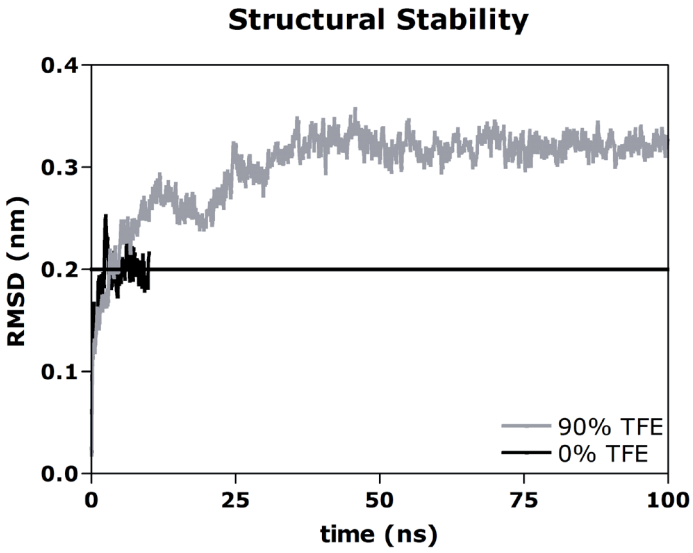

Figure 5.1 – Structural stability analysis for simulations in media with different TFE contents. Root mean square deviation of α-C atoms of cardosin A from X-ray structure (PDB 1B5F) in 0 and 90% TFE.

structure are presented in figure 5.1. Simulations in 0% TFE have reasonable values of RMS deviation from X-ray structure (medium value is 2 Å), showing that the simulation conditions are reproducing the correct physics of the system (Soares *et al.*, 2003).

The MD/MM simulations run for 10% TFE (data not shown) reproduced similar RMSD profile than the aqueous one. This suggests that the protein has largely maintained its native structure, at least during the time scale sampled in these simulations. These data are in agreement with the *in vitro* results discussed in the previous chapter. The conformational alterations promoted by the presence of low amounts of TFE on the *in vitro* system were not detected by the employed techniques in terms of secondary or tertiary structure. In fact DSC results showed a thermal stability decrease. Hydrodynamic volume results could suggest a gentle attack from TFE over cardosin A hydration layer. Simulation

results do not support this idea, since the low amount of TFE molecules present in the simulation medium did not alter the structure stability in a different way than its absence did.

Results for 90% TFE are deviated from the control in more than 3 Å, expressing a consistent stability alteration of the enzyme structure. These structural properties adjustment was expected for such a high content of a polar solvent as TFE (section 7, table 7.1). Previous work from Micaêlo and Soares (2007) showed that the optimal water content that minimizes the difference from the X-ray structure is displaced to higher water level as the polarity of the organic solvent is increased. Simulations ran for the 98 residues α/β protein acylphosphatase in 25% TFE presented RMSD values quite high (5 Å), traducing a considerable instability of the protein in that environment, despite no secondary structure alteration had been found (Flöck *et al.*, 2004). On the other hand different kinds of peptides showed lower RMSD values in TFE/water medium than in pure water medium simulations, stating a more stable and further confirmed ordered structure (Roccatano *et al.*, 2002).

Important information about protein dynamics prediction is reflected by the atoms average positions fluctuation, and is represented in the figures 5.2 via the protein B-factor profiles. Cardosin A is presented according to crystal and simulation predicted structures, and various altered or important domains are marked in cartoon, as well as in surface representations. As expected, the model for aqueous environment (MD/MM simulation 0% TFE, figure 5.2 – B and E) expresses slight different B-factors than the original crystal structure (figure 5.2 – A and D). Locations of the peaks in the RMS fluctuation profile correspond to residues on the enzyme surface, and are well correlated with the temperature factors reported in the crystal structure (Frazão

et al., 1999). Curiously, the model presents the flap region less dynamic than the crystal, and a general increase in the atomic fluctuation. Other crystallographic significantly displaced domain that has this character decreased is the $N_{47}SK$, not implicated in the catalytic cleft. A new domain arises from the model without TFE: $T_{292}LL$, a turn segment located opposite to the flap over the active site.

But both predictions place protein atoms in the same locations, not inducing major secondary or tertiary structural alterations. The presence of TFE in higher proportion than the water molecules (figure 5.2 – C and F, MD/MM simulation 90% TFE) promoted the protein atomic displacement enhancement in general. And also locally, in segments related and closely located to the active site, such as the flap and $T_{292}LL$, respectively. Such a high content of the alcohol in the simulation medium was expected to be translated differently. No large structural change has been observed by this model in the presence of high contents of TFE, in opposition to the fluorescence (section 4.1.1, figure 4.2) and circular dichroism (section 4.1.2, figure 4.3) results obtained. A discussion about the validity of the CD results interpretation was conducted in that section. The obtained high helical content results would not translate an exchanging from β strands to α-helices, but instead, unordered segments would get their helicity increased, masking the dichroic contribution of the maintained β-sheet structures.

All solvation models, even those computationally more demanding, are approximations. Their range of validity is difficult to explore, and some authors defend that experimental approaches and results are essential to validate force field and simulation results (Caflisch and Paci, 2005). For others, the direct comparison between simulations and experimental data is not possible, both due to the limited time scale that can be simulated, and the

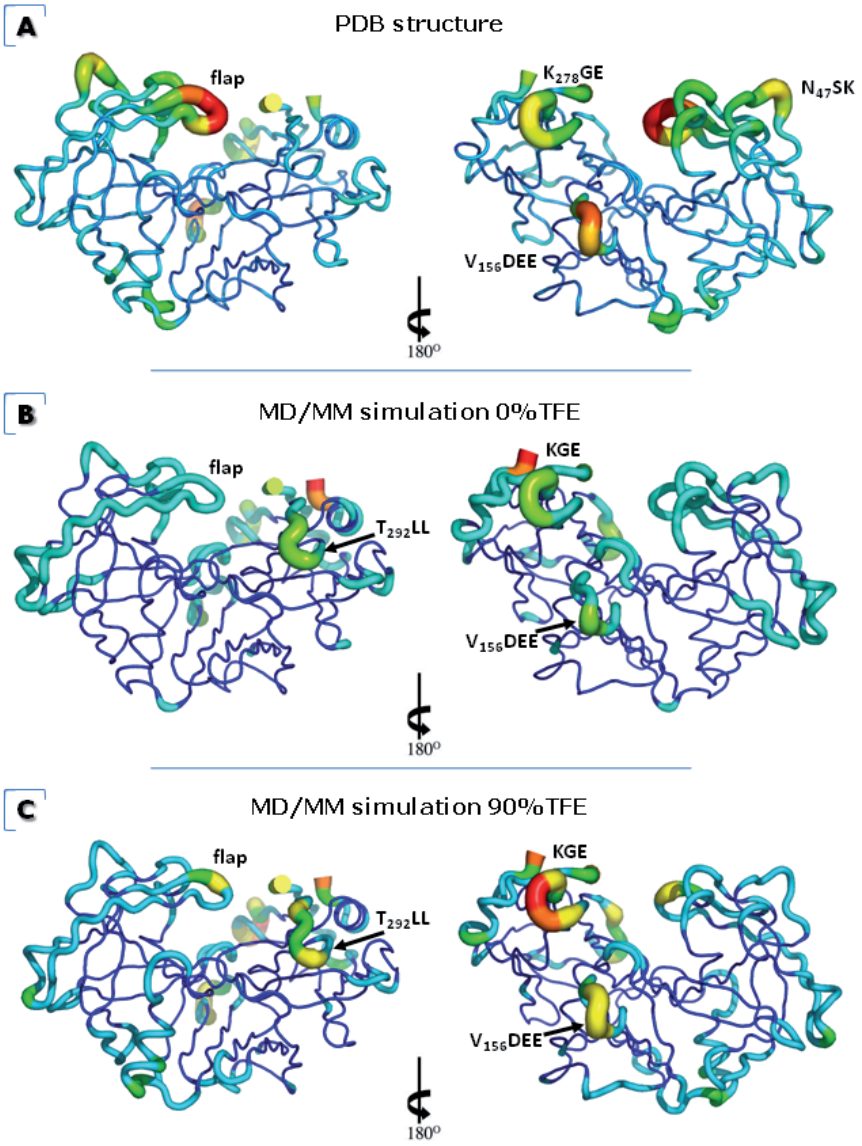

Figure 5.2 - Three-dimensional structure representations of cardosin A crystallographic form (A and D), and MD/MM simulations 0% TFE (B and E) and 90% TFE forms (C and F). Front and back representations according to the B values: warmer colours and/or thicker cartoon segments represent residues with higher

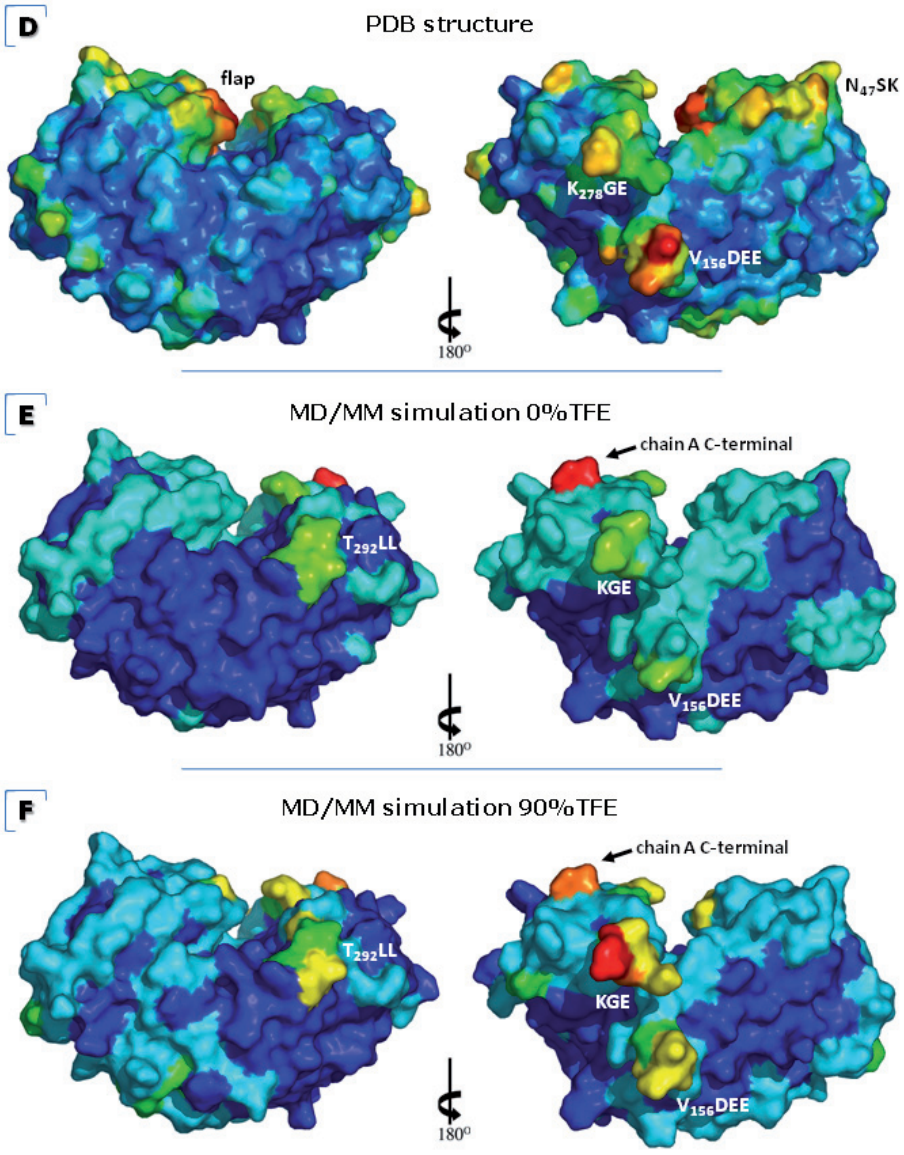

mobility in cartoon (A, B and C) or surface view (D, E and F). PDB 1B5F, flap region corresponds to Y_{75}GT (Frazão *et al*., 1999). The representations were created using *PyMOL* software (DeLano *Scientific LLC*).

fact that the effect of aggregation can never be fully eliminated from the experiment (Villa *et al.*, 2006). But the obtained simulation results will undoubtedly provide usefull information for the discussion of the present work.

The graphical distribution of the RMS fluctuation[2] values for cardosin A in 0% TFE, in 90% TFE, and the difference between the two conditions is presented in figure 5.3. The same values are structurally explored in figure 5.4. Differences higher than 0.5 Å are reported on figure 5.4 – B, and are highlighted in red in the B-factor cartoon structural representation of figure 5.4 – A. The domain with the biggest flexibility increase is KGE, followed by flap. Alanine 291 is also evidenced, and domains M_{140}LNQ, V_{159}DEE and others are shown up in red in figure 5.4 – A. Secondary structure determined by crystallography is exhibited for each residue (figure 5.4 – B), and it was maintained in the 90% TFE simulation structure, except for L_{170}D where the hydrogen bonded turn was lost for a coil[3]. This sequence, as others, is not expected to be related to alterations in the enzyme function, because of its distance to active site.

The effect of the media over the protein structure is also reflected in its exposure to the solvent. Hydration details of enzyme surface, interior, or active site region for a given level of hydration are difficult to obtain from experiments alone (Yang *et al.*, 2004). The MD/MM simulations can help to understand the solvation tendency of the protein structure. Figure 5.5 presents the solvent accessible area of cardosin A in absence and presence of TFE. In the presence of large amounts of the OS the protein structure

[2] When a dynamical system fluctuates about some well-defined average position the RMSD from the average over time can be referred to as the root mean square fluctuation. The size of this fluctuation can be measured and can provide important physical information.

[3] Residues secondary structure comparison run in *VMD 1.8.7* (Humphrey *et al.*, 1996)

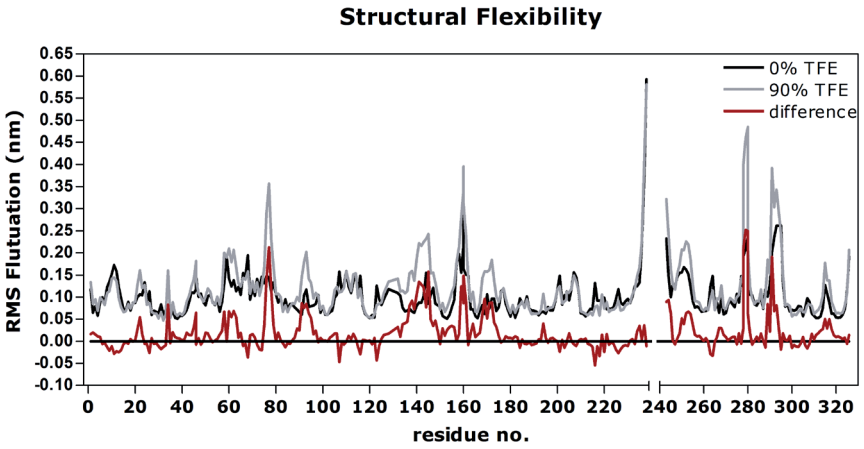

Figure 5.3 – Structural flexibility analysis for simulations in media with different TFE contents. Root mean square fluctuation of cardosin A residues in 0 e 90% TFE, and the difference between these values.

becomes more exposed to the solvent, namely the hydrophobic area (hydrophobic area : hydrophilic area ratio is higher), due to the increase on medium hydrophobicity. These values are consistent with the RMSD results (figure 5.1), that admit the presence of the OS as a structural stability modifier, as seen in other simulation studies (Soares *et al.*, 2003; Villa *et al.*, 2006).

Solvent molecules distribution through the protein surface is represented in figure 5.6, with illustrations depicting cardosin A after 10 ns of MD simulation in water (A), and in the last acquired conformation of the MD simulation at 100 ns in 90% TFE coloured by chain (B), or by residue polarity (C and D). The represented solvent molecules are localised closer than 5 Å from protein atoms.

In aqueous media water molecules are spread all over the enzyme surface (figure 5.6 – A). The presence of high amounts of TFE promotes a very different distribution. By visual inspection we

A

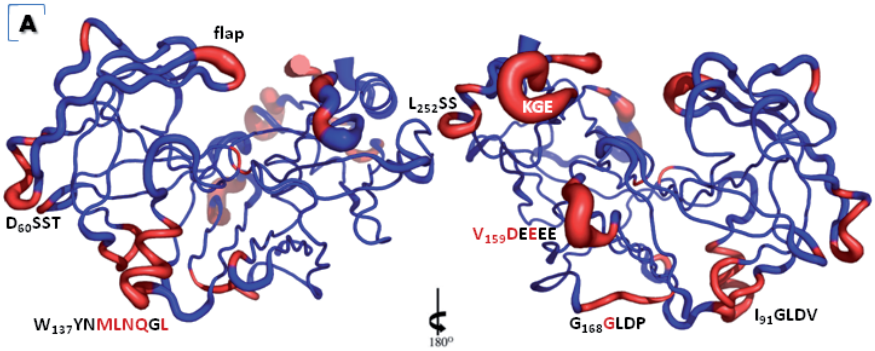

B

Res No.		Amino acid	Variation	Sec. Str.
22		Thr/T	0.05	turn
34	S'2	Gly/G	0.08	turn
46		Ile/I	0.06	turn
58		Ser/S	0.07	3-10 helix
60		Asp/D	0.07	3-10 helix
61		Ser/S	0.05	turn
62		Ser/S	0.07	turn
63		Thr/T	0.05	turn
76	S'1	Gly/G	0.14	turn
77	S 1	Thr/T	0.21	turn
78		Gly/G	0.12	turn
91		Ile/I	0.09	ext. conf.
92		Gly/G	0.08	turn
93		Asp/D	0.08	turn
94		Leu/L	0.06	ext. conf.
95		Val/V	0.05	ext. conf.
137		Trp/W	0.08	α helix
138		Tyr/Y	0.09	α helix
139		Asn/N	0.07	α helix
140		Met/M	0.11	α helix
141		Leu/L	0.13	α helix
142		Asn/N	0.13	α helix
143		Gln/Q	0.12	α helix
144		Gly/G	0.08	coil
145		Leu/L	0.16	coil
159		Val/V	0.12	turn
160		Asp/D	0.12	turn

flap

Res No.		Amino acid	Variation	Sec. Str.
160		Glu/E	0.09	turn
160		Glu/E	0.15	turn
161		Glu/E	0.09	coil
168		Gly/G	0.06	turn
169		Gly/G	0.1	turn
170		Leu/L	0.05	turn *
171		Asp/D	0.09	turn *
172		Pro/P	0.09	3-10 helix
216	triad	Ser/S	-0.05	turn
243		Glu/E	0.09	turn
244		Glu/E	0.09	turn
245		Leu/L	0.06	turn
250		Asn/N	0.05	turn
252		Leu/L	0.06	3-10 helix
253		Ser/S	0.07	3-10 helix
254		Ser/S	0.06	3-10 helix
278		Gly/G	0.07	coil
278		Lys/K	0.21	turn
279		Gly/G	0.25	turn
280		Glu/E	0.25	turn
280		Ala/A	0.08	turn
280		Thr/T	0.06	turn
289	S'1	Met/M	0.08	coil
291		Ala/A	0.19	ext. conf.
293		Leu/L	0.08	turn
315		Tyr/Y	0.05	turn

KGE

Figure 5.4 – Analysis of the residues with higher RMS fluctuation between 0% and 90% TFE. A – Front and back three-dimensional representations of the MD/MM cardosin A in 90% TFE, according to the B values: thicker cartoon segments represent residues with higher mobility in cartoon structure. Highlighted in red are the domains with bigger variation. B – Table presenting the residues with variation values (in nm) higher than 0.5 Å and the respective crystal secondary structure (* mark structures transformed in coil in the 90% TFE simulation structure). Relevant domains are shown up, as well as residues participant on the active site. Variation values higher than 1 Å are underlined in red. The representations were created using PyMOL software (DeLano Scientific LLC).

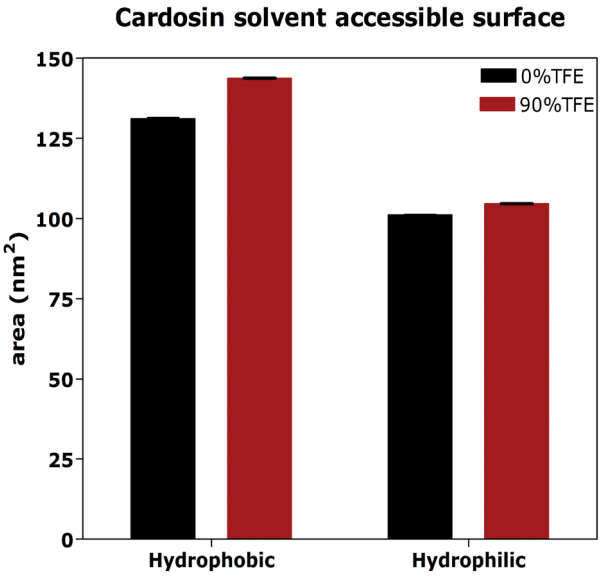

Figure 5.5 – Analysis of cardosin A solvent accessible surface for simulations in the presence of 90% TFE and in water.

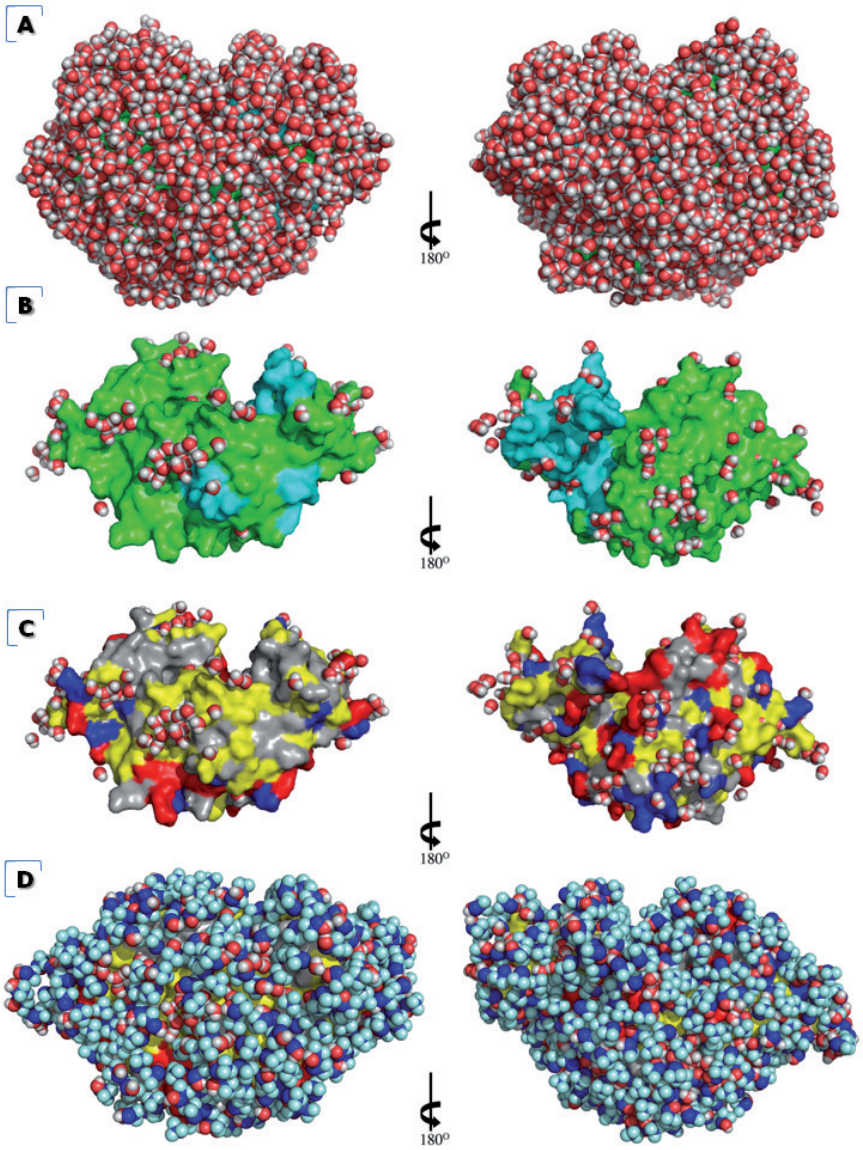

Figure 5.6 – Spatial distribution of solvent molecules in MD simulations for cardosin A. Solvent molecules represented are localised closer than 5 Å from protein atoms. A - Front and back three-dimensional representations of the cardosin A after 10 ns of the MD simulation in water, in a surface representation, coloured according to chains. Water molecules represented as spheres and coloured according to atoms. B, C and D - Front and back three-dimensional representations of the cardosin A in last acquired conformation of the MD simulation 90% TFE at 100 ns, in a surface representation, coloured according to chains (B, green:

are able to identify regions of higher density of water molecules (figure 5.6 – B and C). The tendency is apparently similar to the one followed in aqueous environment. By simple observation, water molecules localisation in TFE/water solvent environment is similar to the localisation of the closest (2 Å) to the protein water molecules in the aqueous simulation (data not shown).

Micaêlo and Soares (2007), by similar simulation studies, compared different OS and water distribution over a protein surface and showed that water is distributed over similar regions of the enzyme in different solvents. For more polar solvents, such as ethanol and acetonitrile, water was found in regions also present in the non-polar solvents. As surface did not change dramatically when the enzyme was placed in different organic solvents, water molecules apparently populated equivalent sites. Sites that corresponded to the areas of exposed charged / polar side chains, hydrated to a higher or lower degree according to the polarity of the organic solvent (Micaêlo and Soares, 2007). In our results no tendentious distribution of the water molecules was found visually, since they are concentrated close to polar and hydrophobic residues. TFE molecules cover the non-hydrated protein surface (figure 5.6 – D). This emphasises TFE role in the protein conformation, given that a significant enzyme surface area is solvated by the OS.

In simulation studies with peptides it was also observed the coating by TFE molecules, limiting the accessibility of water to the surface (Roccatano *et al.*, 2002). A more detailed MD simula-

---

cyan: light chain) or according to residues type (C and D, red: residues with positively charged R groups, blue: residues with negatively charged R groups, yellow: residues with polar uncharged R groups, grey: residues with non-polar R groups). Solvent molecules are represented as spheres (A, C and D) or sticks (B) and coloured according to the Corey, Pauling and Koltun coloring scheme (CPK) (red: oxygen, white: hydrogen, dark blue: carbon, light blue: fluorine). The representations were created using *PyMOL* software (DeLano *Scientific LLC*).

tion study with a protein placed in 25% TFE (acylposphatase, α/β protein with 98 residues) showed that the cosolvent builds dense hydrogen-bonding networks with the charged residues of the protein, while water molecules cannot be found in the immediate neighbourhood. TFE also clusters around hydrophobic side chains with its tri-fluoride head (Flöck *et al.*, 2004). Other study showed by densimetry that the interaction of the amino acids hydrophobic groups with $-CF_3$ and –OH group in TFE dominates over the interaction of the ionic and hydrophilic groups with –OH group of the alcohol (Kundu and Kishore, 2004). Another MD simulation study affirms the strong tendency of the TFE molecules to coat the peptide, but with uniform solvation and no correlation between local TFE concentrations and either the nature of the residues or the secondary structure (Mehrnejad *et al.*, 2007). The interactions between the cosolvent and the peptide are weak, with the formation of a layer over the surface, but the interactions between peptide and TFE do not displace the peptide-peptide interactions (Mehrnejad *et al.*, 2007).

In the X-ray structure of hen egg-white lysozyme (129 residues, mainly α-helical, PDB 1YL1) co-crystallized in 16% TFE, a smaller number of water molecules was found in the primary shell when compared to other less hydrophobic alcohols (Deshpande *et al.*, 2005). Porcine pancreatic elastase (240 amino acid residues, composed of two β-barrel domains, PDB 2FOG) has been crystallised, and transferred to a solution containing 40% TFE. Besides the common water space replacements and alcohol interactions with the protein, no structural alterations were detected when compared to the native crystal (Mattos *et al.*, 2006). In a similar work from the same group ribonuclease A (124 residues, $\alpha + \beta$ protein, PBD 3EV4) was analysed in a crystal in 50%TFE, and once more no significant changes were found besides water space replacement (Dechene *et al.*, 2009). In these study cases,

TFE oxygen atom was found as H-bond donor to threonine or valine main chain oxygens, to hydroxyl oxygen of serine, or to glutamin carboxyamide nitrogen. It also interacted with the protein molecule as an acceptor from the main chain nitrogen of glycine or serine, or from the side chain amino group of lysine. GTPase HRas (166 residues with α and β structures, PDB 1P2S) crystal in 50% of TFE presented a drastic reduction in the number of water molecules, despite no explicit binding of TFE molecule has been observed, and only a single alcohol molecule has been detected in a small hydrophobic cleft. However the secondary structure was slightly altered, with some polar interactions failing to be kept and new being created, contributing for the reinforcement of the α-helical structure (Burhman *et al.*, 2003)[4].

By simple observation of cardosin A last acquired conformation for the simulation with TFE, it cannot be interpreted if it interacts mainly with the -OH group or with the fluorine atoms. Two snapshots of intermolecular interactions formed between TFE and hydrophilic or hydrophobic side chains of the protein are shown in figure 5.7. The illustrations seem to confirm the fluoro-alcohol interaction tendency defended in the references above. Note that in these pictures no water molecule was caught. Moreover, the water molecules in the TFE simulation do not have a marked tendency to remain associated with the protein (data not shown), as occurs for other more hydrophobic OS. This observation proves the solvent polar characteristics, and its claimed hydrophobic effect reduction in water (Luo and Baldwin, 1999).

The simulations may suggest that the stabilizing effect of TFE is

[4] In other protein crystals with TFE, the alcohol is used as substrate analogue (PDB 1A71, Colby *et al.*, 1998), as an inhibitor (PDB 1AXG and 1AXE, Bahnson *et al.*, 1997), or as a ligand (PDB 2NUD, Desveaux *et al.*, 2007; PDB 1SBY, Benach *et al.*, to be published).

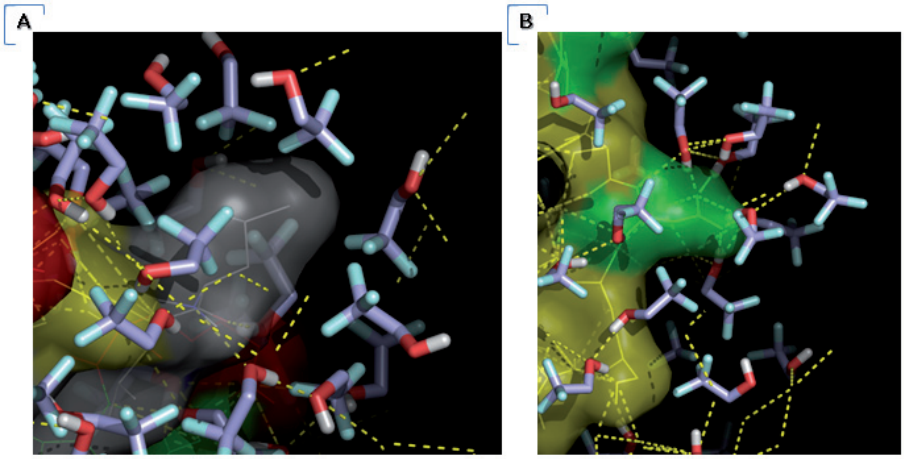

Figure 5.7 – Snapshots of solvent molecules around some cardosin A surface residues in the last acquired conformation of the cardosin A MD simulation in 90% TFE; A – around a hydrophobic residue; B – around a polar residue. Protein portions are represented in surface and coloured according to residues type (red: residues with positively charged R groups, blue: residues with negatively charged R groups, yellow: residues with polar uncharged R groups, grey: residues with non-polar R groups). Solvent molecules are represented as sticks and coloured according to the CPK coloring scheme (red: oxygen, white: hydrogen, dark blue: carbon, light blue: fluorine). Polar interactions are represented as yellow dashes. Representations were created using *PyMOL* software (DeLano *Scientific LLC*).

induced by the preferential aggregation of TFE molecules around the peptides. This coating displaces water, thereby removing alternative hydrogen-bonding partners and providing a low dielectric environment that favors the formation of intrapeptide hydrogen bonds(Roccatano *et al.*, 2002).

The protein secondary structure variation between aqueous and 90% TFE simulations was calculated and is presented in figure 5.8. Contrarily to the results obtained by CD (section 4.1.2, figure 4.3), and to the secondary structure calculation run over them (section 4.1.2, figure 4.4), the results describe secondary structure elements quite undisturbed through the simulation time. As just mentioned, it is known that TFE is able to stabilise individual secondary structure elements by stabilizing the peptide hydrogen

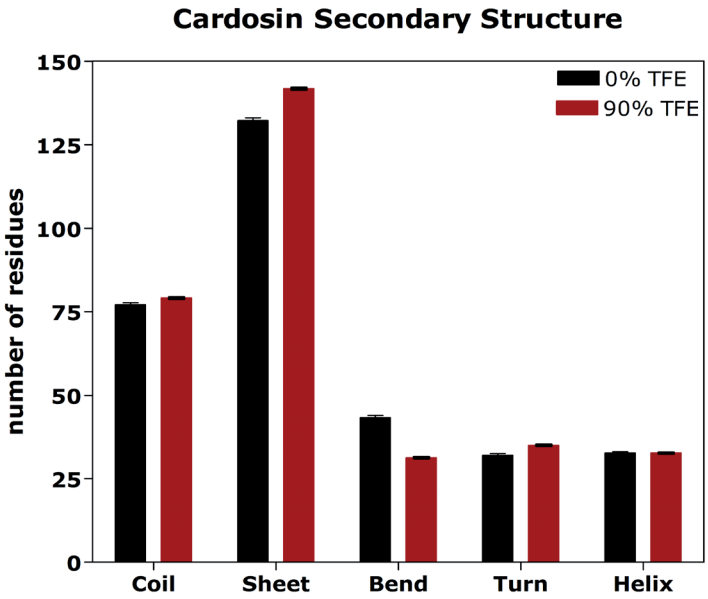

Figure 5.8 – Cardosin A secondary structure proportions for simulations in the presence of 90% TFE and in water.

bond (Luo and Baldwin, 1999). Curiously, despite the structural stability decrease defended by the models, the simulation with OS in the medium denotes an increase in the β-sheets content, and a decrease in poorly structured formations (non-hydrogen-bond based secondary structure) (figure 5.8).

Several studies in the literature also merge *in vitro* results with MD simulations. However, these results are used to complement the *in vitro* results obtained, more than to compare or confirm them[5]. MD simulation studies with TFE are scarce, and most of them use peptides. Peptides showed good agreement between its MD simulation results and CD spectra (Daidone *et al.*, 2004; Kaur

[5] References for MD simulations with TFE: Roccatano *et al.*, 2002; Abbate *et al.*, 2006; Mehrnejad *et al.*, 2007; Kaur *et al.*, 2008.

et al., 2004; Sforça *et al.*, 2004; Villa *et al.*, 2006; Gopal *et al.*, 2009), vibrational CD and infrared absorption (Bour *et al.*, 2008), and NMR structure (Sforça *et al.*, 2004; Mazzini *et al.*, 2007). The MD simulation studies used for a protein (98 residues) in TFE also presented good agreement with the CD spectra data (Flöck *et al.*, 2004).

Our *in vitro* results apparently showed different scenarios. Environment with intermediate TFE content opened the tertiary structure, despite increasing the secondary structure content of the protein. The cosolvent content increase enhanced this tendency. The simulation results confirm the propensity found in similar published studies, with the preferential interaction of the alcohol for protein, limiting water accessible surface. This binding exchange upon water stripping is considered very important in modelling TFE effects over protein structures (Jasanoff and Fersh, 1994). This induced local hydrophobicity may induce the opening of the tertiary structure. This tendency is depicted by the increase in the hydrophobic portion exposed to the solvent (figure 5.5), and is followed *in vitro* by the fluorescence results. Moreover cardosin A conformational alteration in medium with high TFE content resulted in the typical "open helical configuration" (Hamada and Goto, 2005), where the α-helical rods are exposed to the solvent, confirming the previously admitted propensity. The helicity increase may be another result of the surface water stripping promoted by the OS: being less polar than water and less powerful hydrogen-bond competitor, it may promote local backbone H-bond formations.

The structural modifications promoted by the chosen OS would be conclusively characterised by application of techniques such as light scattering and liquid-state NMR.

5.2. UNDERSTANDING FUNCTIONAL ALTERATIONS

Some of the higher RMS fluctuation residues take part in the catalytic cleft. The closer observation of its structure in figure 5.9 – B presents catalytic aspartates in red, and residues with higher variation (values in figure 5.9 – A) in light blue, if belonging to the active cleft, or in magenta, if close located. Alanine 291 and leucine 293 are contiguous to S'1 and S'2 specificity sub-sites respectively. The overall structural changes do not promote a significant loss of the active site residues conformation. The increase in flexibility upon the presence of high amounts of the OS could propose an increase in the enzyme activity (Klibanov, 2001). This may justify the increased *in vitro* activity profile for TFE low percentages (section 4.2, figure 4.9). But for concentrations higher than 20% no activity is detected. The maintenance of the active site conformation is coherent with the nature of the enzyme folding in keeping these residues at their relative positions.

The reduced structural flexibility in typical OS is an important reason for diminished enzymatic activities. In aqueous environments, enzymes possess the conformational mobility necessary for optimal catalysis. In contrast, organic solvents lack water's ability to engage in multiple hydrogen bonds, and also have lower dielectric constants, leading to stronger intra-protein electrostatic interactions. Consequently, enzyme molecules are expected to be much more rigid in organic media (Klibanov, 2001). There is some ambiguity regarding the protonation states of ionisable amino acids of the enzyme in organic solutions. But it is known that the pH of the aqueous solution from which enzymes are extracted influences the enzyme activity in organic solvents, referred to as the ''pH memory'' phenomenon (Zaks and Klibanov, 1985). Another important factor of activity regulation is the solvation. In low aqueous media water preserves the essential function of

controlling the catalytic properties of the enzyme, preserving the sufficient conformational flexibility needed for catalysis. Enzymatic activity in organic media is thus determined by the interactions of the solvent with the water on the enzyme, more than with the enzyme itself (Zaks and Klibanov, 1988a). But the direct effect of the solvent on the protein (e.g. through binding or changing the dielectric constant of the reaction medium) may as well be important and should be considered (Zaks and Klibanov, 1988b). In fact, this activating effect of water can be mimicked by other solvents capable of forming multiple hydrogen bonds, such as alcohols (Klibanov, 2001).

Besides changing enzyme flexibility, the solvation water can affect catalytic activity by affecting specific details of the active site hydration. The observed decrease in enzyme activity with increasing organic solvent polarity reflects the tendency of these solvents to strip water molecules from the enzyme surface, and the extent of water stripping increases with the OS polarity (Yang *et al.*, 2004).

The bound water is usually measured experimentally in terms of the thermodynamic activity of water (a_w), assuming that the level of water associated with the enzyme is essentially the same in different solvents at fixed a_w (Bell *et al.*, 1995; Partridge *et al.*, 1998; Gupta and Roy, 2004). The same enzyme placed in different aqueous/organic mixtures with the same water activity has similar catalytic constants, which supports the idea that it is the enzyme bound water that modulates the catalytic properties of the enzyme. Although there is a good correlation between the thermodynamic activity of water and the amount of hydration water, it does not always capture the true partitioning of water molecules between enzyme and the bulk organic solvent (Bell *et al.*, 1997). And once more this relationship does not hold for

A

	res no.	a.a.	Variation (nm)
catalytic triads	32	Asp/D	-0.01
	33	Thr/T	-0.01
	34	Gly/G	0.08
	215	Asp/D	-0.01
	216	Ser/S	-0.05
	217	Gly/G	-0.01
S'3	36	Ser/S	0.02
	37	Ser/S	0.01
	73	Ile/I	-0.02
	128	Thr/T	0.02
	132	Ile/I	0.03
	188	Tyr/Y	0
S'2	34	Gly/G	0.08
	35	Ser/S	0
	74	Ile/I	-0.02
	76	Tyr/Y	0.04
	189	Tyr/Y	-0.01

	res no.	a.a.	Variation (nm)
S'1	76	Gly/G	0.14
	181	Tyr/Y	0.01
	213	Phe/F	-0.01
	289	Met	0.08
	300	Ile	-0.02
S1	75	Tyr	0.04
	77	Thr	0.21
	112	Phe	0
	117	Phe	0
	120	Ile	0
	128	Thr	0.02
	217	Gly	-0.01
S2	76	Gly	0.14
	79	Thr	0.04
	218	Thr	-0.03
S3	13	Ser	-0.02
	115	Arg	-0.01
	117	Phe	0
	219	Ser	0.01

B

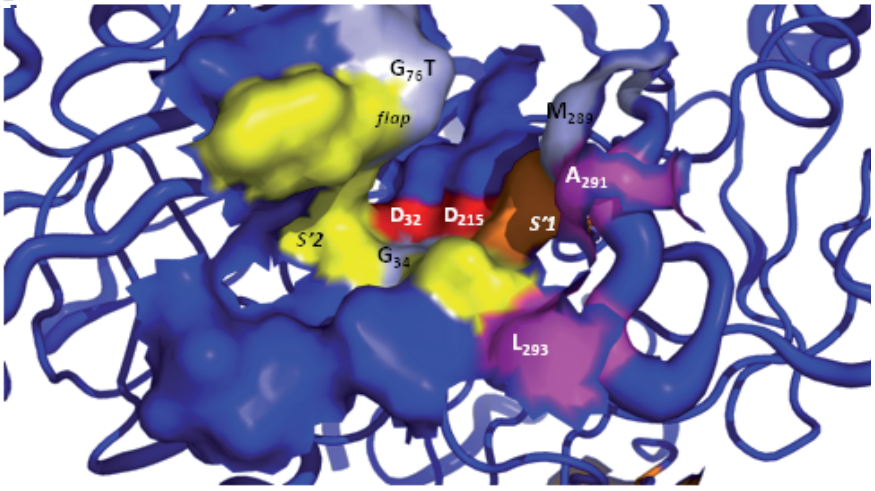

Figure 5.9 – Analysis of the active site residues with higher RMS fluctuation between 0% and 90% TFE. A – Table presenting the active site residues and its variation values. Variation values higher than 0.5 Å are highlighted, and values higher than 1 Å are written in red. B – Active site cleft represented in surface mode with the catalytic aspartates in red, some sub-site specificity mapped (S'1 in orange and S'2 in yellow), and residues with high mobility in light blue. Not participating in the catalytic cleft other high variation residues close located are represented in magenta. The representation was created using *PyMOL* software (DeLano *Scientific LLC*).

polar solvents such as alcohols, where higher water concentrations are required to reach a particular a_w. The capability of acting as hydrogen bond partners with the protein, replacing water, makes water activity comparisons useless (Bell *et al.*, 1997). The decrease in water activity on increasing alcohol concentration might be stronger for alcohols such as hexafluoropropanol and TFE, which have a pronounced tendency to form clusters (Gast *et al.*, 1999).

Cardosin A active cleft sensed the medium alterations. Figure 5.10 compares the two simulation structures (in water: A and D, in 90% TFE: B and E) and the crystal coordinates (C). In the last acquired conformation of the TFE simulation, the active site surface is also filled in with alcohol molecules, along with some water molecules (figure 5.10 - B). As typically, the enzyme surface and the active site region are well hydrated in aqueous medium. TFE stripped the hydration waters from the enzyme surface and active site, confirming the previously studied solvent behaviour. MD simulations ran by Yang *et al.* (2004) showed that water stripping is accompanied by the penetration of polar OS molecules (tetrahydrofuran and acetonitrile) into surface crevices and into the active site. Polar solvents replaced mobile and weakly bound water molecules in the active site and left primarily the tightly bound water in that region. On the other hand, the lack of water stripping in non-polar OS (octane) allowed efficient and uniform hydration of the active site by mobile and weakly bound water and some structural water similar to that in aqueous solution. In addition to polarity, the ability of penetration of the solvent will also depend to some extent on the overall size of the solvent molecules (Yang *et al.*, 2004).

The water molecules that resisted TFE striping attack on cardosin A active site (figure 5.10 – B and E) are thus the more tightly bond

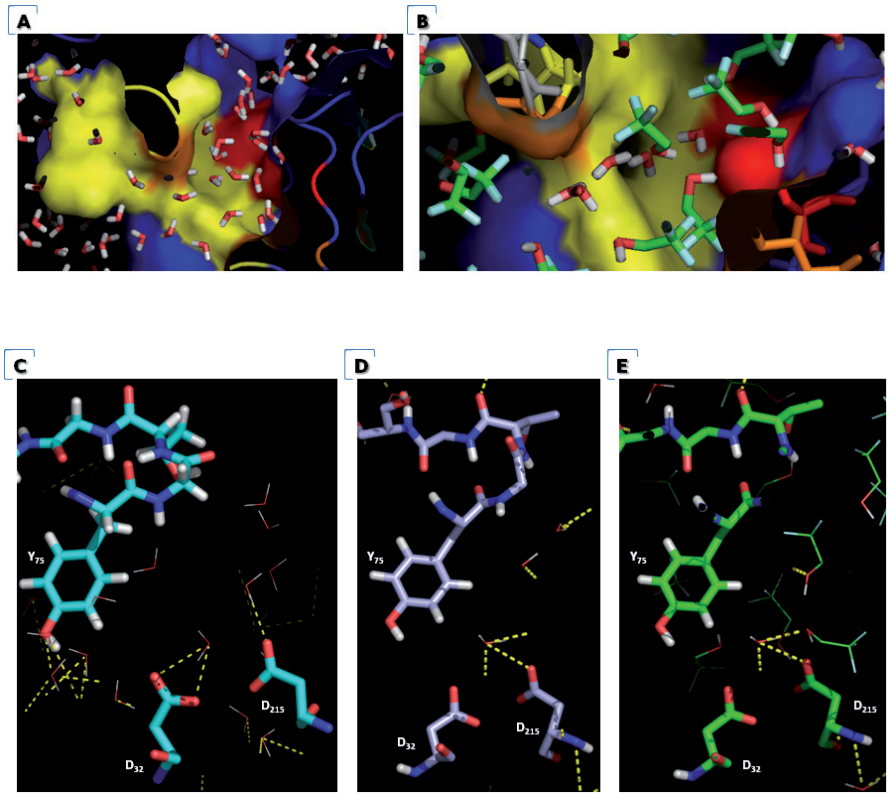

Figure 5.10 – Spatial distribution of solvent molecules in the active site of cardosin A crystal structure (**C**), in the first 10 ns of the MD simulation in water (A and D), and the last acquired conformation of the MD simulation 90% TFE (B and E). A and B - Active site cleft represented in surface mode with the catalytic aspartates in red and some sub-site specificity mapped (S'1 in orange and S'2 in yellow). Solvent molecules are represented as sticks and coloured according to the CPK coloring scheme (red: oxygen, white: hydrogen, green: carbon, light blue: fluorine). B, C and D – Representation of the catalytic aspartates and flap residues (sticks), solvent molecules (lines) and polar interactions (yellow dashes). The representations were created using *PyMOL* software (DeLano *Scientific LLC*).

and actively important. Beyond its solvent role, water molecules mediate enzymatic catalysis: either directly by taking part in the reaction, or indirectly through providing a solvation medium for reactants, transition state, and products (Fersht, 1999). In the aspartic protease catalytic reaction one water molecule, located between the active carboxyl, plays the role of nucleophile, and another water molecule conserved at the vicinity of the active groups forms of a chain of hydrogen-bonded residues between the active site flap and the active carboxyls on ligand binding (Andreeva and Rumsh, 2001).

Observation of snapshots from the simulations in aqueous medium, 90% TFE and of the protein crystal structure can be done in figure 5.10 (D, E and C, respectively). The entrance of TFE molecules on the active site may thus have potential consequences in catalysis. However, single TFE molecules are not perceived bound to specific zones of the active site, suggesting that the interaction between the OS and the protein is fluid like. In the cardosin A crystal, each catalytic aspartate is interacting with a water molecule, while in the simulations snapshots only one aspartate (Asp215) maintains this interaction, and the TFE presence is not impairing this H-bonding to the catalytic water. The proximity of TFE molecules may have disabled other polar interactions with water molecules, but did not replace them.

Sites with similar characteristics, including amino acids sequence homology, have been observed as alcohol common binding sites in other proteins (Dwyer and Bradley, 2000). Pepsin, the archetype of the AP class, has been crystallised in 20% ethanol (Abad-Zapatero *et al.*, 1990). There were ethanol molecules in H-bond donation to backbone carbonyl groups at Ser36 and Ile128, and also H-bond formation to side-chain group of Ser219. The cardosin A correspondent residues found by structural align-

ment (cardosin A PBD 1B5F vs. porcine pepsin in 20% ethanol PDB 3PEP) are 1B5F-Ser36, 1B5F-Thr128 and 1B5F-Ser219, all residues participating in specificity sub-sites. When compared, TFE is a better H-bond donor, and is more polar than ethanol (see section 7, table 7.1), and so these residues may be nominated as good candidates for the fluoroalcohol interaction. Being these residues responsible for interacting with the substrate, this capacity for H-bond with the OS emphasizes the hypothesis of enzyme activity decrease by competition.

Moreover, the simple presence of TFE may well be disabling the substrate access to cardosin A active site. Besides possible conformational alterations that may have changed the affinity for the (MCA-Lys)Lys-Pro-Ala-Glu-Phe-Phe-Ala-Leu(Lys-DNP) peptide, and despite no major changes have been noticed in the active site cleft conformation, the presence of TFE molecules may certainly preclude the catalytic activity. No secondary structure has been found for the peptide in TFE by CD spectra (section 4.2, figure 4.8). But its solvation should also be taken into account.

When considering the presence of the alcohol on the active site as the main reason for the peptidolytic activity loss, the reactivation of the enzyme upon dilution in water medium is easy to understand. The new water molecules would wash out the excess TFE, and compete with the remaining alcohol molecules for the totality of the protein surface. By this way the active cleft would also be left free for hydration, which would repair the activity previously lost.

6. CONCLUSIONS

This work project followed the conformational alterations of an aspartic proteinase promoted by the presence of trifluoroethanol in its vicinity. The different conformational states of cardosin A were monitored and characterised by a combination of *in vitro* (by intrinsic fluorescence, far-UV circular dichroism, differential scanning calorimetry, and size exclusion chromatography) and *in silico* techniques (by molecular dynamics simulations). These results were followed by functional evaluation (through peptidolytic activity measurements *in vitro*).

The presence of 4% TFE content in the medium promoted a decreased structural stability, but also an increase in cardosin A peptidolytic activity (33-59%). A diminished protein stability was detected by calorimetry. This subtle conformational adjustment might have occurred in response to modifications of the solvation layer of the protein, as suggested by the hydrodynamic results

for the lowest TFE contents tested. No alterations were detected in cardosin A secondary or tertiary structures, neither by spectroscopic techniques nor by MD simulations. This conformational alteration was interpreted as reversible. The protein return to aqueous media recovered activity values to normal. These results reinforce the enzyme biological function as being dependent on the delicate relationship with its environment. The structural machine showed to present some structural flexibility before losing its purpose.

Nevertheless, the activity recovery was not possible for higher TFE percentages. TFE medium content over 20% irreversibly inactivated cardosin A, probably due to the detected tertiary structure unfolding, which was characterised as partially reversible. This conformational state showed interesting features, since it was detected some increase in secondary structures content, along with the opening of the native conformation.

The described structural ordering tendency of TFE was intensified for concentrations higher than 70%. A considerable increase in the helicity of cardosin secondary structure was detected, despite the opened tertiary conformation. These characteristic "open helical conformations" promoted by TFE showed to be reversible upon solubilisation in aqueous media, with partial recovery of activity and tryptophans burying.

MD simulations with TFE and water described local alterations in protein flexibility, but no large conformational transformations. Instead, the model could offer an exposition of local competition of TFE with water for surface solvation. TFE molecules were found replacing several hydration molecules in the active site. Despite the catalytic water was not lost in the last acquired conformation of the high TFE content MD simulation, the active site was occupied by several TFE molecules, and this occurrence may

justify the activity loss. The same reasoning would explain the activity recovery upon aqueous dilution, with the release of the active site for substrate binding.

It is our belief that the present work contributed to the comprehension of aspartic proteinases conformational native state as a flexible and mutable form.

7. ANNEXE

Table 7.1 – Chemical and physical parameters for water, ethanol and 2,2,2-trifluoroethanol (TFE). References: [1] Buck, 1998; [2] Perham *et al.*, 2006.

	water	**ethanol**	**TFE**
Molecular formula	H_2O	CH_3CH_2OH	CF_3CH_2OH
Dipole moment (D)	1.84 [2]	1.69 [2]	2.52 [2]
Dielectric constant at 25º C	78.5 [1]	25 [2]	27 [1]
Size (compared to water)			9x
Molecular mass (g/mol)	18.0153	46.07	100.04
Density (g/ml)	0.998	0.789	1.393

8. REFERENCES

Abad-Zapatero C, Rydel TJ, Erickson J. 1990. Revised 2.3 Å structure of porcine pepsin: evidence for a flexible subdomain. *Proteins*, 8: 62–81.

Abbate S, Barlati S, Colombi M, Fornili SL, Francescato P, Gangemi F, Lebon F, Longhi G, Manitto P, Recca T, Speranza G, Zoppi N. 2006. Study of conformational properties of a biologically active peptide of fibronectin by circular dichroism, NMR and molecular dynamics simulation. *Phys Chem Chem Phys*, 8 (40): 4668-4677.

Ahmad S, Gromiha M, Fawareh H, Sarai A. 2004. *ASAView*: Database and tool for solvent accessibility representation in proteins. *BMC Bioinformatics*, 5: 51.

Akitake B, Spelbrink REJ, Anishkin A, Killian JA, de Kruijff B, Sukharev S. 2007. 2,2,2-Trifluoroethanol Changes the Transition Kinetics and Subunit Interactions in the Small Bacterial Mechanosensitive Channel MscS. *Biophysical Journal*, 92: 2771–2784.

Andreeva NS, Rumsh LD. 2001. Analysis of crystal structures of aspartic proteinases: On the role of amino acid residues adjacent to the catalytic site of pepsin-like enzymes. *Protein Sci*, 10: 2439-2450.

Bahnson BJ, Colby TD, Chin JK, Goldstein BM, Klinman JP. 1997. A link between protein structure and enzyme catalyzed hydrogen tunnelling. *PNAS*, 94: 12797-12802.

Baldwin RL. 1991. Molten globules: Specific or nonspecific folding intermediates? *Chemtracts Biochem Mol Biol*, 2: 379-389.

Ball P. 2002. *H_2O – Uma biografia da água*. Ed. Temas e Debates, Lisboa.

Ball P. 2008. Water as an active constituent in cell biology. *Chem Rev*, 108 (1): 74-108.

Banerjee T, Kishore N. 2005. Does the Anesthetic 2,2,2- Trifluoroethanol Interact with Bovine Serum Albumin by Direct Binding or by Solvent-Mediated Effects? A Calorimetric and Spectroscopic Investigation. *Biopolymers*, 78: 78–86.

Barker JA, Watts RO. 1973. Monte-Carlo studies of dielectric properties of water-like models. *Mol Phys*, 26 (3): 789-792.

Barrett AJ, Rawlings ND, Woessner JF. 1998. *The Handbook of Proteolytic Enzymes*. Academic Press, San Diego, chapters 270-272.

Barros MT, Carvalho MGV, Garcia FAP, Pires EMV. 1992. Stability performance of *Cynara cardunculus* L. acid protease in aqueous-organic biphasic systems. *Biotech Lett*, 14 (3): 179-184.

Barros RM, Malcata FX. 2006. Molecular Characterization of Peptides Released from β-Lactoglobulin and α-Lactalbumin via Cardosins A and B. *J Dairy Sci*, 89: 483-494.

Baskakov IV, Kumar R, Srinivasan G, Ji Y, Bolen DW, Thompson EB. 1999. Trimethylamine N-Oxide-induced Cooperative Folding of an Intrinsically Unfolded Transcription-activating Fragment of Human Glucocorticoid Receptor. *JBC*, 274: 10693-10696.

Bell G, Halling PJ, Moore BD, Partridge J, Rees G. 1995. Biocatalytic behaviour in low-water systems. *Trends in Biotechnology,* 13: 468-473.

Bell G, Janssen AEM, Halling PJ. 1997. Water activity fails to predict critical hydration level for enzyme activity in polar organic solvents: interconversion of water concentrations and activities. *Enzyme Microb Technol*, 20: 471–477.

Benach J, Meijers R, Atrian S, Gonzalez-Duarte R, Lamzin VS, Ladenstein R. 1.1-A crystal structure of D. lebanonensis ADH complexed with NAD+ and 2,2,2-trifluoroethanol. *To be published.*

Berendsen HJC, Postma JPM, van Gunsteren WF, DiNola A, Haak JR. 1984. Molecular-dynamics with coupling to an external bath. *J Chem Phys*, 81 (8): 3684-3690.

Berman HM, Westbrook J, Feng Z, Gilliland G, Bhat TN, Weissig H, Shindyalov IN, Bourne PE. 2000. The Protein Data Bank. *Nucleic Acids Res*., 28: 235-242.

Bhakuni V. 1998. Alcohol-Induced Molten Globule Intermediates of Proteins: Are They Real Folding Intermediates or Off Pathway Products? *Archives of Biochemistry and Biophysics*, 357 (2): 274–284.

Bieri O, Kiefhaber T. 1999. Elementary Steps in Protein Folding. *Biol Chem*, 380: 923–929.

Bour P, Kim J, Kapitan J, Hammer RP, Huang R, Wu L, Keiderling TA. 2008. Vibrational circular dichroism and IR spectral analysis as a test of theoretical conformational modeling for a cyclic hexapeptide. *Chirality*, 20 (10): 1104-1119.

Branden C, Tooze J. 1999. *Introduction to Protein Structure*. 2nd Ed., Garland Publishing Inc., New York, USA.

Brodelius PE, Cordeiro MC, Pais MS. 1995. Aspartic proteinases (cyprosins) from Cynara cardunculus spp. Flavescens cv. cardoon; purification, characterisation, and tissue-specific expression. *Adv Exp Med Biol*, 362: 255-266.

Buck M, Radford SE, Dobson CM. 1993. A Partially Folded State of Hen Egg White Lysozyme in Trifluoroethanol: Structural Characterization and Implications for Protein Folding. *Biochemistry*, 32: 669-678.

Buck M. 1998. Trifluoroethanol and colleagues: cosolvents come of age. Recent studies with peptides and proteins. *Quarterly Reviews of Biophysics,* 31 (3): 297-355.

Caflisch A, Paci E. 2005. Molecular Dynamics Simulations to Study Protein Folding and Unfolding. In: Buchner J, Kiefhaber T. eds. *Protein folding handbook*. Part I. Wiley-VCH Verlag GmbH & Co. KGaA, Weinheim. Chapter 32.

Cammers-Goodwin A, Allen TJ, Oslick SL, McClure KF, Lee JH, Kemp DS. 1996. Mechanism of Stabilization of Helical Conformations of Polypeptides by Water Containing Trifluoroethanol. *J Am Chem Soc*, 118: 3082-3090.

Castanheira P, Samyn B, Sergeant K, Clemente JC, Dunn BM, Pires E, Beeumen JV, Faro C. 2005. Activation, Proteolytic Processing, and Peptide Specificity of Recombinant Cardosin A. *JBC*, 280: 13047-13054.

Chatterjee C, Gerig JT. 2007. Interactions of Trifluroethanol with the Trp-Cage Peptide. *Biopolymers*, 87: 115–123.

Chiang CM, Chang SL, Lin HJ, Wu WG. 1996. The role of acidic amino acid residues in the structural stability of snake cardiotoxins. *Biochemistry*, 35 (28): 9177-9186.

Chitra R, Smith PE. 2001. Properties of 2,2,2-trifluoroethanol and water mixtures. *J Chem Phys*, 114 (1): 426-435.

Colby TD, Bahnson BJ, Chin JK, Klinman JP, Goldstein BM. 1998. Active site modifications in a double mutant of liver alcohol dehydrogenase: structural studies of two enzyme-ligand complexes. *Biochemistry*, 37 (26): 9295-9304.

Colombo G, Toba S, Merz KM. 1999. Rationalization of the enantioselectivity of subtilisin in DMF. *J Am Chem Soc*, 121: 3486–3493.

Cooper A, Nutley MA, Wadood A. 2000. Differential scanning microcalorimetry. In: Harding SE, Chowdhry BZ. Eds. *Protein-Ligand Interactions: hydrodynamics and calorimetry*. Oxford University Press, Oxford New York. p 287-318.

Cooper JB. 2002. Aspartic proteinases in disease: a structural perspective. *Curr Drug Targets*, 3 (2): 155-173.

Cooper A. 2004. *Biophysical Chemistry*. The Royal Society of Chemistry, Cambridge, UK. Chapter 2.

Corrêa F, Farah CS. 2007. Different Effects of Trifluoroethanol and Glycerol on the Stability of Tropomyosin Helices and the Head-to-Tail Complex. *Biophys J*, 92: 2463–2475.

Costa J, Ashford DA, Nimtz M, Bento I, Frazão C, Esteves CL, Faro CJ, Kervinen J, Pires E, Verissimo P, Wlodawer A, Carrondo MA. 1997. The glycosylation of the aspartic proteinases from barley (*Hordeum vulgare* L.) and cardoon (*Cynara cardunculus* L.). *Eur J Biochem*, 243 (3): 695-700.

Creighton TE. 1990. Protein folding. *Biochem J*, 270 (1): 1-16.

Daggett V, Fersht AR. 2003. Is there a unifying mechanism for protein folding? *TRENDS Biochem Sci*, 28 (1): 18-25.

Daidone I, Simona F, Roccatano D, Broglia RA, Tiana G, Colombo G, Nola AD. 2004. Beta-hairpin conformation of fibrillogenic peptides: structure and alpha-beta transition mechanism revealed by molecular dynamics simulations. *Proteins*, 57 (1): 198-204.

Damadian R. 1971. Tumor Detection by Nuclear Magnetic Resonance. *Science*, 171: 1151-1153.

Daughdrill GW, Pielak GJ, Uversky VN, Cortese MS, Dunker AK. 2005. Natively disordered proteins. In: Buchner J, Kiefhaber T. eds. *Protein folding handbook*. Part II. Wiley-VCH Verlag GmbH & Co. KGaA, Weinheim. Chapter 8.

Dechene M, Wink G, Smith M, Swartz P, Mattos C. 2009. Multiple solvent crystal structures of ribonuclease A: An assessment of the method. *Proteins,* 76 (4): 861-881.

Deshpande A, Nimsadkar S, Mande SC. 2005. Effect of alcohols on protein hydration: crystallographic analysis of hen egg-white lysozyme in the presence of alcohols. *Acta Crystallogr D Biol Crystallogr*, 61 (Pt 7): 1005-1008.

Desveaux D, Singer AU, Wu AJ, McNulty BC, Musselwhite L, Nimchuk Z, Sondek J, Dangl JL. 2007. Type III Effector Activation via Nucleotide Binding, Phosphorylation, and Host Target Interaction. *Plos Pathog*, 3: e48.

Díaz MD, Fioroni M, Burger K, Berger S. 2002. Evidence of Complete Hydrophobic Coating of Bombesin by Trifluoroethanol in Aqueous Solution: An NMR Spectroscopic and Molecular Dynamics Study. *Chem Eur J*, 8 (7): 1663-1669.

Dill KA, Bromberg S, Yue K, Fiebig KM, Yee DP, Thomas PD, Chan HS. 1995. Principles of protein folding -A perspective from simple exact models. *Protein Sci*, 4: 561-602.

Dill KA, Ozkan SB, Weikl TR, Chodera JD, Voelz VA. 2007. The protein folding problem: when will it be solved? *Current Opinion in Structural Biology*, 17 (3): 342-346.

Dixit S, Crain J, Poon WC, Finney JL, Soper AK. 2002. Molecular segregation observed in a concentrated alcohol-water solution. *Nature*, 416 (6883): 829-832.

Dobbins SE, Lesk VI, Sternberg MJE. 2008. Insights into protein flexibility: The relationship between normal modes and conformational change upon protein–protein docking. *PNAS*, 105: 10390-10395.

Dong A, Matsuura J, Manning MC, Carpenter JF. 1998. Intermolecular β-sheet results from trifluoroethanol-induced nonnative α-helical structure in β-sheet predominant proteins: infrared and circular dichroism spectroscopic study. *Arch Biochem Biophys*, 355 (2): 275-281.

Duarte AS, Pereira AO, Cabrita AMS, Moir AJG, Pires EMV, Barros MT. 2005. The characterisation of the collagenolytic activity of cardosin A demonstrates its potential application for extracellular matrix degradative processes. *Curr Drug Discov Technol*, 2: 37-44.

Duarte P, Figueiredo R, Pereira S, Pissarra J. 2006. Structural characterization of the stigma-style complex of *Cynara cardunculus* (Asteraceae) and immunolocalization of cardosins A and B during floral development. *Can J Bot*, 84: 737–749.

Duarte P, Pissarra J, Moore I. 2008a. Processing and trafficking of a single isoform of the aspartic proteinase cardosin A on the vacuolar pathway. *Planta*, 227(6): 1255-1268.

Duarte AS, Duarte EP, Correia A, Pires E, Barros MT. 2008b. Cardosins improve neuronal regeneration after cell disruption: a comparative expression study. *Cell Biol Toxicol*, DOI 10.1007/s10565-008-9058-x.

Dunn BM. 2002. Structure and mechanism of the pepsin-like family of aspartic peptidases. *Chem Rev*, 102 (12): 4431-4458.

Dwyer DS, Bradley RJ. 2000. Chemical properties of alcohols and their protein binding sites. *Cell Mol Life Sci*, 57 (2): 265-275.

Egas C, Lavoura N, Resende R, Brito RMM, Pires E, Lima MCP, Faro C. 2000. The Saposin-like Domain of the Plant Aspartic Proteinase Precursor Is a Potent Inducer of Vesicle Leakage. *JBC*, 275: 38190-38196.

Ellis RJ. 2001. Macromolecular crowding: obvious but underappreciated. *Trends Biochem Sci*, 26 (10): 597-604.

Ellis RJ, Minton AP. 2006. Protein aggregation in crowded environments. *Biol Chem*, 387 (5): 485-497.

Engel R, Westphal AH, Huberts DHEW, Nabuurs SM, Lindhoud S, Visser AJWG, van Mierlo CPM. 2008. Macromolecular Crowding Compacts Unfolded Apoflavodoxin and Causes Severe Aggregation of the Off-pathway Intermediate during Apoflavodoxin Folding. *J Biol Chem*, 283: 27383-27394.

Fan P, Bracken C, Baum J. 1993. Structural characterization of monellin in the alcohol-denatured state by NMR: evidence for β-sheet to α-helix conversion. *Biochemistry*, 32: 1573–1582.

Faro C, Ramalho-Santos M, Vieira M, Mendes A, Simões I, Andrade R, Veríssimo P, Lin X, Tang J, Pires E. 1999. Cloning and Characterization of cDNA Encoding Cardosin A, an RGD-containing Plant Aspartic Proteinase. *JBC*, 274: 28724-28729.

Fatima S, Ahmad B, Khan RH. 2006. Fluoroalcohols induced unfolding of Succinylated Con A: native like β-structure in partially folded intermediate and α-helix in molten globule like state. *Arch Biochem Biophys*, 454 (2): 170-80.

Fersht A. 1999. *Structure and Mechanism in Protein Science: A Guide to Enzyme Catalysis and Protein Folding.* WH Freeman, New York.

Fink AL. 1995. Compact intermediate states in protein folding. *Annu Rev Biophys Biomol Struct*, 24: 495-522.

Fioroni M, Burger K, Mark AE, Roccatano D. 2000. A New 2,2,2-Trifluoroethanol

Model for Molecular Dynamics Simulations. *J Phys Chem B*, 104: 12347-12354.

Fleming PJ, Rose GD. 2005. Conformational properties of unfolded proteins. In: Buchner J, Kiefhaber T. eds. *Protein folding handbook*. Part I. Wiley-VCH Verlag GmbH & Co. KGaA, Weinheim. Chapter 20.

Flöck D, Daidone I, Nola AD. 2004. A molecular dynamics study of acylphosphatase in aggregation-promoting conditions: the influence of trifluoroethanol/water solvent. *Biopolymers*, 75 (6): 491-496.

Fraczkiewicz R, Braun W. 1998. Exact and efficient analytical calculation of the accessible surface areas and their gradients for macromolecules. *J. Comp. Chem.*, 19 (3): 319-333.

Frazão C, Bento I, Costa J, Soares CM, Veríssimo P, Faro C, Pires E, Cooperi J, Carrondo MA. 1999. Crystal Structure of Cardosin A, a Glycosylated and Arg-Gly-Asp-containing Aspartic Proteinase from the Flowers of *Cynara cardunculus* L. *JBC*, 294 (39): 27694-27701.

Gast K, Zirwer D, Muller-Frohne M, Damaschun G. 1998. Compactness of the kinetic molten globule of bovine α-lactalbumin: A dynamic light scattering study. *Protein Science*, 7: 2004-2011.

Gast K, Zirwer D, Muller-Frohne M, Damaschun G. 1999. Trifluoroethanol-induced conformational transitions of proteins: Insights gained from the differences between α-lactalbumin and ribonuclease A. *Protein Science*, 8:625–634.

Gast K, Siemer A, Zirwer D, Damaschun G. 2001. Fluoroalcohol-induced structural changes of proteins: some aspects of cosolvent-protein interactions. *Eur Biophys J*, 30: 273-283.

Giardini A, Rondino F, Cattenacci G, Paladini A, Piccirillo S, Satta M, Speranza M. 2007. Van der Waals interactions in a monosolvated chiral fluorinated molecule: R2PI vibroelectronic spectra of (R)-1-phenyl-2,2,2-trifluoroethanol clustered with water. *Chem Phys Lett*, 435: 230–235.

Gopal R, Park SC, Ha KJ, Cho SJ, Kim SW, Song PI, Nah JW, Park Y, Hahm KS. 2009. Effect of Leucine and Lysine substitution on the antimicrobial activity and evaluation of the mechanism of the HPA3NT3 analog peptide. *J Pept Sci*, 15 (9): 589-594.

Guha S, Sahu K, Roy D, Mondal SK, Roy S, Bhattacharyya K. 2005. Slow solvation dynamics at the active site of an enzyme: implications for catalysis. *Biochemistry*, 44 (25): 8940-8947.

Gupta MN, Roy I. 2004. Enzymes in organic media - Forms, functions and applications. *Eur J Biochem*, 271: 2575–2583.

Halle B, Denisov VP, Modig K, Davidovic M. 2005. Protein conformational transitions as seen from the solvent: magnetic relaxation dispersion studies of water, co-solvent, and denaturant interactions with nonnative proteins. In: Buchner J, Kiefhaber T. eds. *Protein folding handbook*. Part I. Wiley-VCH Verlag GmbH & Co. KGaA, Weinheim. Chapter 8.

Halling PJ. 2004. What can we learn by studying enzymes in non-aqueous media? *Philos Trans R Soc Lond B Biol Sci*, 359 (1448): 1287-1296.

Hamada D, Chiti F, Guijarro JI, Kataoka M, Taddei N, Dobson CM. 2000. Evidence concerning rate-limiting steps in protein folding from the effects of trifluoroethanol. *Nat Struct Biol*, 7 (1): 58-61.

Hamada D, Goto Y. 2005. Alcohol- and salt-induced partially folded intermediates. In: Buchner J, Kiefhaber T. eds. *Protein folding handbook*. Part I. Wiley-VCH Verlag GmbH & Co. KGaA, Weinheim. Chapter 24.

Henchman RH, McCammon JA. 2005. Protein structural flexibility: molecular motions. *Enc Life Sciences*, 10.1038/npg.els.0003012.

Hermans J, Berendsen HJC, van Gunsteren WF, Postma JPM. 1984. A consistent empirical potential for water-protein interactions. *Biopolymers*, 23 (8): 1513-1518.

Hess B, Bekker H, Berendsen HJC, Fraaije JGEM. 1997. LINCS: A linear constraint solver for molecular simulations. *J Comput Chem*, 18 (12): 1463-1472.

Hess B, Kutzner C, van der Spoel D, Lindahl E. 2008. GROMACS 4: Algorithms for Highly Efficient, Load-Balanced, and Scalable Molecular Simulation. *Journal of Chemical Theory and Computation*, 4 (3): 435-447.

Homouz D, Perham M, Samiotakis A, Cheung MS, Stafshede PW. 2008. Crowded, cell-like environment induces shape changes in aspherical protein. *PNAS*, 105: 11754-11759.

Hong D, Hoshino M, Kuboi R, Goto Y. 1999. Clustering of Fluorine-Substituted Alcohols as a Factor Responsible for Their Marked Effects on Proteins and Peptides. *J Am Chem Soc*, 121: 8427-8433.

Huang K, Park YD, Cao ZF, Zhou HM. 2001. Reactivation and refolding of rabbit muscle creatine kinase denatured in 2,2,2-trifluoroethanol solutions. *Biochim Biophys Acta*, 1545: 305-313.

Humphrey W, Dalke A, Schulten K. 1996. VMD - Visual Molecular Dynamics, *J Molec Graphics*, 14: 33-38.

Iwasaki K, Fujiyama T. 1977. Light-Scattering Study of Clathrate Hydrate Formation in Binary Mixtures of *tert*-Butyl Alcohol and Water. *J Phys Chem*, 81 (20): 1908-1912.

Jackson M, Mantsch HH. 1992. Halogenated alcohols as solvents for proteins: FTIR spectroscopic studies. *Biochim Biophys Acta*, 1118 (2): 139-143.

Jasanoff A, Fersht AR. 1994. Quantitative Determination of Helical Propensities from Trifluoroethanol Titration Curves. *Biochemistry*, 33: 2129-2135.

Jamison JL, Davenport L, Williams BW. 2006. Solvatochromism in the aromatic ketone benzo[*b*]fluorenone. *Chemical Physics Letters*, 422: 30–35.

Jasanoff A, Fersht AR. 1994. Quantitative Determination of Helical Propensities from Trifluoroethanol Titration Curves. *Biochemistry*, 33: 2129-2135.

Javid N, Vogtt K, Krywka C, Tolan M, Winter R. 2007. Protein–Protein Interactions in Complex Cosolvent Solutions. *Chem Phys Chem*, 8: 679 – 689.

Jones DT. 1999. Protein secondary structure prediction based on position-specific

scoring matrices. *J Mol Biol*, 292: 195-202.

Kaur K, Andrew LC, Wishart DS, Vederas JC. 2004. Dynamic relationships among type IIa bacteriocins: temperature effects on antimicrobial activity and on structure of the C-terminal amphipathic alpha helix as a receptor-binding region. *Biochemistry*, 43 (28): 9009-9020.

Kaur K, Sprules T, Soliman W, Beleid R, Ahmed S. 2008. Right-handed 14-helix in beta 3-peptides from L-aspartic acid monomers. *Biochim Biophys Acta*, 1784 (4): 658-665.

Kelly SM, Price NC. 2000. The use of circular dichroism in the investigation of protein structure and function. *Curr Protein Pept Sci*, 1 (4): 349-84.

Kelly SM, Jess TJ, Price NC. 2005. How to study proteins by circular dichroism. *Biochimica et Biophysica Acta*, 1751:119–139.

Kentsis A, Sosnick TR. 1998. Trifluoroethanol Promotes Helix Formation by Destabilizing Backbone Exposure: Desolvation Rather than Native Hydrogen Bonding Defines the Kinetic Pathway of Dimeric Coiled Coil Folding. *Biochemistry*, 37: 14613-14622.

Kerrien S, Alam-Faruque Y, Aranda B, Bancarz I, Bridge A, Derow C, Dimmer E, Feuermann M, Friedrichsen A, Huntley R, Kohler C, Khadake J, Leroy C, Liban A, Lieftink C, Montecchi-Palazzi L, Orchard S, Risse J, Robbe K, Roechert B, Thorneycroft D, Zhang Y, Apweiler R, Hermjakob H. 2007. IntAct—open source resource for molecular interaction data. *Nucleic Acids Res*, 35: D561-D565.

Kervinen J, Tobin GJ, Costa J, Waugh DS, Wlodawer A, Zdanov A. 1999. Crystal structure of plant aspartic proteinase prophytepsin: inactivation and vacuolar targeting. *EMBO J*, 18 (14): 3947-3955.

Khan AR, James MNG. 1998. Molecular mechanisms for the conversion of zymogens to active proteolytic enzymes. *Prot Sci*, 7: 815-836.

Khan AR, Khazanovich-Bernstein N, Bergmann EM, James MNG. 1999. Structural aspects of activation pathways of aspartic protease zymogens and viral 3C protease precursors. *PNAS*, 96: 10968-10975.

Kiselev M, Noskov S, Puhovski Y, Kerdcharoen T, Hannongbua S. 2001. The study of hydrophobic hydration in supercritical water-methanol mixtures. *J Mol Graph Model*, 19 (5): 412-416.

Klibanov AM. 1997. Why are enzymes less active in organic solvents than in water? *Trends Biotechnol*, 15 (3): 97-101.

Klibanov AM. 2001. Improving enzymes by using them in organic solvents. *Nature*, 409 (6817): 241-246.

Koenig SH, Hallenga K, Shporer M. 1975. Protein-Water Interaction Studied by Solvent ^{1}H, ^{2}H, and ^{17}O Magnetic Relaxation. *PNAS*, 72: 2667-2671.

Kohl NE, Emini EA, Schleif WA, Davis LJ, Heimbach JC, Dixon RAF, Scolnick EM, Sigal IS. 1988. Active Human Immunodeficiency Virus Protease is Required for Viral Infectivity. *PNAS*, 85: 4686-4690.

Kumar S, Nussinov R. 2002. Close-range electrostatic interactions in proteins.

Chembiochem, 3 (7): 604-617.

Kundu A, Kishore N. 2004. Interaction of 2,2,2-trifluoroethanol with proteins: calorimetric, densimetric and surface tension approach. *Biophys Chem*, 109 (3): 427-442.

Kuprin S, Gräslund A, Ehrenberg A, Koch MHJ. 1995. Nonideality of water-hexafluoropropanol mixtures as studied by X-ray Small Angle Scattering. *BBRC*, 217 (3): 1151-1156.

Laemmli UK. 1970. Cleavage of structural proteins during the assembly of the head of bacteriophage T4. *Nature* 15:227, 680-5.

Lazaridis T, Karplus M. 2003. Thermodynamics of protein folding: a microscopic view. *Biophys Chem*, 100 (1-3): 367-395.

Lepock JR, Ritchie KP, Kolios MC, Rodahl AM, Heinz KA, Kruuv J. 1992. Influence of Transition Rates and Scan Rate on Kinetic Simulations of Differential Scanning Calorimetry Profiles of Reversible and Irreversible Protein Denaturation. *Biochemistry*, 31: 12706-12712.

Levine IN. 1995. *Physical Chemistry.* 4th Edition, McGraw-Hill, Inc., Singapore.

Liaudet-Coopman E, Beaujouin M, Derocq D, Garcia M, Glondu-Lassis M, Laurent-Matha V, Prebois C, Rochefort H, Vignon F. 2006. Cathepsin D: newly discovered functions of a long-standing aspartic protease in cancer and apoptosis. *Cancer Lett*, 237 (2): 167-179.

Liu ZP, Rizo J, Gierasch LM. 1994. Equilibrium folding studies of cellular retinoic acid binding protein, a predominantly beta-sheet protein. *Biochemistry*, 33 (1): 134-42.

Lo C, Hsu J, Sheu Y, Chiang C, Wu W, Fann W, Tsao P. 1998. Effect of D57N Mutation on Membrane Activity and Molecular Unfolding of Cobra Cardiotoxin. *Biophys J*, 75: 2382-2388.

Luidens MK, Figge J, Breese K, Vajda S. 1996. Predicted and Trifluoroethanol-Induced α-Helicity of Polypeptides. *Biopolymers*, 39: 367-376.

Lu H, Buck M, Radford SE, Dobson CM. Acceleration of the folding of hen lysozyme by trifluoroethanol. *J Mol Biol*, 265 (2): 112-117.

Luo P, Baldwin RL. 1997. Mechanism of Helix Induction by Trifluoroethanol: A Framework for Extrapolating the Helix-Forming Properties of Peptides from Trifluoroethanol/Water Mixtures Back to Water. *Biochemistry*, 36: 8413-8421.

Luo Y, Baldwin RL. 1998. Trifluoroethanol stabilizes the pH 4 folding intermediate of sperm whale apomyoglobin. *J Mol Biol*, 279 (1): 49-57.

Luo P, Baldwin RL. 1999. Interaction between water and polar groups of the helix backbone: An important determinant of helix propensities. *Proc Natl Acad Sci*, 96: 4930–4935.

Ma B, Tsai C, Nussinov R. 2000. A Systematic Study of the Vibrational Free Energies of Polypeptides in Folded and Random States. *Biophys J*, 79: 2739-2753.

Makhatadze GI. 2005. Thermal unfolding of proteins studied by calorimetry. In:

Buchner J, Kiefhaber T. eds. *Protein folding handbook*. Part I. Wiley-VCH Verlag GmbH & Co. KGaA, Weinheim. Chapter 4.

Marcon G, Plakoutsi G, Canale C, Relini A, Taddei N, Dobson CM, Ramponi G, Chiti F. 2005. Amyloid Formation from HypF-N under Conditions in which the Protein is Initially in its Native State. *J Mol Biol*, 347: 323–335.

Matouschek A. 2003. Protein unfolding--an important process in vivo? *Curr Opin Struct Biol*, 13 (1): 98-109.

Mattos C, Bellamacina CR, Peisach E, Pereira A, Vitkup D, Petsko GA, Ringe D. 2006. Multiple solvent crystal structures: probing binding sites, plasticity and hydration. *J Mol Biol*, 357 (5): 1471-1482.

Mazzini S, Fernandez-Vidal M, Galbusera V, Castro-Roman F, Bellucci MC, Ragg E, Haro I. 2007. 3D-Structure of the interior fusion peptide of HGV/GBV-C by ^{1}H NMR, CD and molecular dynamics studies. *Arch Biochem Biophys*, 465 (1): 187-196.

McGuffin LJ, Bryson K, Jones DT. 2000. The PSIPRED protein structure prediction server. *Bioinformatics*, 16 (4): 404-405.

Mehrnejad F, Naderi-Manesh H, Ranjbar B. 2007. The structural properties of magainin in water, TFE/water, and aqueous urea solutions: molecular dynamics simulations. *Proteins*, 67 (4): 931-940.

Melo, EP. 2003. Estabilidade de proteinas. In: Cabral JMS, Aires-Barros MR, Gama M. *Engenharia enzimática*. Eds. Lidel, Edições Técnicas, Lda, pp: 67-90.

Micaêlo NM, Soares CM. 2007. Modeling hydration mechanisms of enzymes in nonpolar and polar organic solvents. *FEBS J*, 274 (9): 2424-2436.

Minton AP. 2006a. How can biochemical reactions within cells differ from those in test tubes? *J Cell Sci*, 119: 2863-2869.

Minton AP. 2006b. Macromolecular crowding. *Cur Biology*, 16 (8): R269-R271.

Miyamoto S, Kollman PA. 1992. SETTLE: An analytical version of the shake and rattle algorithm for rigid water models. *J Comput Chem*, 13 (8): 952-962.

Muñoz V, Serrano L. 1994a. Elucidating the folding problem of α-helical peptides using empirical parameters, II. Helix macrodipole effects and rational modification of the helical content of natural peptides. *J Mol Biol*, 245: 275-296.

Muñoz V, Serrano L. 1994b. Elucidating the folding problem of α-helical peptides using empirical parameters III: Temperature and pH dependence. *J Mol Biol*, 245: 297-308.

Muñoz V, Serrano L. 1997. Development of the Multiple Sequence Approximation within the Agadir Model of α-Helix Formation. Comparison with Zimm-Bragg and Lifson-Roig Formalisms. *Biopolymers*, 41: 495-509.

Munson M, Balasubramanian S, Fleming KG, Nagi AD, O'Brien R, Sturtevant JM, Regan L. 1996. What makes a protein a protein? Hydrophobic core designs that specify stability and structural properties. *Protein Sci*, 5 (8): 1584-1593.

Nakasako M. 2004. Water–protein interactions from high–resolution protein crys-

tallography. *Phil Trans R Soc B*, 359: 1191-1206.

Naseem F, Khan RH. 2004. Fluoroalcohol-induced stabilization of the α-helical intermediates of lentil lectin: implication for non-hierarchical lectin folding. *Archives of Biochemistry and Biophysics*, 431: 215–223.

Neet K, Timm DE. 1994. Conformational stability of dimeric proteins: quantitative studies by equilibrium deneturation. *Protein Sci*, 3: 2167–2174.

Oliveira CSS. 2007. *Estados conformacionais da cardosina A.* Ph.D. thesis. University of Aveiro, Aveiro, Portugal.

Oliveira CS, Sarmento AC, Pereira A, Correia I, Pessoa JC, Esteves VI, Fonseca HMAC, Pires E, Barros MT. 2009. Non-native states of cardosin A induced by acetonitrile: Activity modulation via polypeptide chains rearrangements. *Journal of Molecular Catalysis B: Enzymatic*, 61: 274–278.

Okoniewska M, Tanaka T, Yada RY. 2000. The pepsin residue glycine-76 contributes to active-site loop flexibility and participates in catalysis. *Biochem J*, 349: 169-177.

Oostenbrink C, Villa A, Mark AE, van Gunsteren WF. 2004. A biomolecular force field based on the free enthalpy of hydration and solvation: The GROMOS force-field parameter sets 53A5 and 53A6. *J Comput Chem*, 25 (13): 1656-1676.

Pace NC, Shirley BA, Thomson JA. 1989. Measuring the conformational stability of a protein. In: Creighton CE.*Protein structure, a practical approach*. IRL Press at Oxford University Press, Oxford, GB. Chapter 13

Pace CN, Grimsley GR. 2001 Protein Stability. *Enc Life Sciences*, 10.1038/npg.els.0003002.

Partridge J, Dennison PR, Moore BD, Halling PJ. 1998. Activity and mobility of subtilisin in low water organic media: hydration is more important than solvent dielectric. *Biochimica et Biophysica Acta*, 1386: 79-89.

Payie KG, Tanaka T, Gal S, Yada RY. 2003. Construction, expression and characterization of a chimaeric mammalian-plant aspartic proteinase. *Biochem J*, 372: 671-678.

Pearl LH, Blundell TL. 1984. The active sites of aspartic proteinases. *FEBS Lett*, 174: 96-101.

Pereira AO, Cartucho DJ, Duarte AS, Gil MH, Cabrita AM, Patricio JA, Barros MM. 2005. Immobilisation of cardosin A in chitosan sponges as a novel implant for drug delivery. *Curr Drug Discov Technol*, 2 (4): 231-238.

Pereira AO. 2007. *Cardosina A como modelo para o estudo da estabilidade conformacional de proteases aspárticas.* Ph.D. thesis. University of Aveiro, Aveiro, Portugal.

Pereira CS, Costa DS, Pereira S, Nogueira FM, Albuquerque PM, Teixeira J, Faro C, Pissarra J. 2008. Cardosins in postembryonic development of cardoon: towards an elucidation of the biological function of plant aspartic proteinases. *Protoplasma*, 232: 203-213.

Perham M, Liao J, Wittung-Stafshede P. 2006. Differential Effects of Alcohols on

Conformational Switchovers in α-Helical and β-Sheet Protein Models. *Biochemistry*, 45: 7740-7749.

Pina DG, Oliveira CS, Sarmento AC, Barros M, Pires E, Zhadan GG, Villar E, Gavilanes F, Shnyrov VL. 2003. Thermostability of cardosin A from *Cynara cardunculus* L. *Thermochimica Acta*, 402: 123-134.

Pissarra J, Pereira C, Costa DS, Figueiredo R, Duarte P, Teixeira J, Pereira S. 2007. From Flower to Seed Germination in Cynara cardunculus: A Role for Aspartic Proteinases. *Int J Plant Dev Biol*, 1 (2): 274-281.

Price NC, Stevens L. 1999. *Fundamentals of Enzymology*. 3rd Ed., Oxford University Press, GB.

Privalov PL. 1979. Stability of proteins: Small globular proteins. *Adv Prot Chem*, 33: 167-239.

Provencher SW. 1982. *Comput. Phys. Commun.*, 27: 213-227, 229-242.

Ramalho-Santos M, Pissarra J, Veríssimo P, Pereira S, Salema R, Pires E, Faro CJ. 1997. Cardosin A, an abundant aspartic proteinase, accumulates in protein storage vacuoles in the stigmatic papillae of *Cynara cardunculus* L. *Planta*, 203: 204-212.

Ramalho-Santos M, Veríssimo P, Cortes L, Samyn B, Beeumen JV, Pires E, Faro C. 1998 Identification and proteolytic processing of procardosin A. *Eur J Biochem*, 255: 133-138.

Rand RP, Fuller NL, Butko P, Francis G, Nicholls P. 1993. Measured change in protein solvation with substrate binding and turnover. *Biochemistry*, 32 (23): 5925-5929.

Reiersen H, Clarke AR, Rees AR. 1998. Short elastin-like peptides exhibit the same temperature-induced structural transitions as elastin polymers: implications for protein engineering. *J Mol Biol*, 283 (1): 255-264.

Reiersen H, Rees AR. 2000. Trifluoroethanol may form a solvent matrix for assisted hydrophobic interactions between peptide side chains. *Protein Engineering*, 13 (11): 739-743.

Reyes AM, Ludwig HC, Yañez AJ, Rodríguez PH, Slebe JC. 2003. Native like Intermediate on the Unfolding Pathway of Pig Kidney Fructose-1,6-bisphosphatase. *Biochemistry*, 42: 6956-6964.

Rezaei K, Jenab E, Temelli F. 2007. Effects of water on enzyme performance with an emphasis on the reactions in supercritical fluids. *Crit Rev Biotechnol*, 27 (4): 183-195.

Roccatano D, Colombo G, Fioroni M, Mark AE. 2002. Mechanism by which 2,2,2-trifluoroethanol/water mixtures stabilize secondary-structure formation in peptides: A molecular dynamics study. *Proc Natl Acad Sci*, 99 (19): 12179–12184.

Roccatano D. 2008. Computer simulations study of biomolecules in non-aqueous or cosolvent/water mixture solutions. *Curr Protein Pept Sci*, 9 (4): 407-426.

Sanz JM, Jimenez MA, Gimenez-Gallego G. 2002. Hints of nonhierarchical folding of acidic fibroblast growth factor. *Biochemistry*, 41 (6): 1923-1933.

Sarmento AC, Silvestre L, Barros M, Pires E. 1998. Cardosins A and B, two new enzymes available for peptide synthesis. *J Mol Catalysis B: Enzym*, 5: 327-330.

Sarmento AC. 2002. *A cardosina A uma proteinase aspártica vegetal como modelo para estudos de comportamento em solventes orgânicos. Da biocatálise à química de proteínas.* Ph.D. thesis. University of Aveiro, Aveiro, Portugal.

Sarmento AC, Oliveira CS, Pires EM, Halling PJ, Barros MT. 2003. Cardosin A as a model aspartic proteinase for the study of organic solvent effects. I. An overview on catalytic and structural aspects. *Journal of Molecular Catalysis B: Enzymatic*, 21 (1-2): 19-23.

Sarmento AC, Oliveira CS, Pires E, Amado F, Barros M. 2004. Reverse hydrolysis by cardosin A: specificity considerations. *J. Mol. Cat. B: Enzymatic*, 28:33-37.

Sarmento AC, Oliveira CS, Pires EM, Halling PJ, Barros MT. 2004b. Evaluation of cardosin A as a proteolytic probe in the presence of organic solvents. *J Molecular Catalysis B: Enzymatic*, 31: 137–141.

Sarmento AC, Oliveira CS, Duarte AS, Pires E, Barros MT. 2006. Evaluation of cardosin A as a probe for limited proteolysis in nonaqueous environments – complex substrates hydrolysis. *Enz Microb Technol*, 38: 415-421.

Sarmento AC, Lopes H, Oliveira CS, Vitorino R, Samyn B, Sergeant K, Debyser G, Van Beeumen J, Domingues P, Amado F, Pires E, Domingues MR, Barros MT. 2009a. Multiplicity of aspartic proteinases from *Cynara cardunculus* L. *Planta*, 230 (2): 429-439.

Sarmento AC, Oliveira CS, Pereira A, Esteves VI, Moir AJG, Saraiva J, Pires E, Barros M. 2009b. Unfolding of cardosin A in organic solvents and detection of intermediaries. *J Mol Catal B: Enzym*, 57 (1), p.115-122.

Scharge T, Häber T, Suhm MA. 2006. Quantitative chirality synchronization in trifluoroethanol dimmers. *Phys Chem Chem Phys*, 8: 4664–4667.

Scharge T, Cézard C, Zielke P, Schütz A, Emmeluth C, Suhm MA. 2007. A peptide co-solvent under scrutiny: self-aggregation of 2,2,2-trifluoroethanol. *Phys Chem Chem Phys*, 9: 4472–4490.

Schimmele B, Plückthun A. 2005. Engineering proteins for stability and efficient folding. In: Buchner J, Kiefhaber T. eds. *Protein folding handbook*. Part II. Wiley-VCH Verlag GmbH & Co. KGaA, Weinheim. Chapter 39.

Schmid F. 2005. Spectroscopic techniques to study protein folding and stability. In: Buchner J, Kiefhaber T. eds. *Protein folding handbook*. Part I. Wiley-VCH Verlag GmbH & Co. KGaA, Weinheim. Chapter 2.

Schmid FX. 1990. Spectral methods of characterizing protein conformation and conformational changes. In: Creighton TE. ed. *Protein structure, a practical approach*. IRL Press, Oxford, UK. Chapter 11.

Schmitke JL, Stern LJ, Klibanov AM. 1998. Comparison of x-ray crystal structures of an acyl-enzyme intermediate of subtilisin Carlsberg formed in anhydrous acetonitrile and in water. *PNAS*, 95: 12918-12923.

Schönbrunner N, Wey J, Engels J, Georg H, Kiefhaber T. 1996. Native-like β-structure in a Trifluoroethanol-induced Partially Folded State of the All-β-sheet Protein

Tendamistat. *J Mol Biol*, 260: 432–445.

Sforça ML, Oyama Jr S, Canduri F, Lorenzi CC, Pertinhez TA, Konno K, Souza BM, Palma MS, Neto JR, Azevedo Jr WF, Spisni A. 2004. How C-terminal carboxyamidation alters the biological activity of peptides from the venom of the eumenine solitary wasp. *Biochemistry*, 43 (19): 5608-5617.

Shiraki K, Nishikawa K, Goto Y. 1995. Trifluoroethanol-induced Stabilization of the α-Helical Structure of β-Lactoglobulin: Implication for Non-hierarchical Protein Folding. *J Mol Biol*, 245: 180–194.

Shnyrova AV, Oliveira CS, Sarmento AC, Barros MT, Zhadan GG, Roig MG, Shnyrov VL. 2006. Effect of acetonitrile on *Cynara cardunculus* L. cardosin A stability. *International Journal of Biological Macromolecules*, 39: 273-279.

Simões I, Faro C. 2004. Structure and function of plant aspartic proteinases. *Eur J Biochem*, 271 (11): 2067-2075.

Simões I, Mueller EC, Otto A, Bur D, Cheung AY, Faro C, Pires E. 2005. Molecular analysis of the interaction between cardosin A and phospholipase D(alpha). Identification of RGD/KGE sequences as binding motifs for C2 domains. *FEBS J*, 272 (22): 5786-5798.

Simões I, Faro R, Bur D, Faro C. 2007. Characterization of Recombinant CDR1, an *Arabidopsis* Aspartic Proteinase Involved in Disease Resistance. *JBC*, 282 (43): 31358–31365.

Smith PE, van Gunsteren WF. 1994. Consistent dielectric properties of the simple point charge and extended simple point charge water models at 277 and 300 K. *J Chem Phys*, 100 (4): 3169-3174.

Soares CM, Teixeira VH, Baptista AM. 2003. Protein structure and dynamics in nonaqueous solvents: insights from molecular dynamics simulation studies. *Biophys J*, 84 (3): 1628-1641.

Sönnichsen FD, Eyk JEV, Hodges RS, Sykes BD. 1992. Effect of Trifluoroethanol on Protein Secondary Structure: An NMR and CD Study Using a Synthetic Actin Peptide. *Biochemistry*, 31: 8790-8798.

Stockley JH, O'Neill C. 2008. Understanding BACE1: essential protease for amyloid-beta production in Alzheimer's disease. *Cell Mol Life Sci*, 65 (20): 3265-3289.

Sturtevant JM. 1987. Biochemical applications of Differential Scanning Calorimetry. *Ann. Rev. Phys. Chem.*, 38: 463-488.

Suguna K, Padlan EA, Smith CW, Carlson WD, Davies DR. 1987. Binding of a Reduced Peptide Inhibitor to the Aspartic Proteinase from *Rhizopus chinensis*: Implications for a Mechanism of Action. *PNAS*, 84: 7009-7013.

Sun J, Weinstein H. 2007. Toward realistic modeling of dynamic processes in cell signaling: quantification of macromolecular crowding effects. *J Chem Phys*, 127 (15): 155105.

Sundd M, Kundu S, Dubey VK, Jagannadham MV. 2004. Unfolding of Ervatamin C in the Presence of Organic Solvents: Sequential Transitions of the Protein in the O-state. *J Biochem Mol Biol*, 37(5): 586-596.

Taiz L. 1992. The Plant Vacuole. *J Exp Biol*, 172: 113-122.

Thomas PD, Dill KA. 1993. Local and nonlocal interactions in globular proteins and mechanisms of alcohol denaturation. *Protein Sci*, 2: 2050-2065.

Tironi IG, Sperb R, Smith PE, van Gunsteren WF. 1995. A generalized reaction field method for molecular-dynamics simulations. *J Chem Phys*, 102 (13): 5451-5459.

Törmäkangas K, Hadlington JL, Pimpl P, Hillmer S, Brandizzi F, Teeri TH, Denecke J. 2001. A Vacuolar Sorting Domain May Also Influence the Way in Which Proteins Leave the Endoplasmic Reticulum. *Plant Cell*, 13: 2021-2032.

Torta F, Elviri L, Careri M, Mangia A, Cavazzini D, Rossi GL. 2008. Mass spectrometry and hydrogen/deuterium exchange measurements of alcohol-induced structural changes in cellular retinol-binding protein type I. *Rapid Commun Mass Spectrom*, 22 (3): 330-336.

Tsai CJ, Kumar S, Ma B, Nussinov R. 1999. Folding funnels, binding funnels, and protein function. *Protein Sci*, 8 (6): 1181-1190.

Ulijn RV, Janssen AE, Moore BD, Halling PJ, Kelly SM, Price NC. 2002. Reversible acetonitrile-induced inactivation/activation of thermolysin. *Chembiochem*, 3 (11): 1112-1116.

Umezaki T, Iimura S, Noda Y, Segawa S, Yutani K. 2008. The confirmation of the denatured structure of pyrrolidone carboxyl peptidase under nondenaturing conditions: difference in helix propensity of two synthetic peptides with single amino acid substitution. *Proteins*, 71 (2): 737-742.

Uversky VN. 1993. Use of Fast Protein Size-Exclusion Liquid Chromatography To Study the Unfolding of Proteins Which Denature through the Molten Globule. *Biochemistry*,32: 13288-13298.

Uversky VN. 2002. Cracking the folding code. Why do some proteins adopt partially folded conformations, whereas other don't? *FEBS Lett*, 514 (2-3): 181-183.

Valivety RH, Halling PJ, Peilow AD, Macrae AR. 1994. Relationship between water activity and catalytic activity of lipases in organic media. Effects of supports, loading and enzyme preparation. *Eur J Biochem*, 222 (2): 461-466.

van Gunsteren WF, Berendsen HJC. 1990. Computer simulation of molecular dynamics: Methodology, applications, and perspectives in chemistry. *Angew Chem Int Ed*, 1990. 29: p. 992-1023.

van Holde KE, Johnson WC, Ho PS. 2006. *Principles of Physical Biochemistry*. 2nd edition, Pearson Education Inc, Upper Saddler River, USA. Chapter 10.

Veríssimo P, Faro C, Moir AJ, Lin Y, Tang J, Pires E. 1996. Purification, characterization and partial amino acid sequencing of two new aspartic proteinases from fresh flowers of *Cynara cardunculus* L. *Eur J Biochem*, 235 (3): 762-768.

Viguera AR, Jimenez MA, Rico M, Serrano L. 1996. Conformational analysis of peptides corresponding to β-hairpins and a β-sheet that represent the entire sequence of the α-spectrin SH3 domain. *J Mol Biol*, 255 (3): 507-521.

Villa A, Mark AE, Saracino GA, Cosentino U, Pitea D, Moro G, Salmona M. 2006.

Conformational polymorphism of the PrP106-126 peptide in different environments: a molecular dynamics study. *J Phys Chem B*, 110 (3): 1423-1428.

Viseu MI, Carvalho TI, Costa SM. 2004. Conformational transitions in beta-lactoglobulin induced by cationic amphiphiles: equilibrium studies. *Biophys J*, 86 (4): 2392-2402.

Walgers R, Lee TC, Cammers-Goodwin A. 1998. An Indirect Chaotropic Mechanism for the Stabilization of Helix Conformation of Peptides in Aqueous Trifluoroethanol and Hexafluoro-2-propanol. *J Am Chem Soc*, 120: 5073-5079.

Wangikar PP, Rich JO, Clark DS, Dordick JS. 1995. Probing enzymic transition state hydrophobicities. *Biochemistry*, 34 (38): 12302-12310.

Waterhous DV, Johnson Jr WC. 1994. Importance of environment in determining secondary structure in proteins. *Biochemistry*, 33 (8): 2121-2128.

Wei X, Ding S, Jiang Y, Zeng X, Zhou H. 2006. Conformational Changes and Inactivation of Bovine Carbonic Anhydrase II in 2,2,2-Trifluoroethanol Solutions. *Biochemistry (Moscow)*, 71 (Suppl. 1): S77-S82.

Whitaker JR. 1963. Determination of molecular weights of proteins by gel filtration on Sephadex. *Anal Chem.* 35:1950-1953.

Wikipedia contributors 1. 2009. "File:Water molecule 3D.svg", "File:2,2,2-trifluroroethanol-3D-vdW.png", "File:Acetonitrile-3D-vdW.png". *Wikipedia, The Free Encyclopedia*, 30 December 2009, 16:20 UTC, < http://en.wikipedia.org/wiki/File:Water_molecule_3D.svg>, < http://en.wikipedia.org/wiki/File:2,2,2-trifluroroethanol-3D-vdW.png>, < http://en.wikipedia.org/wiki/File:Acetonitrile-3D-vdW.png>, respectively [accessed 30 December 2009].

Wikipedia contributors 2. 2009. Aspartyl protease mechanism.png. *Wikipedia, The Free Encyclopedia*, 13 May 2009, 01:11 UTC, < http://en.wikipedia.org/wiki/File:Aspartyl_protease_mechanism.png> [accessed 13 May 2009].

Wirmer J, Schlörb C, Schwalbe H. 2005. Conformation and dynamics of nonnative states of proteins studied by NMR Spectroscopy. In: Buchner J, Kiefhaber T. eds. *Protein folding handbook*. Part I. Wiley-VCH Verlag GmbH & Co. KGaA, Weinheim. Chapter 21.

Yamaguchi K, Naiki H, Goto Y. 2006. Mechanism by Which the Amyloid-like Fibrils of a β_2-Microglobulin Fragment Are Induced by Fluorine-substituted Alcohols. J Mol Biol, 363: 279–288.

Yamamoto S, Hasegawa K, Yamaguchi I, Goto Y, Gejyo F, Naiki H. 2005. Kinetic analysis of the polymerization and depolymerization of β_2-microglobulin-related amyloid fibrils in vitro. *Biochim Biophys Acta*, 1753 (1): 34-43.

Yang L, Dordick JS, Garde S. 2004. Hydration of Enzyme in Nonaqueous Media Is Consistent with Solvent Dependence of Its Activity. *Biophysical Journal*, 87 (2): 812-821.

Yuan Z, Bailey TH, Teasdale RD. 2005. Prediction of Protein B-factor Profiles. *PROTEINS: Structure, Function, and Bioinformatics*, 58: 905–912.

Zaks A, AM Klibanov. 1985. Enzyme-catalyzed processes in organic solvents. *Proc Natl Acad Sci*, 82: 3192–3196.

Zaks A, Klibanov AM. 1988a. The effect of water on enzyme action in organic media. *J Biol Chem*, 263: 8017-8021.

Zaks A, Klibanov AM. 1988b. Enzymatic catalysis in nonaqueous solvents. *J Biol Chem*, 263: 3194-3201.

Závodszky P, Kardos J, Svingor A, Petsko GA. 1998. Adjustment of conformational flexibility is a key event in the thermal adaptation of proteins. *PNAS*, 95: 7406-7411.

Zerovnik E, Skarabot M, Skerget K, Giannini S, Stoka V, Jenko-Kokalj S, Staniforth RA. 2007. Amyloid fibril formation by human stefin B: influence of pH and TFE on fibril growth and morphology. *Amyloid*, 14 (3): 237-47.

Zhang YX, Zhu Y, Zhou HM. 2000. Conformational changes and inactivation of calf intestinal alkaline phosphatase in trifluoroethanol solutions. *Int J Biochem Cell Biol*, 32 (8): 887-894.

Zhang J, Li W, Wang J, Qin M, Wu L, Yan Z, Xu W, Zuo G, Wang W. 2009. Protein folding simulations: from coarse-grained model to all-atom model. *IUBMB Life*, 61 (6): 627-643.

Zhao J, Liu H. 2006. The effects of various alcohols on the secondary structural integrity of melittin, TH-10Aox, and Tc1 by molecular dynamics simulations. *Chem Phys Lett*, 420: 235–240.

Zhou HW, Xu Y, Zhou HM. 2002. Activity and conformational changes of horseradish peroxidase in trifluoroethanol. *Biochem Cell Biol*, 80 (2): 205-213.

para o António